Philipps Universität Marburg

Proteomics analysis of exported chaperone/co-chaperone complexes of *P. falciparum* reveals an array of complex protein-protein interactions

Dissertation zur Erlangung des Doktorgrades

der Naturwissenschaften

(Dr. rer. nat.)

dem

Fachbereich Biologie

der Philipps-Universität Marburg

vorgelegt von

Qi Zhang

aus Harbin, P. R. China

Marburg/Lahn, 2016

Vom Fachbereich Biologie der Philipps-Universität Marburg als Dissertation angenommen am:

Prof. Dr. Jude M. Przyborski (Erstgutachter)

Prof. Dr. Uwe G. Maier (Zweitgutachter)

Prof. Dr. Alfred Batschauer

Prof. Dr. Ralf Jacob

Tag der Disputation am:

Publications

1. Qi Zhang, Cheng Ma, Astrid Zinz, Sonja Engels, Jude M. Przyborski. Proteomics analysis of exported chaperone/co-chaperone complexes of *P. falciparum* reveals an array of complex protein-protein interactions. Mol Cell Proteomics. (Under review)
2. Wiebke Petersen, Simone Külzer, Sonja Engels Qi Zhang, Alyssa Ingmundson Melanie, RugAlexander G Maier Jude M. Przyborski J-dot targeting of an exported Hsp40 in P. falciparum-infected erythrocytes (2016). International Journal for Parasitology. pii: S0020-7519(16)30021-2
3. C. Ma, Q. Zhang, J. Qu, X. Zhao, X. Li, P. G. Wang (2015). A precise approach in large-scale core-fucosylated glycoprotein identification with low- and high-normalized collision energy. J of Proteomics. 114:61-70.
4. C Ma, X. Zhao, H. Han, W.Tong, Q. Zhang, P. Qin, C.Chang, W. Ying, and X. Qian (2014). N-linked glycoproteome profiling of human serum using tandem enrichment and multiple fraction concatenation. Electrophoresis 34(16): 2440-2450.

Eigenständigkeitserklärung

Ich versichere hiermit, dass ich meine dem Fachbereich Biologie der Universität Marburg vorgelegte Dissertation, mit dem Titel

“Proteomic analysis of exported chaperone/co-chaperone complexes of reveals an array of complex protein-protein interactions”

selbstständig, ohne unerlaubte Hilfe angefertigt und mich dabei keiner anderen als der von mir ausdrücklich bezeichneten Quellen und Hilfen bedient habe.

Die Dissertation wurde in der jetztigen oder einer ähnlichen Form noch bei keiner anderen Hochschule eingereicht und hat noch keinen sonstigen Prüfungszwecken gedient.

_____ _____

(Ort/Datum) (Unterschrift mit Vor- und Zuname)

Abbreviation

aa	amino aids	PEXEL	Plasmodium export element
ATP	adenosine triphosphate	Pf	*Plasmodium falciparum*
bp	base pairs	PIC	protease inhibitor cocktail
DTT	Dithiothreitol	PMSF	phenylmethylsulphonyl fluoride
ECL	Enhanced chemiluminescence	PTEX	Plasmodium translocon of exported proteins
ER	endoplasmic reticulum	PVM	parasitophorous vacuole membrane
GFP	green fluorescent protein	RBC	red blood cell
Hsp	Heat shock protein	RBCM	red blood cell membrane
HT	host targeting signal	REX 1	ring-exported protein 1 and 2
KDa	kilodalton	SDS	sodium dodecyl sulfate
IAA	iodoacetamide	SERP	serine-rich protein
LC-MS/MS	Liquid chromatography-Tandem mass spectrometry	SLO	Streptolysin O
LTQ	linear trap quadrupole	TFA	trifluoroacetic acid
PAGE	polyacrylamide gel electrophoresis	V	voltage
PBS	phosphate buffered saline	2D	two-dimensional

Summary

In order to grow and survive the human malaria parasite *Plasmodium falciparum* synthesizes and exports hundreds of proteins in order to modify the infected red blood cell. In previous studies, our group found that two members of parasite encoded type II Hsp40s (PEF55, PFA660) associate with highly mobile structure in the infected host cell, which are referred to as J-dots. Furthermore, an exported parasite chaperone, *Pf*Hsp70x was identified which also associated with these structures. To understand the role of J-dots in host cell modification, we aimed to purify J-dots and identify the proteome of these parasite-induced intra-erythrocytic structures. This would allow us to further construct a protein-protein interactions network of the *P. falciparum* infect red blood cell.

In this study, multiple proteomics methods were used to profile PFE55-*Pf*Hsp70x chaperone/co-chaperone protein complexes (J-dots). By using differential centrifugation as well as immunoblotting of BN-PAGE and 2D BN/SDS PAGE, PFE55 and *Pf*Hsp70x were visualized in the same complex with a high molecular weight >223KDa. Furthermore, two exported proteins, *Pf*PHISTc and *Pf*GEXP18 were identified by co-immunoprecipitation (co-IP) and LC-MS/MS to interact with PFE55 and *Pf*Hsp70x, and subsequently to localize to J-dots In addition, further protein complexes containing PFE55 and *Pf*Hsp70x were found not only in the parasite infected erythrocyte cytosol but also in the parasitophorous vacuole. Surprisingly, *Pf*Hsp70x was also found associated with a protein translocon at the parasitophorous vacuole, termed PTEX. Proteomic analysis of the co-IP also suggested an interaction between human Hsp70 and PFE55. Taken together, our data indicates *Pf*Hsp70x-PFE55 chaperones/co-chaperone complexes are involved in exported protein trafficking from the parasitophorous vacuole into the erythrocyte cytosol. Potentially, these complexes could be aiding in protein folding and unfolding during passage through the PTEX translocon. Moreover, the fact that many exported proteins were found associated with *Pf*Hsp70x, further highlights the role of *Pf*Hsp70x in coordinating exported protein trafficking.

Zusammenfassung

Der humane Malaria Parasit *Plasmodium falciparum* ist für sein Überleben darauf angewiesen die von ihm infizierten Erythrozyten mittels exportierter Proteine zu modifizieren. In vorausgehenden Studien konnte gezeigt werden, dass zwei parasiten-codierte Typ II Hsp40s (PEF55, PFA660) mit mobilen Strukturen in der Wirtszelle, den sogenannten J-dots, assoziieren. Außerdem konnte ein exportiertes Chaperon des Parasiten *Pf*Hsp70x identifiziert werden, dass ebenfalls mit diesen Strukturen assoziiert. Ziel dieser Arbeit ist es J- dots aufzureinigen und deren Proteom zu bestimmen, um die Funktion dieser parasitären Strukturen im Wirtszellcytosol für die Modifikation der Wirtszelle besser zu verstehen. Das könnte uns ermöglichen, weitere Teile des komplexen Netzwerks aus Protein-Protein Interaktionen in *P. falciparum* infizierten Erythrozyten zu entziffern.

In dieser Arbeit wurden mehrere Methoden benutzt, um das Proteom der PFE55-*Pf*Hsp70x Ko-Chaperon- Chaperon Komplexe (J-dots) zu bestimmen. Dabei konnte durch differentielle Zentrifugation und Immunoblot von BN-PAGE und 2D BN/SDS PAGE gezeigt werden, dass PFE55 und *Pf*Hsp70x Teil eines Komplexes mit hoher molekularer Masse (>223 kDa) sind. Außerdem konnten mittels Ko-Immunpräzipitation und LC- MS/MS zwei exportierte Proteine identifiziert werden, die mit PFE55 und *Pf*Hsp70x interagieren und ebenfalls mit J-Dots assoziieren: *Pf*PHISTc und *Pf*GEXP18. Zusätzlich wurden PFE55 und *Pf*Hsp70x nicht nur in Komplexen im Zytosol der infizierten Erythrozyten sondern auch in weiteren Komplexen in der parasitophoren Vakuole nachgewiesen. Außerdem tritt PfHsp70x überraschender Weise auch in Assoziation mit einem Translokon in der parasitophoren Vakuole (PTEX) auf. Des Weiteren weißt die proteomische Analyse der Ko-Immunpräzipitation auf eine Interaktion von PFE55 und humanem Hsp70 hin.

Insgesamt zeigen unsere Daten, dass *Pf*Hsp70x und PFE55 als Chaperon- Ko-Chaperon Komplexe am Transport von exportierten Proteinen durch das PTEX Translokon an der parasitophoren Vakuole beteiligt sind. Dabei könnten sie insbesondere bei der Entfaltung und Faltung von Proteinen während dem Export durch das PTEX Translokon eine Rolle spielen. Zusätzlich unterstreicht die Vielzahl an exportierten Proteinen, die mit *Pf*Hsp70x interagieren die Rolle, die dieses Chaperon in der Koordination des Proteinexports von *P. falciparum* spielt.

Table of Contents

List of tables and figures

1 INTRODUCTION

1.1 Malaria

Malaria is one of the most serious fatal blood diseases in the world. Nearly half of the world population living in the endemic areas has been infected, include South America, Africa and Indonesia, covering more than 100 countries. In 2013, an estimated 198 million cases of malaria occurred worldwide with 584,000 to 855,000 people dead. Over 90% of these cases happened in Africa; majority of them were children with a burden occurring age younger than 5 years old (WHO, 2014). Malaria is caused by parasites that are transmitted from the bites of female *Anopheles* mosquito. These parasites are transferred from mosquito's saliva into human blood steams after biting then travel to human livers for maturation and reproduction. There are five different species of the genus *Plasmodium* known to cause malaria, including *Plasmodium vivax, Plasmodium ovale, Plasmodium malariae, P falciparum* and *Plasmodium knowlesi*. Among them, *P. falciparum* leads to the most fatal infection; while *P. vivax, P. ovale,* and *P. malariae* generally cause a milder form of malaria that is rarely fatal. Additionally, *P. knowlesi* mostly causes the disease in macaques; however, recently, it has been also found to infect human (Singh *et al.*, 2004).

1.2 Overview of the *P. falciparum* life cycle

P. falciparum has a complicated life cycle includes multiple reproduction stages in human host cells. In general, sporozoites migrate into the host during the bite of the female *Anopheles* mosquito, then enter the bloodstream and eventually get into the liver cell, which is referred as the exo-erythrocytic stage. In the liver cell, the sporozoites re-differentiate and release thousands of merozoites into the bloodstream. Next, once the merozoites invade the red blood cell successfully, the erythrocytic stage starts. The invasion is a fast process that takes approximately 60 seconds for escaping the immune detection and invading the red blood cell. The invasion is accomplished via the interaction between merozoite surface proteins and red blood cell membrane surface proteins. After invasion, parasites replicate and go through three distinct stages including ring, trophozoite and schizont stages. One merozoite can reproduce 20-30

daughters in 48 hours. First of all, merozoite grows from ring like stage by take the hemoglobin as nutrition (0-12 hours after invasion) into more mature trophozoites (12-30 hours), afterwards, the nucleus of trophozoite is divided and become multinucleated schizont (30-48 hours) (Shortt, 1951), followed by growing into many individual merozoite forms. Once the red blood cell is ruptured, merozoites are released in order to invade new red blood cells and restart a new life cycle (Cowman and Crabb, 2006). Moreover, parasites can also commit to the asexual stage by differentiating into male or female gametocytes, the sexual form of parasites is able to stay in the host for 60 days without any further development except been taken by mosquito for complete *P. falciparum* cycle by development in the mosquito midgut (mosquito stage) (figure 1.1) (Talman *et al.*, 2004; Alano, 2007; Ay *et al.*, 2015).

As malaria parasites rapidly reproduce and spread in the erythrocyte and blood stream, and export Erythrocyte Membrane Protein-1 (*Pf*EMP1) to the red blood cell membrane surface lead to infected erythrocytes cytoadherence. Many symptoms appear on infected hosts, such as coldness or fever, significantly reduced or even halted blood flows due to the cytoadherence of infected erythrocytes. All of these are vital to body organs such as hearts, lungs, and kidneys. For some serious form of malaria, there is even the brain function deficiency, which can lead to convulsions, paralysis, coma and even death (Idro *et al.*, 2010).

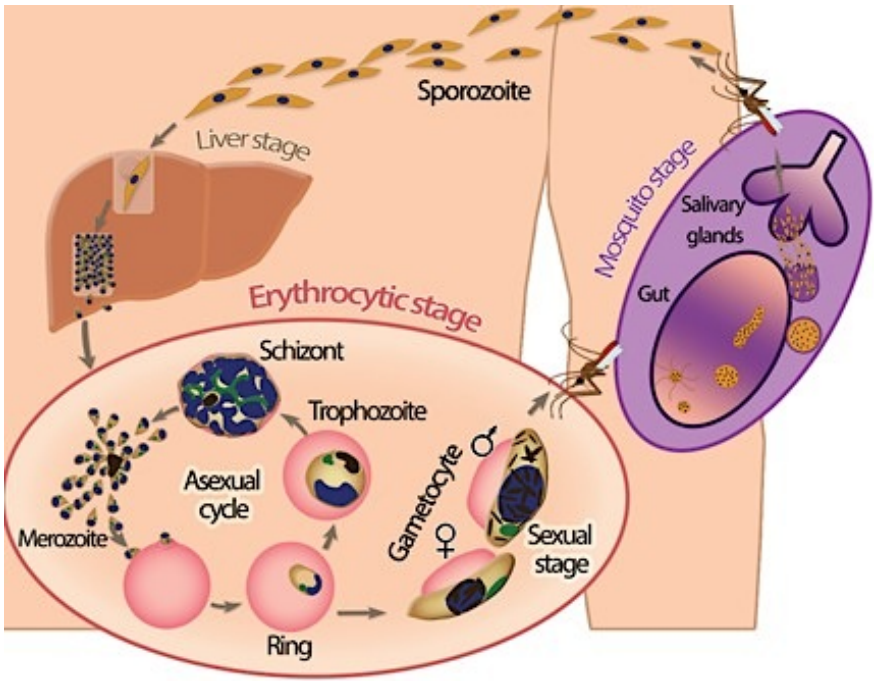

Figure 1.1: *P. falciparum* life cycle overview.

During the bite of mosquito, malaria parasites migrate into the human host. Asexual reproduction occurs in live cell; then merozoites invade into red blood cells and develop through ring, trophozoite and schizonet stages and finally are released from host cells to initial a new invasion cycle. (Ay *et al.*, 2015)

1.3 Intraerythrocytic stages of *P. falciparum*

1.3.1 The function of novel structures in *P. falciparum* infected red blood cell

There are several structures and compartments formed during the development and maturation of the parasite in the red blood cell (Figure 1.2). First of all, parasitophorous vacuole (PV) is present in some apicomplexan parasites such as *Toxoplasma* and *Plasmodium* and formed during merozoite invasion, which surrounds the parasite as a barrier between it and the host cell. The parasite reproduces and develops inside the PV. It is suggested that PV is involved in the parasite nutrition uptake as well as protecting the parasite from erythrocyte cytosol potentially harmful substances (Lauer *et al.*, 2000; Murphy *et al.*, 2004). Also many proteases and chaperones have been found in PV by proteome studies; and these proteins are likely involved in many

processes such as nutrient acquisition and parasite release (Lingelbach and Joiner, 1998; Lauer *et al.*, 2000; Marti *et al.*, 2004; Murphy *et al.*, 2004). Surrounding the side PV, there is a membrane compartment so-called parasitophorous vacuole membrane (PVM); however, it is still under debate whether the source of PVM is from human red blood cell membrane or the or parasite origin is still in a debate (Bannister and Dluzewski, 1990). In addition, there is a set of membranous network called tubovesicular network (TVN) locating at the erythrocyte cytosol (van Ooij *et al.*, 2008), which seems to connect with PVM and plays a role in the nutrient acquisition (Atkinson and Aikawa, 1990). Another unique, complex structure likely generated from PVM or TVN and formed in parasites during erythrocyte infection, is called Maurer's clefts. This structure has a diameter of ~30nm, consisting of an electron-dense coat and a translucent lumen. It is most likely close to the erythrocyte membrane and has been revealed to be associated with several parasite encode export proteins such as *Pf*EMP1, RIFIN and SURFIN during their delivery to the red blood cell membrane surface, indicating its function to help deliver export proteins through red blood cell (Tobie and Coatney, 1961; Aikawa *et al.*, 1986; Waterkeyn *et al.*, 2000; Przyborski *et al.*, 2005; Lanzer *et al.*, 2006).

Since malaria parasites are known to export more than 400 hundreds protein to the infected erythrocyte in order to modify the morphology, physiology and function of the host cell, it is essential for parasites to make sure these proteins cross not only parasite plasma membrane (PPM) but also the PVM (Marti *et al.*, 2005; Sargeant *et al.*, 2006; Maier *et al.*, 2008). The transport to the PV is usually accomplished by going through endoplasmic reticulum (ER), a classical secretory system; and these proteins contain a hydrophobic sequence at the N-terminus similar as the signal peptide (Blobel and Dobberstein, 1975; Blobel and Dobberstein, 1975; Kirchhausen, 2000). Recently, a novel translocon of exported proteins complex (PTEX) is found to be located at PVM, which may play an important role for protein transport from PV to erythrocyte cytosol (de Koning-Ward *et al.*, 2009; Beck *et al.*, 2014; Elsworth *et al.*, 2014).

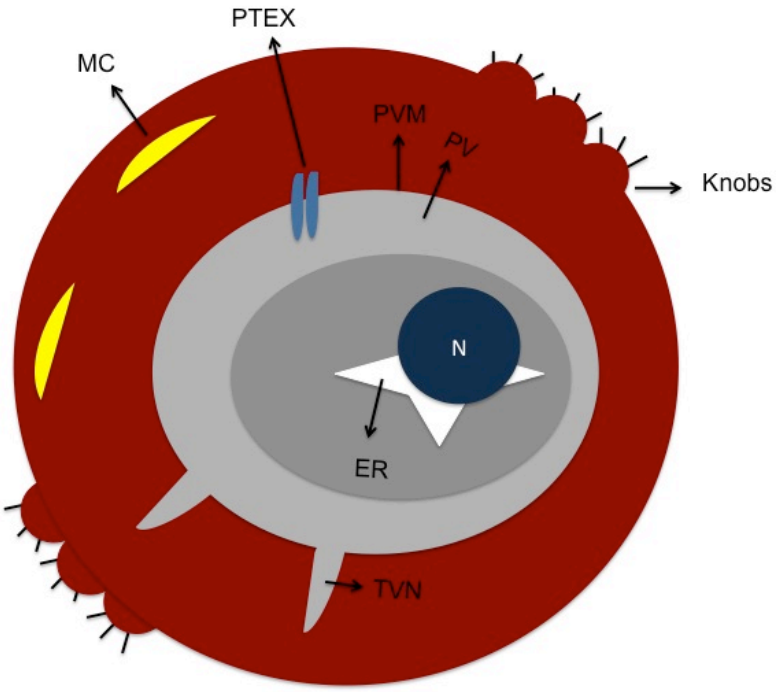

Figure 1.2: The structure of malaria parasites in the host cell.

N: nucelus; PV: parasitophorous vacuole; PVM: parasitophorous vacuole membrane; PPM: parasite plasma membrane; MC: Maurer's clefts; NPP: new permeation pathways in the red blood cell membrane; V: transport vesicles and protein aggregates; mCS: modified cytoskeleton of the red blood cell; Knobs; structures on the host cell surface

1.3.2 Modification of the host cell by *P. falciparum* exported protein

Parasites have to modify the infected red blood cell for escaping human immune system in order to develop and reproduce inside. For these purposes, parasites export many proteins to the membrane surface of red blood cells, which form an electron-microscopically visible, sticky structure referred as “Knobs” during plasmodium trophozoite stage change the morphology, physiology and function of infected red blood cells (Leech *et al.*, 1984). So far, there are several of these surface proteins identified, such as *P. falciparum*-infected erythrocyte membrane protein-1 (*Pf*EMP-1), *P. falciparum*-infected erythrocyte membrane protein-2 (*Pf*EMP2), erythrocyte membrane protein-3 (*Pf*EMP-3) as well as submembranous structural proteins knob-associated histidine-rich protein (KAHRP) that is essential for Knobs conformation (Pologe and

Ravetch, 1986; Pasloske *et al.*, 1993; Crabb *et al.*, 1997; Waller *et al.*, 1999; Smith, 2014). *Pf*EMP-1 is a protein with a molecular weight of 200-350KDa that is responsible for the adhesion of infected erythrocytes to the endothelial lining of blood vessels. Since membrane surface proteins like *Pf*EMP-1 can adhere together to endothelial cells in the blood vessel, the blood stream flow is significantly reduced or even completely halted; as a result, lots of organs such as heart, lung, kidney and brain fail to function properly (Grau *et al.*, 1990; Baruch *et al.*, 1995; Smith *et al.*, 2000; Miller *et al.*, 2002; Maier *et al.*, 2009). Therefore, the Knob proteins are important for the malaria parasites to escape from immunotherapeutic agents, suggesting that these proteins are a hot research topic for malaria remedy.

1.3.3 *P. falciparum* proteins transport

Once the parasites invade into erythrocyte, hundreds of proteins are exported to modify the host cell for parasite survival. Up to 8% of the parasite's gene products contain a five amino acid motif sequence (RxLxE/D/Q) called PEXEL/HT (Protein Export Element/Host targeting motif). This sequence is located ~35 amino acids downstream from the signal peptide and can be cleaved by the enzyme plasmepsin V in order to produce the mature protein. The PEXEL motif can be used to predict exported proteins (Hiller *et al.*, 2004; Marti *et al.*, 2005; Sargeant *et al.*, 2006; Chang *et al.*, 2008; Boddey *et al.*, 2009; Maier *et al.*, 2009). Exported proteins have various destinations including the cytoplasm of host red blood cells, Maurer's cleft, as well as the erythrocyte membrane (Maier *et al.*, 2009). This unique export element defines the secretome; however, the principle of the secretion pathway is still not fully understood. Particularly, this PEXEL/HT peptide sequence shares between soluble and membrane proteins. Another type of exported proteins, which lacks the PEXEL motif sequence but can still export to the cytoplasm, is called PEXEL-negative exported proteins (PNEPs). This group of protein includes skeleton binding protein 1(SBP1) and membrane associated histidine-rich protein (MAHRP1). By far, its export mechanism is also not clear (Blisnick *et al.*, 2000; Spielmann *et al.*, 2006; Maier *et al.*, 2009). Recent studies found that a new *Plasmodium* translocon of exported proteins (PTEX) on PVM was responsible for exporting both PEXEL-containing proteins and PNEP proteins to the cytoplasm of the infected cell (de Koning-Ward *et al.*, 2009; Gruring *et al.*, 2012; Beck *et al.*, 2014; Elsworth *et al.*, 2014).

1.3.4 *Plasmodium* translocon of exported proteins (PTEX)

In order to reach the erythrocyte cytosol, the exported proteins are supposed to cross parasitophorous vacuole membrane (PVM) by going through a specific translocon. Proteome analysis of lipid-raft-like, detergent resistant membrane fractions of parasites revealed a majority of PVM proteins. This suggests that the components of the translocon are PVM proteins (de Koning-Ward *et al.*, 2009). By co-immunoprecipitation and the LC-MS/MS identification, it has been found that *Plasmodium* translocon of exported proteins (PTEX) is a protein complex locating at PVM, which consists of five proteins. Among them, a heat shock protein 101 (Hsp101) is a ClpB-like AAA+ ATPase component of PTEX, providing the power to unfold the protein going through the channel formed on the PVM by export protein 2 (EXP2), a PVM protein. Another partner, PTEX 150, seems to directly associate with EXP2 and a small thioredoxin-like protein (TRX2) that assist protein oxidation and reduction, as well as an unknown protein PTEX88 (Figure 1.3) (de Koning-Ward *et al.*, 2009; Elsworth *et al.*, 2014). This PTEX translocon can help exported protein cross the membrane for entering the infected erythrocytes (de Koning-Ward *et al.*, 2009). It has been found that Hsp101 was more likely binding with exported protein than others, which indicated that Hsp101 played a role in associating with exported proteins and serving as protein cargos for the secretion (Bullen *et al.*, 2012). To verify the function of PTEX translocon, several knockdown cell lines were generated. In the PTEX150 knockdown parasite cells, the expression level of *P. falciparum*-infected erythrocyte membrane protein-1 (*Pf*EMP-1) on the surface was found to be lower. By knocking down Hsp101, PEXEL contain proteins REX3 and KAHRP transport were found be blocked in the infected red blood cell while the PNEP protein export has also been blocked like REX1 (Ring-exported protein 1) (Beck *et al.*, 2014; Elsworth *et al.*, 2014; Molloy, 2014). However, the mechanism and function of PTEX translocon remains poorly understood For instance, how the PTEX translocon recognizes and selectively allows some of the proteins passing through; while the other proteins remain in parasitophorous vacuole? Also, since exported proteins have to keep unfolded for going through the translocon and refold after crossing PVM, it is still not clear whether Hsp101 or other chaperones assist it (Gehde *et al.*, 2009; Gruring *et al.*, 2012).

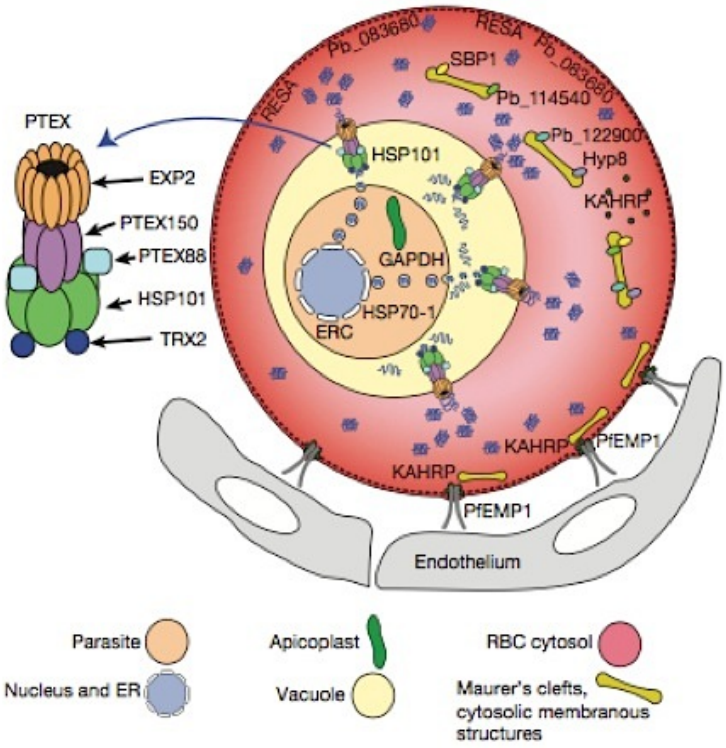

Figure 1.3: location and composition of PTEX translocon in the infected erythrocyte.

PTEX translocon localizes at PVM and consists of five subunits: EXP2, Hsp101, PTEX150, PTEX88, TRX2, and EXP2. EXP2 forms the pore in the PVM; while Hsp101 unfolds the protein before translocation. PTEX150 forms the structure of PTEX. TRX2 assists protein oxidation and reduction and helps to regulate PTEX. The function of PTEX88 remains unknown (Elsworth *et al.*, 2014).

1.4 Important heat shock proteins in *P. falciparum*

Heat shock proteins are a family of proteins produced to response to the environmental stress (Ritossa, 1962; Matz *et al.*, 1995; Cao *et al.*, 1999). Many of these heat shock proteins act as chaperones and are essential for many cellular processes including protein folding, unfolding, protein trafficking as well as repair of proteins upon damage under stress condition like UV radiation, cold, or oxidative stress (De Maio, 1999). Normally, heat shock proteins (Hsp) are named according to molecular weight, such as Hsp60, Hsp70, Hsp90, and Hsp110. Some of heat shock proteins function as chaperones or co-chaperones such as Hsp40 and Hsp70. These two Hsps assist protein folding and prevent proteins from abnormal aggregation (Walter and Buchner,

2002; Li and Srivastava, 2004; Kampinga and Craig, 2010). Recent studies suggest that *Plasmodium* encode export Hsp40s and Hsp70s that are involved in many cellular processes during the infection, including cell cycle regulation and signal transduction (Botha *et al.*, 2007; Shonhai *et al.*, 2007).

1.4.1 *P. falciparum* encodes Hsp40

P. falciparum genome encodes Hsp40 that can be divided into four classes. Type I Hsp40 contains J-domain that is crucial for interacting with Hsp70, Gly/Phe-rich region (GF domain), and a Zinc finger but without any export element. It has a chaperone function in the parasite (Mayer *et al.*, 1999; Rug and Maier, 2011). Type II Hsp40 has the J domain and Zinc domain but lack the cysteine-rich domain (Botha *et al.*, 2007), there are eight Hsp40 belonging to type II, with three of them having an export motif (PFA0660w, PFB0090c, and PFE0055c) (Bhattacharjee *et al.*, 2008). Most of the Hsp40s belong to type III, which has only a J domain. Some of them have a predicted export element; while the others lack a PEXEL sequence (Young *et al.*, 2004). Type IV has a J domain as well as a HPD tripeptide; this type of Hsp40 is parasite specific with no homolog in human; and its function is hypothesized to be function differently from other types, there are ten out of the total twenty molecular Hsp40 with a export element (Cheetham and Caplan, 1998; Botha *et al.*, 2007). Recently studies reveal that PFE0055c (referred to as PFE55) as well as PFA0660W (referred to as PFEA660) localize at the parasite-infected erythrocyte as a highly mobile dot structure that is referred as J-dots; moreover, these two proteins co-localize with parasite-encoded *Pf*Hsp70x, but not with any known Maurer's clefts markers. So far, the function and composition of J-dots are not yet clear (Kulzer *et al.*, 2010; Kulzer *et al.*, 2012). There is a hypothesis that type II Hsp40 proteins possibly interact with the human-encoded Hsp70 since they are homologous with the human DnaJB4 gene; however, no direct evidence has been found. Some non-exported type II Hsp40s also have been found to interact with cytosolic parasite-encoded Hsp70s, such as Pfj4 interacting with Hsp70-1 (Pesce *et al.*, 2008; Rug and Maier, 2011).

1.4.2 *P. falciparum* heat shock proteins 70 (*Pf*Hsp70s)

P. falciparum heat shock proteins 70 (*Pf*Hsp70s) are important chaperones critical for protein folding, refolding, degradation, and especially for transporting exported proteins into the infected red blood cell (Shonhai *et al.*, 2007; Njunge *et al.*, 2013). There are six Hsp70 proteins identified in the *P. falciparum* life: Hsp70-1, Hsp70-2, Hsp70-3 and Hsp70x, y, z (Njunge *et al.*, 2013). *Pf*Hsp70-1 is a cytosolic protein locating at cytosol or nucleus and plays a role as the co-chaperone with the parasite-encoded Hsp90 for the stress response (Gitau *et al.*, 2012). *Pf*Hsp70-2 is *Pf*Hsp70-1's endoplasmic reticulum homolog. *Pf*Hsp70-1, *Pf*Hsp70-2 and *Pf*Hsp90 form as various isoforms by different post-translational modification (Foth *et al.*, 2011). *Pf*Hsp70-y and *Pf*Hsp70-z belong to Grp110.Grp170 (Hsp110) group, *Pf*Hsp70-y localizes at ER and is possibly responsible for the protein quality control (Shonhai *et al.*, 2007). *Pf*Hsp70-z acts as nucleotide exchange factors (NEF) to facilitate the nucleotide exchange function of *Pf*Hsp70-1 (Shonhai *et al.*, 2007). *Pf*Hsp70x is only identified in two Laverania subgenus malaria parasite, *P. falciparum* and chimpanzee parasite *Plasmodium reichenowi* (Kulzer *et al.*, 2012). *Pf*Hsp70x contains an ER signal peptide with a C-terminal region, and is found to locate at the PV as well as cytosol erythrocyte. *Pf*Hsp70x is highly expressed in the early ring stage; and its protein level reaches the peak during the schizonts stage. *Pf*Hsp70x lack the PEXEL/HT motif; while the peptide from 25 to 32 amino acids seems be responsible for its export (Hiller *et al.*, 2004; Grover *et al.*, 2013; Przyborski *et al.*, 2015). Recently, it has been found that *Pf*Hsp70x co-localizes with parasite Hsp40 that as known as J-dots (Kulzer *et al.*, 2010; Kulzer *et al.*, 2012).

1.4.3 A novel structure in parasite infected erythrocyte

There is a novel uncharacterized highly mobile structure that is identified in cytosol of *P. falciparum*-infected red blood cell recently (Kulzer *et al.*, 2010). This structure contain two exported type II Hsp40s (PFE0055c, PFA660w) which showed by immunofluorescence and not marked by Maurer's marker and already visible in the ring stage, as refers as J-dots since the Hsp40 have a J domain (Kulzer *et al.*, 2010). Investigations have revealed that the outer side of the J-dots is derived from parasite Hsp40 (Kulzer *et al.*, 2010). In addition, co-immunoprecipitation and immunofluorescence assays show that parasite-derived Hsp70x directly interacts and

partially co-localizes with PEF0055c as well as PFA660w (Kulzer et al., 2012) (Figure 1.4). This chaperone/co-chaperone structure (PFA0660w/PFE0055c-PfHsp70x) may be involved in the intracellular or intercellular protein trafficking and responsible for the protein folding, unfolding and trafficking within the infected red blood cell cytosol (Kulzer *et al.*, 2012; Grover *et al.*, 2013). Formation of 30nm pores in the membrane of infected erythrocytes by Streptolysin O permeabilization failed to isolate the J-dots indicating that the J-dots are greater than 30nm (Kulzer *et al.*, 2012). Immunofluorescence assay also revealed that *Pf*EMP1 and J-dots partially co-localized during the early stage, which indicated that J-dots were possibly involved in *Pf*EMP1 transport through the infected erythrocytes (Kulzer *et al.*, 2012). A merger with the cell membrane of the host cell could also not be observed, which seems the J-dots not to be anchored in the infected erythrocytes. The exact composition and function of J-dots remain unclear.

As known that the parasite-encoded exported proteins are involved in the host cell modification process (Maier *et al.*, 2008). In particular, a set of proteins that are transported to the surface of red blood cells hold responsibility for the cytoadhesion and immune evasion of host cells (Maier *et al.*, 2008). To ensure the proper protein transport to the erythrocyte cytosol or the red blood cell membrane, parasite-secreted proteins have to cross the parasite membrane by un-folding and refolding after passing the membrane (Gehde *et al.*, 2009). Furthermore, exported heat shock proteins are implicated to work as chaperones that mediate the protein translocation, folding and unfolding (Przyborski *et al.*, 2015).

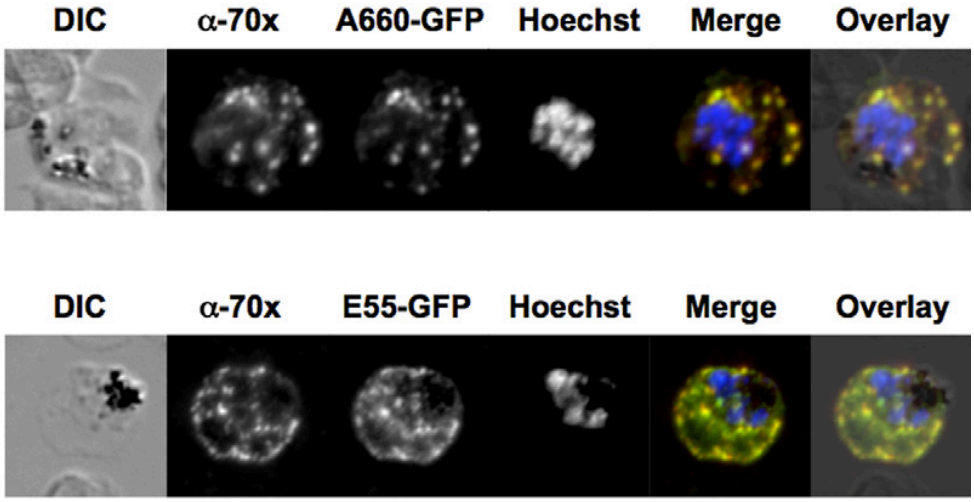

Figure 1.4: A novel structure was found in the parasite infected erythrocyte cytosol contained PFA660w/PFE055c-*Pf*Hsp70x referred as J-dots.

Co-localization of *Pf*Hsp70x and exported Hsp40s (PFE55/PFA660w), Fluorescence channels are shown individually in black and white, co-localization was indicated in merge and overlay. The analysis was performed using monoclonal anti-GFP (green) and polyclonal anti-*Pf*Hsp70x (red) (Kulzer *et al.*, 2012).

1.5 Protein-protein interactions studies

Proteomics is a large-scale study on functions and structures of proteins (Wilkins, 2009). It focuses on the dynamics of gene regulation, quantities of the protein expression, the identification of the impact on disease and drug (Heath *et al.*, 2015). All of subjects study base on protein structure and function study to illuminate the changes of the life mechanisms under pathological condition (Tyers and Mann, 2003).

Many aspects have to be taken into account for understanding the protein structure and function, which includes the post-translational modification (PTM), protein-protein interactions (PPIs) and protein conformation. PTM can be achieved by protein phosphorylation, acetylation, methylation, ubiquitination or glycosylation (Krishna and Wold, 1993; Phizicky and Fields, 1995; Jensen, 2004). PPIs are essential for many biological processes including cell-cell communication, cell metabolism and transcriptional regulation (Braun and Gingras, 2012). Moreover, PPIs also play a role in forming protein complex to receive exogenous and endogenous signals and transmit them (Berggard *et al.*, 2007; Yamada and Bork, 2009; Petta *et al.*, 2015). Therefore,

investigating the protein interaction network has become a hotspot of proteomics research. So far, there are several methods developed for studying PPIs such as yeast two-hybrid system (Fields and Song, 1989), phage body display technology (Smith and Petrenko, 1997), GST pull-down assays (Smith and Johnson, 1988), co-immunoprecipitation (co-IP) (Operana and Tukey, 2007) and tandem affinity purification (TAP) (Rigaut *et al.*, 1999). Yeast two –hybrid system has a high sensitivity for analyzing the biologically active and instant protein-protein interaction. GST pull-down assays are able to identify stable protein complexes *in vivo*. This approach takes advantage of the strong affinity of glutathione-transferase tags for GSH beads, which leads to the isolation of GST fusion proteins and the closely associated molecules in the sample (Smith and Johnson, 1988). TAP is also a method to study PPIs by purifying target proteins with a fusion protein, TAP tag was first use to characterize protein complexes in 1999 (Rigaut *et al.*, 1999).

1.5.1 Co -immunoprecipitation (co-IP) analysis protein-protein interaction

Co-immunoprecipitation is a classic and sufficiency technique to study protein interaction *in vivo*. In order to capture proteins that interact with the target protein, the target protein in the sample is isolated using its specific antibody, followed by the identification of immunoprecipitation protein complexes using the two-dimensional electrophoresis (2-DE), SDS-PAGE, western blot and Mass spectrometry (Phizicky and Fields, 1995; Lee, 2007). This assay can reveal the protein interaction *in vivo* under native condition and has been widely used in various biological systems (Golemis and Brent, 1992; Dobson *et al.*, 2001; Monti *et al.*, 2005). However, some weak or transient interactions may be difficult to detect without maintaining a more stable physiological interaction using strong wash buffers- However, less washing often leads to more non-specific bindings and higher false positive alerts. The critical factor of a successful co-IP experiment is to maintain the complex with suitable lysis and wash buffers (Monti *et al.*, 2005).

In order to compensate this disadvantage of co-IP, cross-linking can be combined to use. This step is meaning to covalently crosslinked two or more molecules within a close contact, which further strengthen the binding. The crosslinking is often achieved using chemical reagents with reactive groups, such as amine, sulfhydryl- and photo-

reactive chemicals (Suchanek *et al.*, 2005; Qin *et al.*, 2011). Recently, there are many commercially cross linkers generated, including N-hydroxysuccinmide (NHS)-ester cross linker BS3, DSP; dimethyl subberimidate and formaldehyde (Uckert *et al.*, 1983; Mattson *et al.*, 1993; Gavazzi *et al.*, 2007). It becomes critical to choose the appropriate crosslinkers First of all, due to the range of distance, an important factor to choose crosslinkers is the spacer arm length (Zhang *et al.*, 2009). In addition, some crosslinkers are available to target the cell surface while the others can go through the membrane; therefore, the surface or intracellular proteins require different crosslinkers (Schweizer *et al.*, 1982; Knoller *et al.*, 1991). Moreover, cleavable and un-cleavable crosslinkers should be chosen differently depending on the variety of following analysis techniques (Knoller *et al.*, 1991; Yang *et al.*, 2012). With crosslinking, the transient and loose protein-protein interactions can be stabilized, captured and analyzed.

1.5.2 Blue native polyacrylamide gel electrophoresis (BN-PAGE)

Blue native polyacrylamide gel electrophoresis (BN-PAGE) is another efficient method with high resolution to isolate multiple protein complexes (Sali *et al.*, 2003). Unlike normal SDS-PAGE gel, BN-PAGE does not use any denaturing reagent. One can separate the protein complexes from various samples such as cell lysates (Vahsen *et al.*, 2004), tissue homogenates as well as membranes (Schagger, 2001; Pfeiffer *et al.*, 2003) with the complex size ranged from 10 KDa to 10 MDa (Schagger *et al.*, 1994). It is widely used for many purposes including native protein purification, 2D crystallization, and analysis of physiological protein-protein interactions (Poetsch *et al.*, 2000; Schagger and Pfeiffer, 2000). In principle, proteins are separated according to their hydrodynamic size and appear as blue bands in the BN gel. Interesting bands are excised and subjected for either proteomic experiments or a second SDS PAGE (Wittig *et al.*, 2006). In addition, the percentage of gels used has to be taken into account according to the expected protein complex size. Gradient gel or many commercially gel systems with suitable buffers are also available now (Fiala *et al.*, 2011). BN-PAGE has been widely used for many studies, such as the isolation of mitochondrial ATP synthase complex with size of ~600kDa from *Arabidopsis* by 3D BN/IEF/SDS-PAGE (Wittig *et al.*, 2006). Seven merozoite surface proteins complex were also identified by separating detergent-resistant membrane proteins using BN-PAGE (Sanders *et al.*,

2007). Often several approaches are applied for interaction studies. For instance, by using two-dimensional blue native/SDS-PAGE, two protein complexes were characterized in HepG2.2.15 cells; then by using mass spectrometry, 20% of these proteins were identified to be heat shock proteins, including Hsp60, Hsp70 and Hsp90. Furthermore, it was verified with co- immunoprecipitation assays that Hsp60, Hsp70, Hsp90 interacted with each other (Liu *et al.*, 2009).

1.6 *P. falciparum* proteomics

Despite that the genome study of the *P. falciparum* has been completed (Gardner *et al.*, 2002), a large- scale comprehensive study of its proteome is still required for understanding the mechanism of parasite development and survival in the host cell. Therefore, the large-scale quantification of protein levels during different stages of development can provide more insights toward understanding the extraordinarily complicated plasmodium and erythrocyte reorganization mechanism immune response of host cell (Florens *et al.*, 2002). The dynamics of proteomic profiles during different stages of *P. falciparum* development provide further information for the interaction between parasites and human host cells. In addition, the improvement of *Plasmodium* proteomics study could clarify the signal pathway of the host cell under physiological and disease condition as well as search for potential biomarkers to establish new therapies strategies (Florens *et al.*, 2002; Lasonder *et al.*, 2002).

So far, 2,415 parasites proteins were identified in the strain 3D7 by LC-MS/MS; as expected, only 6% of total proteins were found in all four stages (sporozoites, merozoites, trophozoites and gametocytes) such as transcription factors, ribosomal proteins, and cytoskeletal proteins (Lasonder *et al.*, 2002). Sporozoite stage has the most abundant stage-specific proteins (nearly 50%). By analyzing the sequence of these proteins, 439 of them were identified with one or more transmembrane domains; while 309 proteins contain a signal sequence (Lasonder *et al.*, 2002). Surface proteins have been found be widely expressed in different stages, indicating that these surface proteins may be involved in the parasite–host interactions during immune evasion (Lasonder *et al.*, 2002). Through two-dimensional gel electrophoresis with LC-MS/MS, 27 novel antigens were found to be extracellular secreted into the medium at asexual blood stages of *P. falciparum*. And half of the proteins were suggested to be involved in encoding parasite putative antigenic determinants (Singh *et al.*, 2009). During invasion,

P. falciparum recognizes various erythrocyte surface receptors in order to switch on the invasion pathway. The quantitative proteomics suggested that merozoite protein levels have a significant change during invasion (Kuss *et al.*, 2012). After the merozoites invade into new erythrocytes to start a new parasite life cycle, they develop, divide and modify the host cell by exporting proteins, which cross the parasite plasma membrane (PPM) and the parasitophorous vacuole membrane (PVM), then were secreted into the erythrocyte cytosol. Some of these proteins cross the erythrocyte membrane and locate at the surface to change the physiology of erythrocytes (Marti *et al.*, 2004). Furthermore, by comparing the composition of membrane proteins of infected and non-infected erythrocyte using two-dimension electrophoresis (2D-DIGE), over 100 proteins were identified over represented. Most of them were human proteins in the infected sample. Surprisingly, many of these proteins are not membrane proteins and present in the erythrocyte cytosol under normal conditions, such as heat shock protein 70 that was identified in the infect red blood cell membrane as well as another chaperone TCP1 (Fontaine *et al.*, 2012). The proteome expression study under life and physiological conditions allows us to identify proteins related to intracellular and intercellular signaling pathways, which may be the potential targets for establishing new diagnosis and therapy strategy.

1.6.1 Protein-protein interactions studies in *P. falciparum*

In general, proteins often require interaction with others to function. Although some progress has been made using the proteomics study for *P. falciparum*, the knowledge of protein-protein interactions remains insufficient. The first *P. falciparum* protein-protein interactions (PPIs) study was made in 2005, where 2,846 potential protein-protein interactions were identified in *P. falciparum* via yeast two-hybrid assays (LaCount *et al.*, 2005). This was the first time where a large-scale investigation of protein-protein interactions has been performed to understand the interaction network in *P. falciparum*. Investigators have also tried to study the PPIs under the physiological condition for fundamental biological processes. How proteins contact with each other to function properly during *Plasmodium* invasion, parasite development and the modification of the host cell is always a research hotpot. BN-Page has become a powerful technique for purifying potential protein complexes. While studying the merozoite surface proteins complexes, the detergent-resistant membrane proteins

were separated using BN-PAGE and identified by HPLC-MS/MS. There are seven known protein complexes, including MSP-1/7, RAP1/2 and RAP1/3, high molecular weight rhoptry complexes (RhopH1/H2/H3), and the invasion motor complex (GAP45/GAP50/myosin A) were found among 62 identification proteins (Sanders et al., 2007). Other than BN-PAGE, co-immunoprecipitation (co-IP) has also been widely used. For instance, a novel translocon protein complex PTEX (PTEX150, Hsp101, PTEX88, EXP2, TRX2) on PVM was found using Co-IP followed by mass spectrometry (de Koning-Ward *et al.*, 2009; Elsworth *et al.*, 2014). Similarly, co-IP is also used for studying co-chaperones. For example, the interaction of two important chaperones (*Pf*HSP70 and *Pf*HSP90) that play a role in assisting protein folding was identified by co-IP as well (Gitau *et al.*, 2012). Moreover, this approach also works for the purification of large molecular-weight protein complexes. One of these complexes contains *P. falciparum* WD40 -repeat protein *Pf*WLP1 that is expressed both in schizonts and gametocyte stages which was found to associate with cell adhesion protein *Pf*AMA1 in schizonts stage and interact with *Pf*CCp1 and *Pf*s230 in gametocytes (von Bohl *et al.*, 2015).

1.7 Mass spectrometry base proteomic analysis

1.7.1 Mass spectrometry

Mass Spectrometry analysis is a method to identify molecules based on the mass to charge ratio. In general, mass spectrometry use an ion source to convert molecules into gas-phase ions; then a mass analyser separates ionized analytes base on the m/z ratio, in parallel with a detector to record the number of ions for each m/z value. As two types of soft ionization technologies, MALDI-MS (matrix-assisted laser desorption/ionization-M) and ESI-MS (electrospray ionization), have been developed, it is possible to analyze high polar, thermally unstable and involatile samples, especially peptides or proteins (Karas and Hillenkamp, 1988; Fenn *et al.*, 1989). MALDI-MS uses ions samples from dry crystalline matrix by pulsing with laser and is normally used for analyzing less complicated peptide mixtures, such as two-dimensional gel protein spots or purified proteins that are digested into peptides (Aebersold and Mann, 2003). ESI-MS can analyze molecules without fragmentation, and can be always combined with a

high performance liquid chromatography (HPLC), which pre-chromatographic separated samples (Fenn et al., 1989). Therefore, ESI-MS can be used to analyze complicated mixtures, such as total protein mixtures, mixed gel bands from SDS-PAGE. A remarkable feature of ESI-MS is that it is suitable to work as a tandem mass spectrometry; this is because ESI-MS can produce multiple charged peaks that make charged ions break more easily, and induce ion collision by selection, in order to get the target peptide sequence (Ho et al., 2003)

The mass analyzer is a core element of mass spectrometry, which determines the sensitivity, resolution, and accuracy of MS. The popular mass analyzers include ion traps (Chi *et al.*, 2007), time-of-flight (TOF) (Loo *et al.*, 2001), quadrupoles (Salamonsen *et al.*, 1986) and Fourier transform-based instruments (FTICR) (Zabrouskov and Whitelegge, 2007). Recently, there is a new tandem mass spectrometry developed, named LTQ-Orbitrap (Thermo Fisher Scientific) (Hu *et al.*, 2005). It contains a LTQ with a C-trap as well as the Orbitrap. This tandem MS take the advantage of the high sensitive, robustness, MS/MS capability of LTQ as well as the high resolution and high mass accuracy of the Orbitrap, becoming one of the top choices to use (Macek *et al.*, 2006; Han *et al.*, 2008).

1.7.2 Mass spectrometry based proteomics analysis

Along with mass spectrometry development, this becomes a powerful proteomic instrument for protein purifications as well as studying protein-protein interactions and protein post-translational modification. In addition, high sensitivity and resolution of mass spectrometry make the identification of low abundant proteins possible. Therefore, mass spectrometry provides the foundation for a systematic study of the function and dynamics of proteins in a large scale. In general, the isolation protein from cell and tissue by affinity purification and biochemistry extraction is normally either separated in one dimension gel or dissolve in the buffer, subsequently, the protein can be enzymatically fragmented into peptides from gel or directly in solution. The enzyme is used for digestion normally by trypsin, which cleaves the lysine and arginine residues at the carboxyl side. Normally, the mixture peptides are separated by high-pressure liquid chromatography (HPLC) especially by using reverse-phase HPLC before injection in the mass spectrometry. Peptides are separated and eluted to the electrospray ion source by the hydrophobic interaction intensity between the peptide

and hydrocarbonaceours materials, the stronger interaction, the longer of peptides retention time in the column (Meek, 1980). Followed, protonated peptide enters to the mass spectrometry, and the mass to charge ration (precursor ions) of the peptide eluting is taken immediately at the first mass spectrometry (MS1). At the second mass spectrometry, the precursor ions are fragmented by the collision-induced dissociation (CID) in to product ions and MS/MS spectra are taken and searched against the protein sequence database (Han *et al.*, 2008) (Figure 1.5)

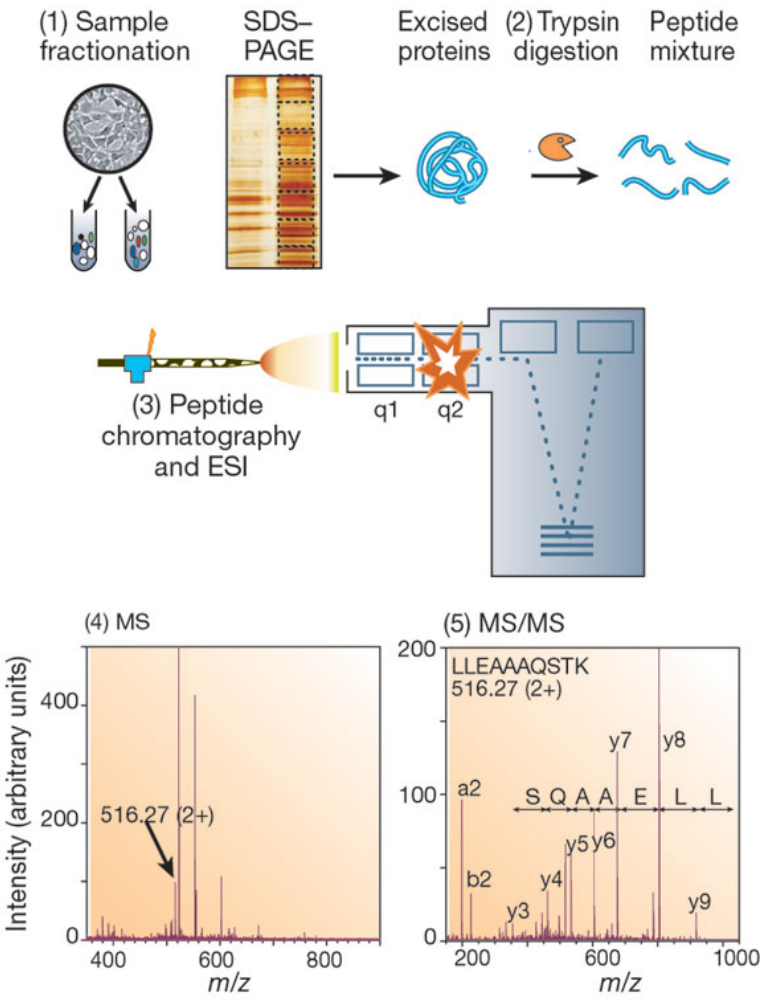

Figure 1.5: proteomics analysis basic strategy. (Aebersold and Mann, 2003)

1.8 Objective

Over 400 parasite-encoded proteins are predicted to be exported to the infected red cell cytosol by *Plasmodium falciparum* and involved in modify the host cell including cytoadhesive and permeability for their own survival. During the transport, parasite exported protein need to cross the plasma membrane of the parasite (PPM) and the parasitophorous vacuole membrane (PVM) to the infected erythrocyte cytosol sites, and further deliver to the surface of red blood cell membrane to alter the morphology, physiology and function of red blood cell membrane. Exported parasite proteins are also involved in inducing new membrane structure in parasite infected erythrocyte cytosol such as Maurer's clefts and tubulovesicular network (Maier *et al.*, 2009).

Recently, Our group found a novel highly mobile structure in the infected erythrocyte cytosol referred to as J-dots, which were contained members of exported co-chaperones Hsp40s (PFE55, PFA660) (Kulzer *et al.*, 2010). Subsequently, we could also identify a parasite-encoded exported Hsp70 (*Pf*Hsp70x) in complex with PFE55 at the J-dots (Kulzer *et al.*, 2012). The aim of our work is to further understand the importance of this structure for parasite protein trafficking and parasite survival in the red blood cell. Therefore multiple proteomics methods will be used to purify and characterize of the entire proteome of the J-dots, and further address out the potential functional of J-dots by study protein-protein interaction between PFE55/*Pf*Hsp70x and other protein candidates.

2 MATERIALS AND METHOD

2.1 Materials and Chemicals

2.1.1 Appliances

Appliances	Company	Company headquarters
Autoclave	Thermo Scientific	USA
Blotting apparatus	Phase	Lübeck
Centrifuge (5804R)	Eppendorf	Hamburg
Electroporator (gene PulserII)	Bio-Rad	USA
Glass slides	IDL	Italy
LTQ-Orbitrap Elite Mass spectrometry	Thermo Fisher	USA
Nano-LC UltiMate 3000	Thermo Fisher	USA
pH meter	Bio-Rad	München
Thermoblock	Heidolph	Schwabach
Thermomixer 5436	Eppendorf	Hamburg
Vortexer (Reax 2000)	Heidolph	Schwabach
Weighing machine (1205)	Sartorius	Germany
Weighing machine (P1200)	Mettler Toledo	

2.1.2 Materials

Appliances	Company	Company headquarters
Centrifuge tubes	Eppendorf	Hamburg
Culture flasks (25 cm2 and 75 cm2)	Greiner	Frickenhausen
Falcon tubes	Greiner	Frickenhausen
Pipette tips	Sarstedt/Greiner	Nümbrecht/Frickenhausen
Plastic material	Sarstedt//Greiner	Nümbrecht/Frickenhausen
Whatman paper	Schleicher & Schuell	Dassel
Gel loader tips	VWR	Darmstadt

2.1.3 Chemicals

Chemicals	Company	Company headquarters
0.1% Trifluoroacetic	Fluka	Neu-Ulm
1,4-dithio-DL-threitol (DTT)	Fluka	Neu-Ulm
10% Dodecylmaltoside (DDM)	Thermo Fisher	USA
Acetonitrile (HPLC grade)	Fluka	Neu-Ulm
Ammonium peroxodisulfate (APS)	Roth	Karlsruhe
Ammonium sulfate ($(NH_4)_2SO_4$)	Roth	Karlsruhe
Comassie Brilliant Blue	AppliChem	Darmstadt
Dimethylsulfoxide (DMSO)	Fluka	Neu-Ulm
Dipotassium phosphate (K_2HPO_4)	Roth	Karlsruhe
Disodium phosphate (Na_2HPO_4)	Roth	Karlsruhe
DSP (dithiobis(succinimidyl	Thermo Fisher	USA

propionate))		
Glycerol anhydrous	AppliChem	Darmstadt
Glycine	Roth	Karlsruhe
Iodoacetamide (IAA)	Sigma	USA
Isopropanol	Merck	Darmstadt
Luminol	AppliChem	Darmstadt
Method	Roth	Karlsruhe
N,N,N',N'-tetramethylethane-1,2-diamine	Roth	Karlsruhe
Phenylmethylsulfonyl fluoride (PMSF)	Serva	Heidelberg
Potassium dihydrogen phosphate (KH_2PO_4)	Roth	Karlsruhe
Protease Inhibitor Cocktail Set III	Calbiochem	USA
Proteinase K	AppliChem	Darmstadt
Protein Prestained Ladder	Thermo Fisher	USA
Rotiphorese Gel 30	Roth	Karlsruhe
Sodium dodecyl-phosphate (SDS)	AppliChem	Darmstadt
Streptolysin O	S.Bhakdi	
Tris	AppliChem	Darmstadt
Triton X-100	Roth	Karlsruhe
Trypsin	Promega	USA

2.1.4 Cell Culture Materials

Cell culture materials	Company	Company headquarters
AlbuMaxII	Invitrogen	Groningen
D-Sorbitol	Roth	Karlsruhe
Gelafundin	B. Braun AG	Melsungen
Giemsa	Merck	Darmstadt
Human erythrocyte concentrate (A/rh+)	University medical centre Marburg, Bloodbank	Marburg
Human Plasma (A/rh+)	University medical centre Marburg/Giessen, Bloodbank	Marburg
Hypoxanthine	PAA	Cölbe
RPMI 1640	Gibco	Karlsruhe
WR 99210	Jacobus Pharmaceuticals	USA

2.1.5 Molecular Biology Kit

Molecular Kits	Company	Company headquarters
Pierce Co-Immunoprecipitation Kit	Thermo Fisher Scientific	USA

2.1.6 Antibody

Primary Antibody	Dilution Factor (IFA)	Dilution Factor (Western blotting)	Original
Mouse anti-GFP (monoclonal)	1:100	1:500	Abcam
Mouse anti-Glycophrin A/B (monoclonal)	---	1:1000	Abcam
Mouse anti-human Hsp70 (monoclonal)	---	1:500	Santa Cruz Biotechnology
Mouse anti-*Pf*GBP130 (monoclonal)	1:1000	1: 1500	Group Holder
Mouse anti-*Pf*Hsp101(monoclonal)	1:1500	1:1000	Group Holder
Rabbit anti-*Pf*SBP1 (monoclonal)	1:1000	1:500	Group Przyborski
Rabbit anti-*Pf*Aldolase (polyclonal)	---	1:5000	Group Przyborski
Rabbit anti-*Pf*Exp1 (monoclonal)	---	1:500	Group Przyborski
Rabbit anti-*Pf*GBP130 (monoclonal)	---	1:500	Group Przyborski
Rabbit anti-*Pf*Hsp70x (polyclonal)	1:100	1:500	Group Przyborski
Rabbit anti-*Pf*PhistC(monoclonal)	1:1500	1:1500	Group Holder
Rabbit anti-*Pf*SBP (monoclonal)	1:1000	1:500	Group Przyborski
Rabbit anti-*Pf*SERP (polyclonal)	---	1:1000	Group Przyborski

Secondary antibody	Dilution	Company	Company Headquarter
Goat anti-mouse HRP	1:2000	DAKO	Glostrup
Goat anti-rabbit HRP	1:2000	DAKO	Glostrup
Goat anti-chicken Cy2	1:2000	JacksonImmuno Research Laboratories	USA
Goat anti-mouse Cy3	1:2000	JacksonImmuno Research Laboratories	USA
Goat anti-rabbit Cy3	1:2000	JacksonImmuno Research Laboratories	USA

2.1.7 Solutions and buffers

Solutions and buffers used for molecular and biochemical work are listed.

Solutions and buffers	Individual components
Sample buffer (2x) for proteins	100 mM Tris/HCl pH 6.8 5 mM EDTA 20 % glycerol 4 % SDS 0.2 % bromphenolblue 100 mM dithiothreitol
Separating buffer (4x)	1.5 M Tris/HCl pH 8.8
Stacking buffer (4x)	500 mM Tris/HCl pH 6.8 0.4 % SDS
Sample buffer (2x) for proteins	100 mM Tris/HCl pH 6.8 5 mM EDTA 20 % glycerol 4 % SDS 0.2 % bromphenolblue 100 mM dithiothreitol
Western blot transfer buffer	48 mM Tris/HCl pH 9.5

	39 mM glycine 0.04 % SDS 20 % methanol
Phosphate buffered saline (PBS)	140 mM sodium chloride (NaCl) 2.7 mM potassium chloride (KCl) 1.4 mM monopotassium phosphate 0.8 mM disodium phosphate
Electrophoresis running buffer	124 mM Tris 960 mM glycine 0.05 % SDS
Blocking solution for IFA	3 % BSA in PBS (pH 7.4)
BN sample buffer	20mM bis-tris 500mM 6-aminocaproic acid 20mM NaCl 2mM PH 8.0 EDTA 10% Glycerol PH 7.0 0.01% coomassie Brilliant G-250
3x BN-Gel Buffer	Bis-tris 150mM ε-aminocaproic acid 200mM

Solutions used for culturing *P. falciparum* are listed as following:

Solutions	**Individual components**
RPMI medium	500 ml RPMI medium supplemented with 50 ml of heat-activated human plasma 50 mg neomycin 200 µM hypoxanthine
Freezing solution	28 % glycerol 3 % d-sorbitol 0.65 % sodium chloride
Thawing solution	12 % sodium choride (NaCl) 1.6 % sodium chloride (NaCl)

	0.9 % sodium chloride, 0.2 % glucose
WR99210	20 mM stock (8.6 mg in 1ml DMSO) working concentration: 5 nM

2.1.8 Cells strains

Strain	Reference
P. falciparum strain 3D7	The Walter and Eliza Institute of Medical Research, Melbourne, Australia
P. falciparum PFE55^{GFP}	Simone Külzer, et al., 2010
P. falciparum PFA660^{GFP}	Simone Külzer, et al., 2010

2.2 Methods

2.2.1 Cultivation of *P. falciparum*

The asexual stages of *P. falciparum* were cultivated in RPMI medium containing 4% hematocrit A^+ human erythrocytes, 0.2 % hypoxanthine, 10 % human plasma and 0.1mg/ml neomycin in the suspension culture flasks. The parasites were incubated at 37 °C and supplied with gas containing 90 % N_2, 5 % O_2 and 5 % CO_2. Every 24h the medium was changed with a glass pipette without disturb the cells. The parasitemia was checked with Giemsa stain solution: ~5ul of blood drops were taken from the bottom of the flask onto a glass slide; after the smear was dry, we fixed the slide in Methanol for 30s and stained it with Giemsa solution (1:10 diluted with H_2O) for 5-10 min. Next, we washed off the excess staining solution and examined the slide with light microscope at a hundred-fold magnification.

2.2.2 Parasites synchronization

The whole cycle of *P. falciparum* mainly consists of four stages: ring, trophozoite, schizont and merozoite stages. In this study, most of the work was performed on parasites during the thophozoite stage. In order to get more synchrony parasites and

high parasitemia, parasites during ring stage were synchronized using 5% of sorbitol solution (Lambros and Vanderberg, 1979) ; while at trophozoites stage, parasites were enriched by gelafundin flotation (Pasvol *et al.*, 1978).

Synchronization of *P. falciparum* with sorbitol:

Cultures were transferred into a falcon tube and centrifuged at 3000 rpm for 2 min; the pellet was then resuspended in 5 times volume of pre-warm sorbitol solution (5%). After incubating the mixture in water bath for 10-12 min at 37 °C, we centrifuged the mixture at 3000 rpm for 2 min, followed by washing the pellet twice with 10 times volume of medium. In order to get more synchronized parasites, the parasites can be treated with sorbitol again after 4 hours.

Trophozoite-stage parasites enrichment via gelafundin flotation:

Cells were collected by centrifugation at 3000 rpm for 2 min and resuspended with 10 ml of pre-warmed gelafundin flotation buffer. The mixture was then incubated in water bath for 12 min at 37 °C. During the incubation, knob-associated cells floated into the upper phase of the gelafundin cell mixture; while most of non-infected and ring-stage parasites were found at the bottom. The upper phase was collected and centrifuged at 3000 rpm for 2 min to obtain trophozoite-infected cells. Cells were suspended in 10 times volume of medium for further use.

2.2.3 Freezing and thawing of *P. falciparum*

Freezing *P. falciparum*:

Ring-stage parasites were transferred with 5%-10% parasitemia culture into a falcon tube, centrifuged at 3000 rpm for 2min; the resulting pellet was resuspended with freezing solution. The resuspension was then transferred into the freezing tube and kept in the liquid nitrogen for long-term preservation.

Thawing *P. falciparum*:

First of all, we pre-warmed all the solutions. Frozen cells stored in the liquid nitrogen were then thawn for several minutes in the flow at room temperature. Cells were then transferred from the freezing tube to a falcon tube; 200-250 ul of 12% NaCl solution was then added drop by drop into cells and gently mixed. After incubation for 3 min, 5 ml of 1.6% NaCl solution was added into the mixture slowly and incubated for another

3 min. Finally, 5 ml of 0.9% NaCl solution was also added followed with 3-min incubation time. Cells were collected by centrifugation at 3000 rpm for 2 min and washed with 10 ml of RPMI medium before further use.

2.2.4 SLO (Streptolysine O) permeabilization of *P. falciparum*-infected erythrocytes

SLO (streptolysine O) is a membrane damage toxin secreted by *Streptococcus pyogenes*. SLO can permeabilize the host red blood cell membrane while leave the PV (parasitophorous vacuole) intact by binding to surface exposed membrane cholesterol induce a 30nm hole on the membrane (Bhakdi *et al.*, 1985; Jackson *et al.*, 2007). The SLO treatment assay is used to analyze the subcellular localization of protein complexes in *plasmodium*-infected red blood cells in this study.

2 x 10^8 of trophozoite-stage parasite-infected red blood cells were treated with 3 hemolytic units (HU) of SLO in 188 µl of PBS (pH 7.4) and incubated for 6 minutes at room temperature while gently mixed every 2 minutes, followed by centrifugation at 1,000 x g for 3 minutes. The supernatant was transferred into a new 1.5 ml tube while the pellet was washed two more times with PBS supplemented with 1mM PMSF and protease inhibitor cocktail (Knoller *et al.*) (1:200 dilution).The supernatant and pellet were either used for western blotting or co-immunoprecipitation (co-IP) assays.

2.2.5 Saponin lysis of *Plasmodium falciparum*-infected erythrocytes

Saponin is a glycoside, which is commonly found in plants and known to disintegrate the erythrocyte membrane and the parasitophorous vacuolar membrane of *P. falciparum* but leaves the parasite interacting with cell membrane cholesterol, leading to the permeabilization of the membrane (Beaumelle *et al.*, 1987). In this study, saponin lysis was also used to analyze the subcellular localization of protein complexes in *plasmodium*-infected red blood cells.

The trophozoite-stage infected erythrocytes were enriched with gelafundin flotation. A total of 2 x 10^8 cells were treated with 0.02 % saponin dissolved in PBS (pH 7.4) supplemented with 1 mM PMSF. The cells were incubated for 10 min on ice while

gently mixed, followed by the centrifugation at 5000 rpm for 5 minutes at 4 °C. The supernatant was then transferred into a new 1.5 ml tube; while the pellet was washed for two and more times with PBS (pH 7.4) supplemented with 1 mM PMSF and PIC (1:200 diluted). The supernatant and pellet were used for either western blotting or co-IP assay.

2.2.6 Protease K protection assay

In this study, protease K protection assay was used to analyze the subcellular localization of protein complexes in *P. falciparum* infected red blood cells.

The trophozoite-stage parasites were treated either with 0.02 % saponin or SLO (3 HU); afterwards, the pellet fraction was collected and mixed with 0.5 µl of 10 mg/ml protease K diluted in PBS. After 30 min incubation time on ice, 2 mM PMSF and PIC (1:100 diluted) was added into cells in order to inactivate Protease K activities. The pellet was then collected by centrifugation at 13,200 g for 30 s, and then washed with PBS for two or more times. The pellet was used for either western blotting or co-IP assay.

2.2.7 Differential ultracentrifugation

Differential centrifugation is a centrifuge optimized at different speeds to separate the organelles from whole cell lysate according to the size and density. Here, this method was performed to isolate the J-dot fraction.

The trophozoite-stage *P. falciparum*-infected red blood cell were lysed by 5mM Na_2HPO_4 buffer containing PIC (1:100 diluted) and 1 mM PMSF, followed by the ultracentrifugation at 4°C with following steps: 5000 g for 10min, 10,000 g for 10min, 20,000 g for 10min, 33,000 g for 30min, 80,000 g for 1 hour, and 100,000 g for 2 hour. The pellet was then washed for twice with lysis buffer with the above centrifugation protocol. Finally, the pellet was dissolved in 2 x SDS sample buffer supplemented with 100mM DTT, and analyzed by immunoblot assays. Antibodies used included monoclonal mouse anti-GFP (1:1000 diluted), polyclonal rabbit anti-*Pf*Hsp70x (1:500 diluted), monoclonal rabbit anti-*Pf*SERP (1:1000 diluted), monoclonal rabbit anti-*Pf*Aldolase (1:5000 diluted), monoclonal rabbit anti-*Pf*SBP (1:500 diluted), monoclonal

rabbit anti-*Pf*Exp (1:500 diluted), and monoclonal mouse anti-Glycophrin A/B (1:1000 diluted).

2.2.8 SDS-polyacrylamide gel electrophoresis (SDS-PAGE)

Sodium dodecyl sulfate polyacrylamide gel electrophoresis (SDS-PAGE) is used to separate proteins according to their molecular weights (Laemmli, 1970). The sodium dodecyl sulfate (SDS) is an anionic detergent that linearizes proteins by disturbing the 3-dimensional structure of proteins. Proteins migrate from the negative-charged to positive-charged side and get separated in the polyacrylamide gel according to their molecular weights. As for further denaturation, some additional reducing reagents can be used, such as dithiothreitol (DTT) or 2-mercaptoethanol (beta-mercaptoethanol/BME).

In this study, samples for SLO, saponin permeabilization, ultracentrifugation and co-IP were resuspended in 2 x SDS loading buffer containing 100mM DTT and boiled at 100 °C for 10 minutes. The denatured protein samples were separated in a 12 % SDS-PAGE gel (Table 2.1). The running voltage was initially set up at 90 V before protein entered into separate gel from stacking gel, then the voltage was increased to 120 V until finished and a pre-strain protein ladder was used to determine protein molecular weight. The SDS-PAGE gel was either stained with coomassie brilliant blue buffer containing 20 % methanol or subjected for the western blotting assay.

Table 2.1: SDS-PAGE.

Reagent	4% Stacking gel (ml)	12% Separating gel (ml)
ddH_2O	2.56	3.1
Gel Buffer	1.875	1.25
30 % acrylamide	3	0.65
APS	0.05	0.025
TEMED	0.005	0.005

2.2.9 Western blotting

After electrophoresis, the protein can be transferred to PVDF (polyvinylidene fluoride) or nitrocellulose membrane from SDS-PAGE gel for immunoblot analysis (Towbin *et al.*, 1979). In this study, all the western blotting was performed by a semi-dry system. Six pieces of Whatman paper and a PVDF membrane were prepared according to the gel size, and wetted with transfer buffer. The membrane was placed on the polyacrylamide gel and made it like a 'sandwiched'positioned between 3 pieces of Whatman paper on either side; then this 'sandwich' was placed in a blotting chamber. The whole transfer was carried out at 1-2mA/cm^2 for 1.5 hours allowing protein transfer to occur from negative-charged to positive-charge end. After the transfer finished, for checking the efficiency of the transfer, the membrane was stained with Ponceau S solution for 5-10 min until protein bands were visible. Afterwards, the Ponceau S solution was washed out with ddH_2O before proceed the immunoblot detection. Briefly, the membrane was blocked with 5% of the milk solution for 1 hour at room temperature with gentle agitation, and then washed with PBS (pH 7.4) for 3 times (10 min each) at room temperature, in order to remove the non-specific binding of antibodies. After washing, the membrane was incubated with primary antibody diluted in 5% of milk solution overnight at 4 °C with gently shaking. The next day, the membrane was washed for 3 times with PBS (pH 7.4), and incubated with the secondary antibody conjugated to Horseradish Peroxidase (HRP) (1:2000 diluted in 5% of milk solution) for 2 hours at room temperature with gently shaking. After incubation, the membrane was washed for 3 times with PBS (pH 7.4). The detection was carried out using the Enhanced Chemiluminescence (ECL) detection system. The membrane was incubated with a luminol, which is a substrate reacting with the conjugated secondary antibody to produce the light signal. The chemiluminescence can be captured on X-ray film.

2.2.10 Blue native polyacrylamide gel electrophoresis (BN-PAGE)

Blue native polyacrylamide gel (BN-PAGE) is used to separate protein complexes as well as identify physiological protein–protein interactions (PPIs) and subunit composition of protein complexes without denaturing proteins. BN-PAGE provides a higher resolution than gel filtration or sucrose density ultracentrifugation. In BN-PAGE,

protein complexes were separated according to the hydrodynamic size and structure in the polyacrylamide matrix. In this study, BN-PAGE was used for separating the multiple complexes in *P. falciparum*-infected erythrocytes.

The trophozoite-stage *P. falciparum*-infected red blood cells were enriched by gelafundin flotation and lysed with 5mM Na_2HPO_4. After ultracentrifugation with 800000 g force, the pellet was dissolved in blue native sample buffer (20mM bis-tris, 500mM 6-aminocaproic acid, 20mM NaCl, 2mM PH 8.0 EDTA, 10% Glycerol, PH 7.0) containing 0.5% of dodecylmaltoside and 0.01% of coomassie Brilliant G-250. The electrophoresis was performed in the 4 % stacking gel followed by 4%-15% gradient separating gel (Table 2.2). The voltage setup was 100V for running within the stacking gel and 180V while running in the gradient separating gel. HMW Native marker was used as a standard (GE Healthcare). The aminocaproic acid was used for improving the solubilization of membrane proteins; while Blue G induced a charge shift on the constituent proteins (Van Coster *et al.*, 2001).

Table 2.2: BN-PAGE.

Reagent	3.2% Stacking gel (ml)	4% Separating gel (ml)	15% Separating gel (ml)
ddH_2O	5.04	4.5	1.25
3 x BN buffer	3.00	2.5	2.5
30 % acrylamide	0.96	1	3.7
APS	0.12	0.054	0.042
TEMED	0.012	0.0054	0.0042

2.2.11 Western blotting of two dimension BN /SDS –PAGE

In the first dimension of BN-PAGE, proteins complexes were separated without destroying the protein-protein interaction under a native condition; while the protein subunits from the one protein were separated in a secondary SDS-PAGE. In this study, this method was used for analyzing the multiple complexes from parasite infect red

blood cell.

Once the first dimension of BN-PAGE gel was finished, the lane with protein samples was sliced and boiled in 2 x SDS sample buffer containing 100mM DTT for 20 s, followed by the incubation for 0.5 hour at room temperature with gentle shaking. For the second dimension, the denatured sample was separated in a 10% of 18x20 cm SDS-PAGE running at room temperature with a voltage at 100 V for stacking gel and 160V for separating gel, respectively. The secondary SDS-PAGE was followed by either immunoblot detection or LC/MS/MS identification (Figure 2.1). Antibodies used in this section were listed as following: monoclonal mouse anti-GFP (1: 1000 diluted), polyclonal rabbit anti-*Pf*Hsp70x (1:500 diluted), polyclonal rabbit anti-*Pf*PHISTC (1: 1000 diluted), and polyclonal rabbit anti-*Pf*GBP130 (1: 1000 diluted).

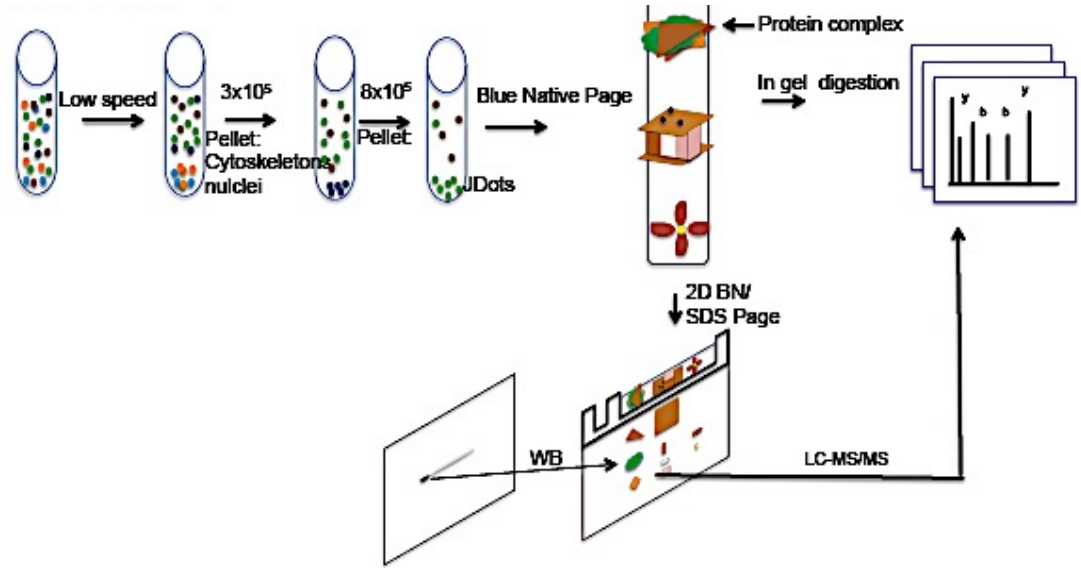

Figure 2.1: Two-dimension BN/SDS-PAGE analyses of the cellular lysates.

Multiple protein complexes were purified by ultracentrifugation, followed by BN-PAGE. The protein complexes were either analyzed with LC-MS/MS or a second dimension SDS-PAGE. The components of multiple protein complexes can be verified by either immunoblot analysis or LC-MS/MS.

2.2.12 In-vivo cross-linking

Cross-linking is a bond active links from one polymer chain (protein) to the other. It has been widely used in protein chemistry study especially in protein-protein interactions (PPIs) research because cross-link would help to binding the week and instantaneous interaction between proteins in vivo. By using chemical reagents with reactive groups, like amnie, sulfhydryl- and photo-reactive, formed the cross-link and they are mostly used in protein crosslinking. Recently, there are many commercially cross linkers have been generated such as N-hydroxysuccinmide (NHS)-ester cross linker BS3 (bis(sulfosuccinimidyl)suberate), DSP (dithiobis(succinimidyl propionate)), dimethyl subberimidate and formaldehyde (Uckert *et al.*, 1983; Mattson *et al.*, 1993; Gavazzi *et al.*, 2007). In this study, DSP was used for crosslinking, since it is lipophilic and membrane–permeable and useful for intracellular and intramembranous conjugation.

The trophozoite-stage *P. falciparum* infected red blood cell were enriched by gelafundin flotation as described above, washed two times by PBS (PH 7.2) reaction buffer, followed by cross-linking with 1.5mM DSP on ice for 2 hour. The reaction was then terminated by15mM Tris-HCl (PH 7.5) at room temperature for 15 min. Afterwards, cells were washed with PBS (PH 7.2) for 3 times, and ready for the further co-immunoprecipitation assays.

2.2.13 Co- immunoprecipitation (co-IP)

Co-immunoprecipitation (co-IP) is a technique to identify relevant protein-protein interactions (PPIs) by using target protein-specific antibodies to indirectly capture proteins that bind to the target protein. This approach is often used to identify new interaction partners of the target protein followed by two dimensional electrophoresis (2-DE), SDS-PAGE and Mass spectrometry (Figure 2.2) (Phizicky and Fields, 1995; Lee, 2007).

In this section, trophozoite-stage parasites were enriched by gelafundin flotation as mentioned above followed by crosslinking with 1.5mM DSP on ice for 2h. The reaction was terminated by incubation with 15mM Tris-HCl at room temperature for 15 min. The crosslinked cells were lysed with lysis buffer containing PIC (1:200 diluted) and 1 mM PMSF, and centrifuged at 1300 g, 4 °C for 10 min to remove cell debris. The supernatant of the lysis was used for co-IP (IP, Pierce co- immunoprecipitation kit,

Thermo Scientific, Rockford, IL, USA). Antibody beads needed were generated as describe The AminoLink Plus Coupling Resin and reagents were equilibrated at room temperature. The 20x couple buffer was diluted to 1 x. Next, 50µl of resins were added into the column and centrifuged at 3000 rpm for 1 min, followed by washing for twice with 1X coupling buffer. Gently tapped the bottom of the spin column on a paper towel to remove the excess liquid and inserted the bottom plug. 5-10 µg of antibodies were used for coupling by adjusted the volume to 200 µl with PBS and 3 µl of Sodium Cyanoborohydride Solution. The antibody solution and beads were incubated for 90-120 min with gentle agitation at room temperature. And then the flow was collected for the further analysis by centrifugation. The coupling reaction was terminated by incubating with 200 µl of quenching buffer at room temperature for 15 min. After that, the antibody-resin was washed for twice with 1X coupling buffer, followed by washing with 150 µl of wash buffer for 6 times. The antibodies used for generating antibody-bound beads were as following: monoclonal mouse anti-GFP, polyclonal rabbit anti-*Pf*Hsp70x, monoclonal mouse anti-*Pf*Hsp101 and polyclonal rabbit anti-*Pf*GBP130. For immunoprecipitation, after pre-incubating the lysate the empty agarose resin at 4°C for 1h, the lysate was collected and mixed with the antibody-coupled resins overnight with gentle agitation at 4°C. The next day, after collecting the remaining lysate, the antibody-protein-coupled resin was washed for two or more times to remove nonspecific binding proteins. The Proteins that were specifically bound to the antibody-coupled resins were eluted using 0.1% TFA, and further analyzed by both western blotting and LC-MS/MS.

2.2.14 Trypsin in gel digestion

In gel digestion is an important step when preparing the peptide samples for mass spectrometric identification (Rosenfeld et al., 1992). After separated by 1D or 2D-PAGE, protein bands were visualized by coomassie staining. The interest bands or spots were excised and destained for further protein digestion. The trypsin enzyme is widely used for protein digestion by cleaving peptide chains at carboxyl side of lysine and arginine.

In this study, gel slices were washed by milli-Q water and sliced into 1mm^3 pieces with incubating in 25 mM NH_4CO_3 with vortexing for 20 min for several times until the NH_4CO_3 solution was clean, moreover the gel piece was distained with 25 mM

NH_4CO_3/CH_3CN 1:1 for 20 min, repeated this step until the color completely gone. Threw the supernatant and covered the gel piece with acetonitrile until the gel piece shrank. Removed the extra acetonitrile, gel particles were dried by centrifugation under vacuum at room temperature for 30 min. Proteins were reduced by covering the gel particle with 25 mM NH_4CO_3 containing 10 mM DTT for 1 hour at 56 °C, followed by alkylation of proteins by the addition of 25 mM NH_4CO_3 containing 55 mM iodoacetamide for 45 min in the dark at room temperature. Gel pieces were then washed with 25 mM NH_4CO_3 and subsequently 25 mM NH_4CO_3/CH_3CN 1:1 for 20 min each. Finally, the gel was covered with acetonitrile until shranking and then dried by centrifugation under vacuum. In-gel digestion was performed by adding 10 ng/µl of trypsin dissolved in 25 mM NH_4CO_3 at 37 °C overnight. The next day, peptides was extracted from the gel by adding 2 times gel volumes of 50% CH_3CN/0.1%TFA solution and mixed by vortexing for 20 min. All of the peptide solution was collected and dried in vacuum at room temperature.

2.2.15 LC-MS/MS identification and data analysis

LC-MS/MS is a technique combines a high performance liquid chromatography (HPLC) that pre-chromatographic separation samples with mass spectrometry (MS). Here, digested peptides were concentrated and further analyzed by LTQ-Orbitrap Elite Mass spectrometry (Thermo Fisher) equipped an EASY-Spray source and a nano-LC UltiMate 3000 high-performance liquid chromatography system (Thermo Fisher). A full-scan survey MS experiment (m/z range from 375 to 1600; automatic gain control target, 1,000,000 ions; resolution at 400 m/z, 60,000; maximum ion accumulation time, 50 ms) was performed using the Orbitrap mass spectrometer, where ten most intense ions were selected and fragmented by collision-induced dissociation (CID). Raw data were converted to mgf files by Proteome Discoverer 1.3 (Thermo fisher) and analyzed using pFind 2.1 software to search against the human Uniprot TrEMBL database (release on April 2012, human, 65,493 entries) and *P. falciparum* DB database (release on October 2013, plasmodium 3D7), respectively (Li *et al.*, 2005). The modification was set as following: static modification of carbamidomethyl (Cys), dynamic modification of deamination (Asn), oxidation (Van Coster *et al.*), and acetylation (Lys). Trypsin was selected as the enzyme; while two missed cleavages were allowed. The mass tolerance was set to 20 ppm for the precursor ions and 0.5 Da for the fragment ions. A

false discovery rate (FDR) of 1% was estimated and applied to all data sets at the total peptide levels.

2.2.16 Live cell imaging

Cells were harvested by centrifugation, followed by washing for 3 times with RPMI medium. Cells were stained with 10 µg/ml Nuclear DNA Hoechse dye and incubated at room temperature with gentle shaking for 10 min; After a blood-drop applying to the slide, samples were visualized using Zeiss Axio Observer inverse epifluorescence microscope system at room temperature.

2.2.17 Immunofluorescence assays

Immunofluorescence assays were performed using acetone/methanol (90%/10%) fixation. 5-8µl of *P. falciparum*-infected and non-infected red blood cell mixture were taken from the culture and applied to the slide; the smear of cells was then dried and fixed with pre-cooled acetone/methanol (90%/10%) solution at -20 °C for 10 min. After the smear was completely dry, samples were blocked with 3 % BSA in PBS for 1 hour at room temperature. For the primary antibody incubation, the antibody was diluted in 3 % BSA in PBS and applied onto the smear followed by the overnight incubation at 4 °C. The next day, the slide was washed with PBS (PH 7.4) for 3 times (10 min each) to remove non-binding primary antibody and incubated with the secondary antibody for 2 hours at room temperature. The slide was then washed with PBS (PH 7.4) for 3 times. To visualize the nuclear DNA of the fixed parasites, samples were stained with Hoechst 33258 (50 ng/ml) for 10 min prior to visualization by epifluorescence microscopy. The primary antibodies used in this assay include polyclonal rabbit anti-*Pf*Hsp70x (1:2000 diluted), monoclonal mouse anti-GFP (1:500 diluted), monoclonal mouse anti-*Pf*GBP130 (1:1000 diluted), monoclonal mouse anti-*Pf*Hsp101 (1:500 diluted), and polyclonal rabbit anti-*Pf*PhistC (1:1000 diluted). The conjugated secondary antibodies include anti-rabbit-Cy2, anti-rabbit-Cy3, and anti-mouse-Cy3 (Dianova, 1:2000 diluted). Images were acquired using a Zeiss Axio Observer inverse epifluorescence microscope system, with appropriate filter sets.

2.3 Bioinformatics analysis

2.3.1 Mass spectrometry data analysis

Raw data were analyzed as mentioned in 1.2.11. The more details of databases used were shown in Table 2.3.

Table 2.3: Protein database information.

Protein database	Website
Plasmodium DB	http://plasmodb.org/plasmo/
Uniprot	http://www.uniprot.org
GeneDB	http://www.genedb.org/Homepage
ExPASy	http://www.expasy.org/

2.3.2 Image processing with Image J

In this study, microscopic images were analyzed using ImageJ, which is an open source with Java-written program (http://rsbweb.nih.gov/ij/). Images were taken with the aforementioned epifluorescence microscope and imported into ImageJ64. The channels were spited into separate windows and converted into 8-bit grayscale mode. Every image was subjected to background subtraction. The RGB channels were split into red, green and blue channels before the individual images were merged. All images were adjusted with the brightness/contrast tool before saved as TIF files.

3 RESULTS

In previous studies, our group discovered two members of parasite-encoded type II Hsp40s family (PEF55, PFA660) that forming highly mobile structures in the parasite-infected red blood cell, which was referred as J-dots. Furthermore, *Pf*Hsp70x was identified to partially co-localize with J-dots by immunocolocalization and immunoprecipitation. This observation indicates that J-dots are involved in protein transport through the erythrocyte. In this current study, multiple proteomics approaches were used to characterize the parasite-induced intra-erythrocytic protein complex and further construct a protein-protein interactions network in the *P. falciparum* infected red blood cell, which will expand our understanding their importance in parasite survival and virulence.

3.1 Isolation of J-dots fraction by differential centrifugation

In our studies, mainly work was performed on PFE55^{GFP} transfection parasite line, which expresses full-length PFE55 fused to GFP, on the basis of 3D7 strain (Kulzer *et al.*, 2010).

In this section, PFE55^{GFP} parasites infected red blood cells were subjected to hypotonically lysis, which was followed by a differential centrifugation. During the differential centrifugation protein contaminations were removed and in the end pure J-dot fractions were obtained.

The pellets from 1000 g-10x10^4 g fractions were investigated for the purification efficiency by immunoblots with several antibodies including checked for the purification efficiency by immunoblots with antibodies including anti-GFP (J-dots), anti-*Pf*Hsp70x (J-dots), anti-*Pf*SERP (soluble protein of parasitophorous vacuole), anti-*Pf*SBP1 (a protein marker of Maurer's clefts), anti-*Pf*Aldolase (soluble protein of parasite cytosol), anti-*Pf*EXP1 (protein marker of parasitophorous vacuole membrane (PVM)) and anti-Glycophorin A/B (a protein marker of erythrocyte plasma membrane). As shown (Figure 3.1), strong signals were detected by using anti-GFP, anti-*Pf*Hsp70x, anti-

*Pf*SERP or anti-*Pf*Aldolase for immunoblots with samples from this fraction. This indicated that the signal came from from the non-lysed cell.

Since *Pf*SBP1 and *Pf*EXP1 were mostly present in 5000 g, 10,000 g, 20,000 g, 30,000 g pellets which indicates that these fractions contained parasitophorous vacuole (PV) proteins and Maurer's clefts proteins while 5000g-30,000 g pellets showed mostly erythrocyte marker proteins. In the 80,000 g fraction, we detected the presence of PFE55-GFP as well as *Pf*Hsp70x, but not *Pf*SERP, *Pf*SBP1 and *Pf*EXP1, indicating that the J-dots fraction was pure without containing any marker proteins of Maurer's clefts and parasitophorous vacuole membrane (PVM). However, red blood cell membrane protein marker Glycophorin A/B was present in every fraction including the 80,000 g fraction suggesting that this fraction also contained some fragments of erythrocyte plasma membrane. In the 10x 10^4 g fraction, the signal from PFE55-GFP and *Pf*Hsp70x as well as the others protein markers were absent.

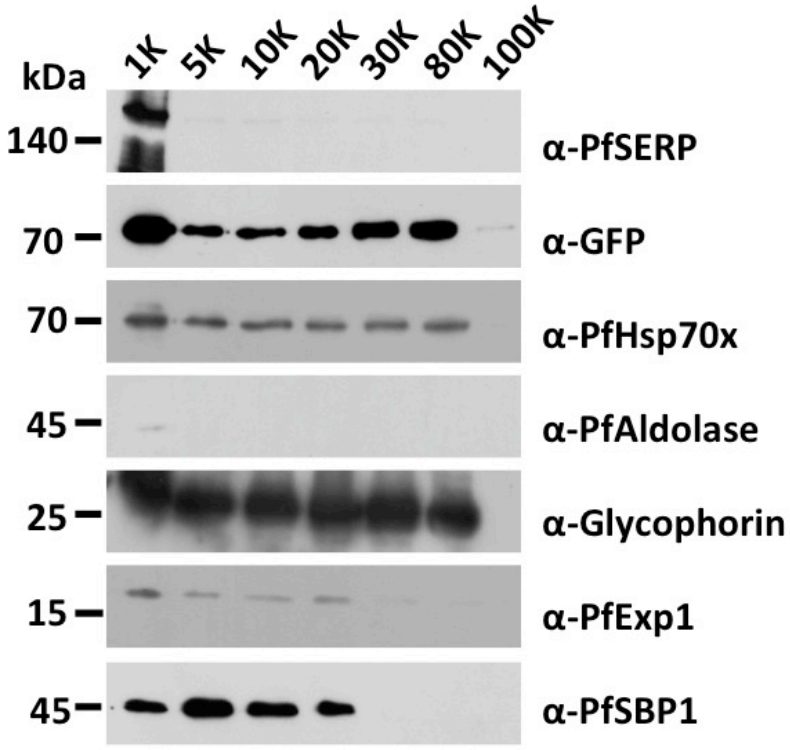

Figure 3.1: Western blot analysis of different fractions from differential ultracentrifugation

The pellets from 1000 g-10x 10^4 g by different centrifugation were verified by using anti-GFP (J-dots), anti-*Pf*Hsp70x, anti-*Pf*SERP, anti-*Pf*SBP1, anti-*Pf*Aldolase, anti-*Pf*EXP1 and anti-GlycophorinA/B.

3.2 Detection and identification of protein complexes separated by BN-PAGE and 2D BN/SDS-PAGE

In order to characterize the molecular PFE55-*Pf*Hsp70 chaperone/co-chaperone complex in the J-dot fraction, a BN-PAGE gel was applied to separate the multiple protein complexes of the 80,000 g fraction, followed by with the detection via immunoblot analysis and identification by LC-MS/MS. In addition, an immunoblot of 2D BN/SDS-PAGE was performed for further analysis of the J-dot complexes.

3.2.1 Immunoblot analysis and protein identification of BN-PAGE by LC-MS/MS

Proteins of the 80,000 g fraction of PFE55^{GFP} transfection cell line and control 3D7 wild type cell line were separated on the BN-PAGE, followed by immunoblot analysis using anti-GFP as well as mass spectrometry identification.

In this experiment, the non-ionic detergent digitonin and dodecylmaltoside (DDM) were chosen for solubilsation as well as stabilization of protein complexes in the J-dots fraction. By adding the DDM, a clear signal was observed at the height of >232kDa (Figure 3.2) in immunoblot analysis with anti-GFP and anti-*Pf*Hsp70x. However, with digitonin solubisation, two clear signals were found, one signal at around 232kDa, and the other one around 440 kDa~669kDa (Figure 3.2A), As digitonin was more solubilizes and stabilizes supercomplexes while DDM possible leads to the dissociation of these structures into a single protein complexes. This result suggests that a *Pf*Hsp70x and PFE55 chaperones/co- chaperones complex in J-dots has a molecular weight of at least of ~223-440kDa.

Based on these observations, five bands were chosen and sliced from the corresponding gel, followed by in gel-digestion with trypsin and proceeded protein identification by LTQ-Orbitrap Elite Mass spectrometry (Figure 3.2 B). The peptides masses and sequences information were searched against the *Plasmodium* DB database by using Pfind (2.0) engine and identified by two unique peptides matching. Here, the proteins were selected based on the presence of an export domain, transmembrane domain or signal peptide (Table 3.1, Table 3.2). *Pf*Hsp70x was found in two samples, band 2 (Table 3.1) and band 3 (Table 3.2) with two unique peptides

matching, respectively. In band 2 (Table 2.1), the following exported proteins from *P. falciparum* were identified including: *Pf*Hsp70x, *Pf*SEMP1, *Pf*G174, REX1, *Pf*GBP130, DnaJ protein, *Pf*j2, CPN60, RON3, MSP7, SEC7, RAP3, RAP2, RhopH3 and RhopH2. In band 3 (Table 2.2), several exported *Pf*Hsp70x, *Pf*SEMP1, *Pf*GEXP18, MSP1, CPN60 and RhopH2. Among those, most of the proteins belong to known protein complexes with a high abundance in the infected red blood cell. For example, RAP2 and RAP3 are members of low molecular weight rhoptry complexes (Baldi *et al.*, 2000), in contrast to RhopH3 and RhopH2 which are components of high molecular weight rhoptry complexes (Doury *et al.*, 1994). RON3 associates to the *Plamodium* rhoptry neck (RON) protein complex (Cowman *et al.*, 2012). *Pf*SEMP1 is a new Maurer's clefts membrane protein and was identified during a co-immunoprecipitation with *Pf*Hsp70x (Dietz et al., 2014). In addition, more unknown proteins were identified along with *Pf*Hsp70x, in the same band, PfG174 is a PHISTb family protein with unknown function and found in the infected erythrocyte ghosts (Vincensini *et al.*, 2005). Moreover, *Pf*GBP130 was detected which is a soluble protein found in the host cell cytoplasm with an unknown function (Benting *et al.*, 1994). DnaJ and *Pf*j2 are both belonged to type II J-protein family (Hohfeld *et al.*, 1995). *Pf*GEXP18 is a *Plasmodium* exported protein with unknown function. Further, CPN60 was identified in all five bands, which is a chaperone protein with a molecular weight of 60kDa. Unfortunately, the PFE55-GFP was not detected in all five bands. Considering the high abundance of identified proteins like the high RhopH2 with 17 unique peptides identified and SCE with 11 unique peptide identified, it might be that either PFE55 was not presented in these bands or the identification was shadowed by the high abundance of other proteins.

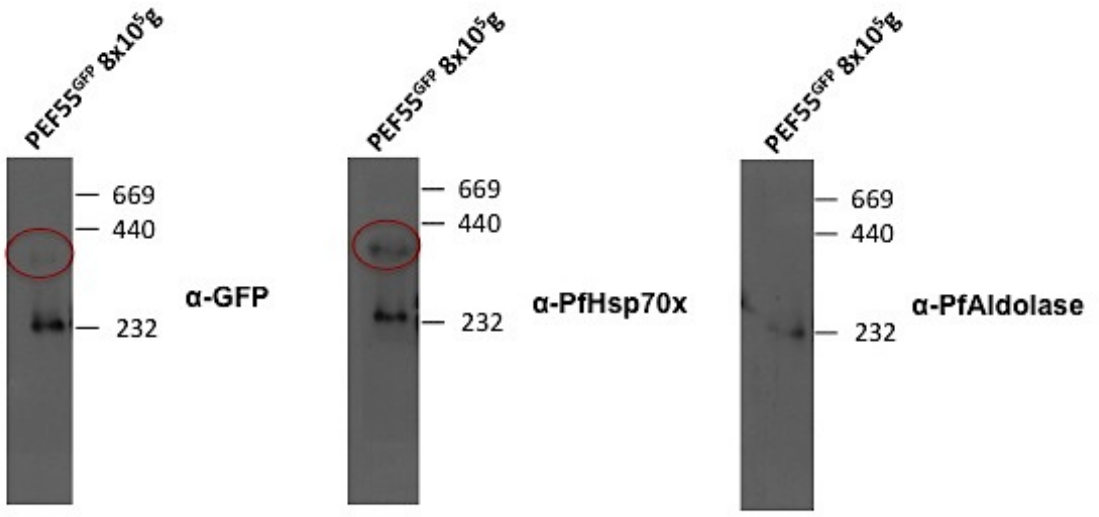

Figure 3.2: Immunoblot analyses protein complexes isolated by BN-PAGE in J-dots fraction.

The 80,000 g fraction pellet from trophozoite stage parasite of PFE55^{GFP} transfection cell line and 3D7 cell line was solubilsation by dodecylmaltoside (DDM) and separated on the BN-PAGE followed by western blotting using anti-GFP (PFE55-GFP), anti-*Pf*Hsp70x and anti-*Pf*Aldolase (control). HMW Native markers were used as a standard (kDa).

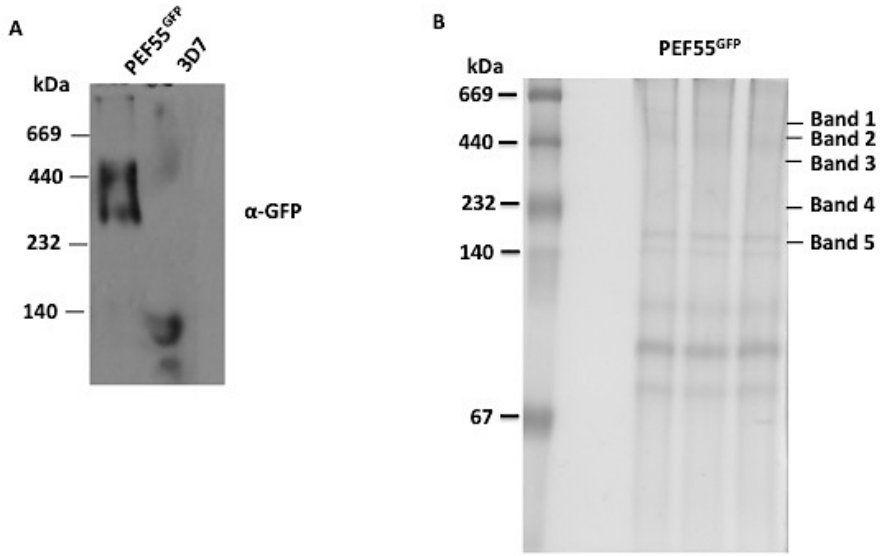

Figure 3.3: Immunoblot analyses and LC-MS/MS identification of protein complexes isolated by BN-PAGE in J-dots fraction.

A: The 80,000 g fraction pellet from trophozoite stage parasite of PFE55GFP transfection cell line and 3D7 cell line was separated on the BN-PAGE followed by western blotting using anti-GFP (PFE55-GFP), HMW Native markers were used as a standard (GE Healthcare) B: Five bands were excised form BN-PAGE and digested with trypsin for further LC-MS/MS analysis.

Table 3.1: Protein identification of band 2 by LC/MS/MS (exported protein list).

Accession Number	Protein names	Unique Peptide Number	Percent Coverage	Molecular Weight
PF3D7_0629200	DnaJ protein, putative	3	6.316	44,669
PF3D7_0702400	small exported membrane protein 1 (SEMP1)	2	15.447	14,195
PF3D7_0731300	Plasmodium exported protein (PHISTb), unknown function (PfG174)	2	6.309	37,723
PF3D7_0831700	heat shock protein 70 (HSP70x)	2	3.829	75.054
PF3D7_0935900	ring-exported protein 1 (REX1)	4	4.067	83,041
PF3D7_1016300	glycophorin binding protein (GBP)	3	18.932	95,844
PF3D7_1108700	heat shock protein DnaJ homologue Pfj2	2	5	62,377
PF3D7_1232100	60 kDa chaperonin (CPN60)	5	9.053	81,484
PF3D7_1252100	rhoptry neck protein 3 (RON3)	4	1.851	263,155
PF3D7_1335100	merozoite surface protein 7 (MSP7)	2	5.698	41,276
PF3D7_1442900	protein transport protein SEC7, putative (SEC7)	11	1.684	404,583
PF3D7_0501500	rhoptry-associated protein 3 (RAP3)	2	4.75	47,004
PF3D7_0501600	rhoptry-associated protein 2 (RAP2)	3	8.543	46,739
PF3D7_0905400	high molecular weight rhoptry protein 3 (RhopH3)	6	7.581	104,856
PF3D7_0929400	high molecular weight rhoptry protein 2 (RhopH2)	17	13.57	162,665

Table 3.2: Protein identification of Band 3 by LC/MS/MS (exported protein list).

Accession Number	Protein names	Unique Peptide Number	Percent Coverage	Molecular Weight
PF3D7_0402400	Plasmodium exported protein, unknown function (GEXP18)	2	8.661	31,019
PF3D7_0702400	small exported membrane protein 1 (SEMP1)	2	15.447	14,195
PF3D7_0831700	heat shock protein 70 (HSP70x)	2	3.387	75.054

PF3D7_0929400	high molecular weight rhoptry protein 2 (RhopH2)	5	3.193	162,665
PF3D7_0930300	merozoite surface protein 1 (MSP1)	6	4.128	195,726
PF3D7_1016300	glycophorin binding protein (GBP)	2	17.112	95,844
PF3D7_1232100	60 kDa chaperonin (CPN60)	3	5.153	81,484
PF3D7_1456800	V-type H(+)-translocating pyrophosphatase, putative (VP1)	2	3.347	76,417

3.2.2 2D BN/SDS-PAGE and western blot analysis of protein complexes that contained PFE55/*Pf*Hsp70x in J-dots fraction

Multiple complexes that contained PEF55-GFP and *Pf*Hsp70x were isolated from 80,000 g J-dot fraction by BN-PAGE and following western blotting; while an additional secondary dimension SDS-PAGE was performed to prove the presence of PEF55-GFP and *Pf*Hsp70x from the same protein complex with high molecular weight.

After multiple complexes were separated on the first dimension BN-PAGE, the gel lane with the protein complexes was subsequently denatured and further separated on a 10% SDS-PAGE. Western blotting was performed using anti-GFP and anti-*Pf*Hsp70x, respectively. As shown in Figure 3.3, by usage of the anti-*Pf*Hsp70x antibody three to four signals with a molecular weights ~75kDa could be detected Signals were initially identified on BN-PAGE at height of >669kDa, 440kDa~669kDa and 232kDa~440kDa (it seems like there was more than one signal detected at the height of 440kDa~669kDa). With the anti-GFP, were two strong signals and a week signal spot with a molecular weights of ~70kDa was detected. Signals were present at the height of >669kDa, 440kDa~669kDa and 232kDa~440kDa on BN-PAGE, respectively. Comparing the signal from anti-GFP and anti-*Pf*Hsp70x which were running at a similar molecular mass as in the initial BN-gel, which was indicated that PFE55-GFP and *Pf*Hsp70 came from the same high molecular weight complex. The first lane was loaded with 80,000 g fraction and severed as a positive control.

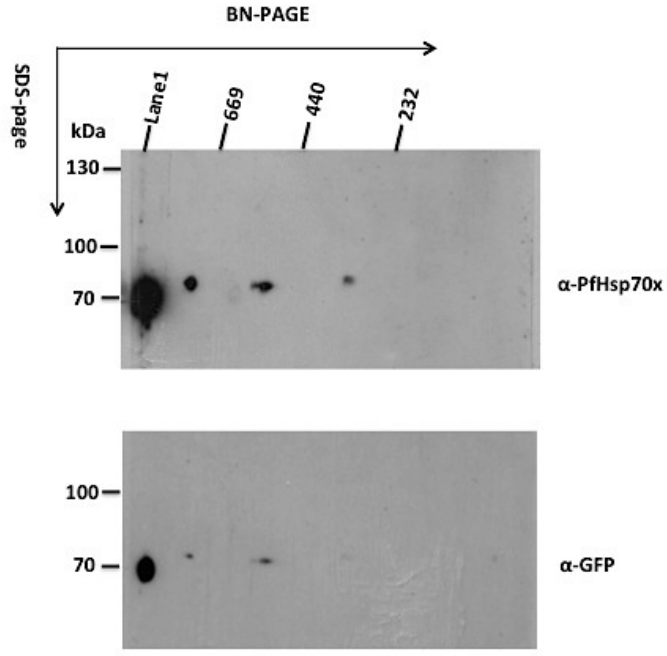

Figure 3.4: 2D BN/SDS-PAGE immunoblotting analysis J-dots protein complex.

The protein sample of 80000 g fraction was subjected to 2D BN/SDS-PAGE (4–15% and 10%, respectively), and further preceded for immunoblot analysis with anti-*Pf*Hsp70x and anti-GFP (*Pf*Hsp40-GFP). Lane1: Positive control (80,000g cell lysate fraction).

3.3 *In vivo* crosslinking and co-immunoprecipitation (co-IP)

The result from 2D BN/SDS PAGE immunoblotting suggests that PFE55-GFP and *Pf*Hsp70x were present in the same high molecular complex. In order to investigate other interaction partners PFE55-*Pf*Hsp70x, co-immunoprecipitation (co-IP) was performed. In addition to this and in order to enhance the protein-protein interaction as well as to stabilise transient protein-protein interactions, an *in vivo* cross-linking reaction was done in prior the to the co-IP analysis, an overview of the experimental set up is shown in Figure 3.4.

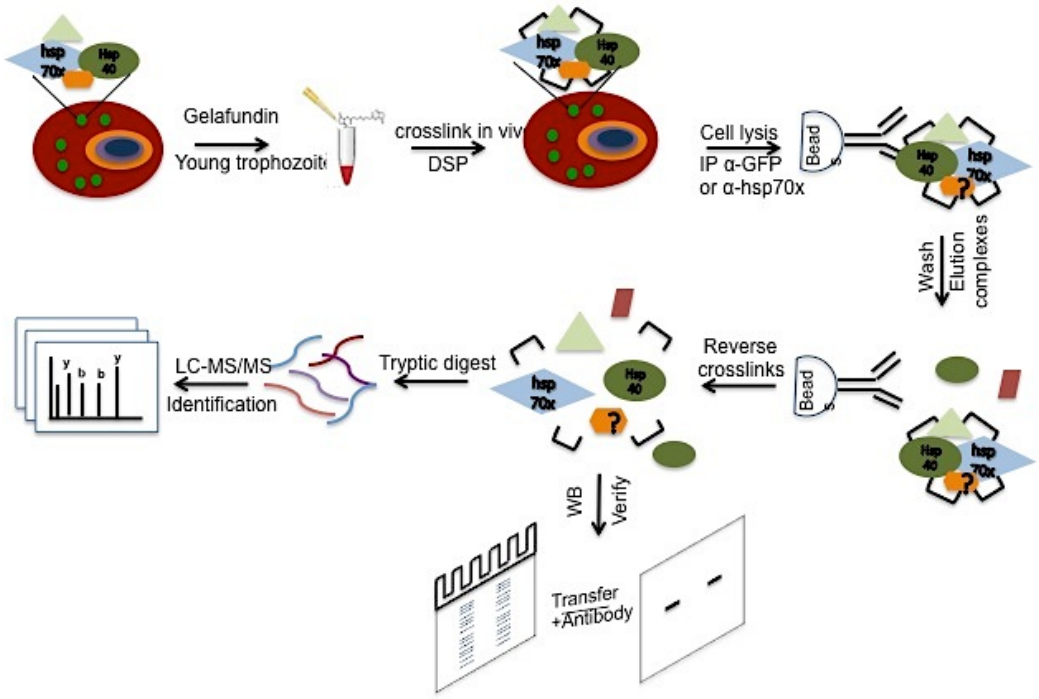

Figure 3.5: The diagram shows the experimental setup of *in vivo* crosslinking and co-Immunoprecipitation assays.

3.3.1 Identification of interacting proteins partners by immunoprecipitation via PMF

The western blotting of 2D BN /SDS PAGE suggests a molecular weight of J-dot protein complexes of more than 223 kDa, in order to detect the association of *Pf*Hp70x with both exogenous PFE55-GFP and endogenous PFE55, a pull-down experiment with anti-GFP antibody was performed on PFE55-GFP parasites cell line and 3D7 parent parasites as control.. The eluted proteins were separated on a 12% SDS-PAGE and visualized by commassie staining. Compared to the negative control, two unique bands were present in the elution from co-IP assays using GFP as baits. The first band has a molecular weight of ~70kDa, while the other ~40kDa. These two bands were excised and subject to an in gel digestion with trypsin. Thereby samples were prepared for MALDI-TOF mass spectrometry to obtain peptide mass fingerprinting (PMF). Proteins were identified by a search against *Plasmodium* DB database and Uniprot human database. The proteins from band one including consist of PFE55 (PFE55-

GFP), *Pf*Hsp70x, and human HSC70 while PFE55 was identified in band two (Figure 3.5).

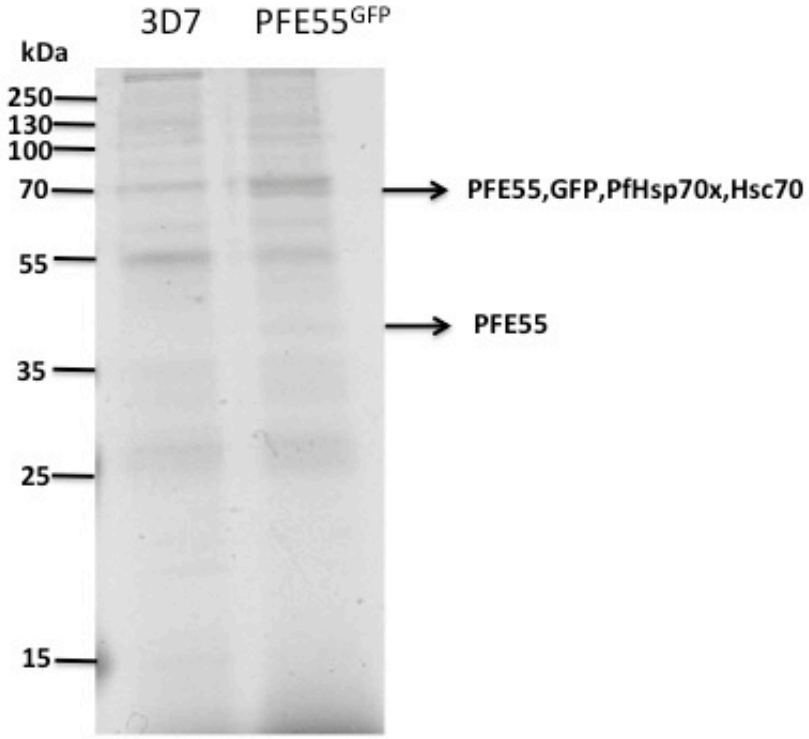

Figure 3.6: Protein identification in unique coomassie stained band by MALDI-TOF mass spectrometry.

Coomassie stained SDS–PAGE gels of the elution from immunoprecipitation performed using GFP antibody on parasite lysates from PFE55-GFP and 3D7, two unique bands were excised and analyzed by MALDI-TOF mass spectrometry. A pre-stain protein marker was used as a standard.

3.3.2 *In vivo* crosslink with DSP

We used an amine-reactive, thiol-cleavable and membrane permeable cross linker named DSP with a bond length of 12 Å for *in vivo* crosslinking of the cell in order to strengthen protein-protein interactions as well as capturing the instantaneous protein inactions. Western blotting with anti-GFP and anti-*Pf*HSP70x was used for verifying the efficiency of *in vivo* cross-link *in vivo* by a comparison with non-crosslinked sample.

As shown in the western blotting (Figure 3.6), the crosslinked and non-crosslinked cells were lysed and separated into three fractions: membrane fraction, J-dot fraction and

supernatant fraction. For the sample with crosslinking, the *Pf*Hsp70x was observed in complexes (>250kDa) present mostly in the membrane fraction (30,000 g) and J-dot fraction (80,000 g) but rarely in the supernatant fraction. Most of the monomeric *Pf*Hsp70x was present in the supernatant while only a small amount was detectable in the membrane fraction at a size of around 70 kDa. This data imply that most of the *Pf*Hsp70x is present as higher ordered structure in the J-dot fraction and membrane fraction (Figure 3.6).

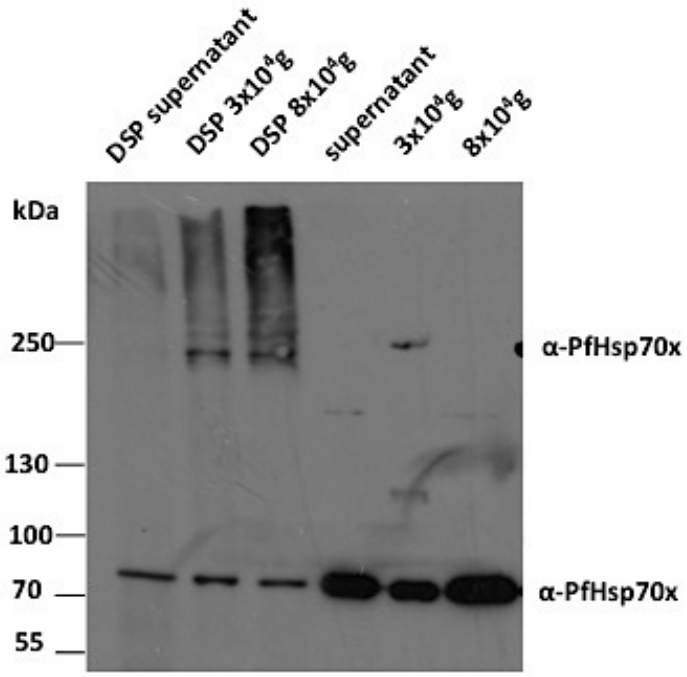

Figure 3.7: Cross-link captures *Pf*Hsp70x complexes in different cell fraction.

Trophozoite stage *P. falciparum* infected red blood cell parasites were treated with cross-linker DSP at 1.5mM, then differential centrifuged at $3x10^4$ g, $8x10^4$ g after lysed. The supernatant, and the pellet from membrane fraction and J-dots fraction was separated by SDS-PAGE under non-reduced conditions. A: western blotting analysis with a polyclonal anti-*Pf*Hsp70x antibody.

3.3.3 Identification of the protein from co-immunoprecipitation (co-IP) using LC-MS/MS

As the results above show, the protein complex contained PFE55-GFP and *Pf*Hsp70x in a high molecular weight. In order to investigate the other proteins associating with *Pf*Hsp40 and *Pf*Hsp70x, we performed two groups' co-IP assays with anti-GFP and anti-*Pf*Hsp70x on PFE55^{GFP} transgenic cell line. The interaction partners of PFE55 were captured by co-elution with PFE55-GFP after incubating cell lysates with anti-GFP affinity beads; while lysates from the 3D7 control cell line were used as a negative control. Meanwhile, *Pf*Hsp70x associating proteins were identified by co-IP assays using anti-*Pf*Hsp70x affinity beads in PFE55^{GFP} lysate and non-antibody beads were used as a control.

The elution protein was subject to 12% SDS-PAGE gel and visualized by commassie blue. Proteins from both IP and control were in gel digested with trypsin and analyzed by LTQ-Orbitrap Elite mass spectrometry. The entire protein list is shown in Table S1. All identified proteins were using ≥ 2 unique peptides matches were used and we further selected the interaction partners by either of the following characteristics: i) proteins containing a classical N-terminal signal sequence only, ii) proteins having a predicted PEXEL/HT export motif OR an annotation as "exported", iii) proteins exhibiting a hydrophobic domain. In addition, the specific binding proteins were picked up by the ratio ≥2 of identified unique peptide number in comparison to the control. In theory, the higher ratio value it has, the more specific binding opportunity of identification protein.

In total 73 *P. falciparum* proteins co-eluted with PFE55-GFP. Amongst of these, four exported proteins, two proteins with a signal peptide and one protein containing a transmembrane domain (Table 3.3). The proteins were further selected by a peptide ratio ≥ 2 compared to control identified unique peptide number. We ended up with are PFE55, *Pf*Hsp70x, *Pf*PHISTc, DnaJ protein, plasmepsin IV, *Pf*Hsp101.

From the co-IP assays with *Pf*Hsp70x as a bait protein, there were 190 *P. falciparum* proteins identified with ≥ 2 unique peptides matching, including nine exported proteins, 20 proteins with signal peptide and eight proteins containing transmembrane domain (Table 3.4). By comparison with the negative control, 23 proteins were with a unique peptide number ratio ≥ 2. Interestingly, two *P. falciparum* proteins, *Pf*PHISTc and

*Pf*Hsp101 were found to be potentially binding to both PFE55-GFP and *Pf*Hsp70x. In addition, these two proteins exhibit different subcellular location. *Pf*Hsp101 is a component of PTEX translocon complex that localizes to the PVM and faces to PV (de Koning-Ward *et al.*, 2009). PHISTc belongs to the PHIST protein family protein, and is potentially localized in the erythrocyte cytosol. In previous study, J-dots have been demonstrated to localize in the erythrocyte cytosol, which suggests that PHISTc is a member of the J-dot protein complex by binding to PFE55 and *Pf*Hsp70x. Moreover, *Pf*Hsp101 was identified by LC-MS/MS with a five fold and four fold of unique peptide in co-IP with anti-GFP and anti-*Pf*Hsp70x, respectively. This is highly suggestive that a protein complex containing PFE55/*Pf*Hsp70x is also found in the PV. Besides *Pf*Hsp101 and *Pf*PHISTc, there were more proteins identified that highly associate with *Pf*Hsp70x, including *Pf*GEXP18, *Pf*GBP130, PHIST protein, *Pf*EXP2, and *Pf*PV1. Interestingly, *Pf*EXP2, another protein component of PTEX translocon as well as *Pf*Hsp101 were found in *Pf*Hsp70x pull down. Furthermore, in a recent study, *Pf*PV1 and *Pf*Hsp70x were identified to immunoprecipitation with an essential PTEX translocon component-PTEX150 (Elsworth *et al.*, 2016). As two components of PTEX translocon bound *Pf*Hsp70x, further analysis of the interaction between members of the PTEX translocon and *Pf*Hsp70x was carried out.

It has long been suggested that parasite encoded Hsp40s potentially interact with human Hsp70. In order to verify the interaction between PFE55, *Pf*Hsp70x and human protein, all of the raw data were search against Uniprot human database. With ≥ 2 unique peptides matching, in total 87 proteins and 59 proteins were identified by co-immunoprecipitation with anti-GFP and anti-*Pf*Hsp70x respectively. We first excluded removed high abundant proteins including trypsin, keratin, myosin, and ribosomal proteins. The remaining proteins with unique peptide number ratio ≥ 2 are selected. In our study, we only interested the interactions between human Hsp70 and PFE55/*Pf*Hsp70x. As shown in the list (Table 3.5), two HsHsp70 proteins were identified in immunoprecipitation with PFE55-GFP. HSP74_HUMAN, a heat shock 70kDa protein 4 (HSP70RY) and GRP78_HUMAN, a 78 kDa glucose-regulated protein (GRP-78) with unique peptide ratio of three fold and four fold compared to control, respectively. This is highly suggests that PFE55 interacts with human Hsp70. Because of high homology, between GRP_human and parasite encoded heat shock protein 70 (HSP70-2) (64.384% identity), HSP70RY shares 30-40% homology with many parasite-encoded heat shock proteins, such as Hsp70x and Hsp110c. Therefore, it is

difficult to verify these data without more specific antibodies working with double species systems. In our study, although many of human Hsp70 protein peptides were found by precipitated with *Pf*Hsp70x. However, most of the peptide was not unique peptide, therefore, they couldn't take into account in our analysis. However, GRP-78, only was identified by binding with anti-*Pf*Hsp70x with 1 unique peptide and 2 peptide identification, but not found in control sample, which was still suggested the possibility the interaction between GRP-78 and *Pf*Hsp70x.

Table 3.3: Proteome identification of co-immunoprecipitation against with anti-GFP by LC/MS/MS (Plasmodium DB database).

Exported N=5						
Accession Number	**Protein names**	**Unique Peptide Number**	**Peptide Coverage**	**Unique Peptide Number**	**Peptide Coverage**	**Ratio**
PF3D7_0501100.1/2	heat shock protein 40, type II (PFE55)	6	15.423	0	0	6/0
PF3D7_0801000	Plasmodium exported protein (PHISTc), unknown function	3	4.102	0	0	3/0
PF3D7_1401100	DnaJ protein, putative	8	22.561	1	1.829	8
PF3D7_1407800	plasmepsin IV (PM4)	3	12.695	1	4.677	3
PF3D7_0831700	heat shock protein 70 (HSP70x)	17	34.866	6	15.464	2.83
Signal peptide N=3						
PF3D7_0929400	high molecular weight rhoptry protein 2 (RhopH2)	7	7.329	4	5.007	1.75
PF3D7_1116800	heat shock protein 101 (HSP101)	5	9.272	0	0	5/0
PF3D7_1471100	exported protein 2 (EXP2)	3	9.756	2	8.362	1.5
TM Domain N=2						
PF3D7_1408100	plasmepsin III (HAP)	2	5.965	0	0	2/0

Table 3.4: Proteome identification of co-immunoprecipitation with anti-PfHsp70x by LC/MS/MS (Plasmodium DB database).

Exported N=9						
Accession Number	**Protein names**	**Unique Peptide Number**	**Peptide Coverage**	**Unique Peptide Number**	**Peptide Coverage**	**Ratio**
PF3D7_0401800	Plasmodium exported protein (PHISTb), unknown function (PfD80)	2	4.46	0	0.00	2/0
PF3D7_0402400	Plasmodium exported protein,	6	36.61	0	0.00	6/0

	unknown function (GEXP18)					
PF3D7_0501100.1/2	heat shock protein 40, type II (PFE55)	4	15.92	0	0.00	4/0
PF3D7_0721100	conserved Plasmodium protein, unknown function	2	9.84	0	0.00	2/0
PF3D7_1001400	alpha/beta hydrolase, putative	2	3.47	0	0.00	2/0
PF3D7_1016300	glycophorin binding protein (GBP)	6	46.48	0	0.00	6/0
PF3D7_1201000	Plasmodium exported protein (PHISTb), unknown function	4	6.28	0	0.00	4/0
PF3D7_0831700	heat shock protein 70 (HSP70x)	38	57.44	3	12.08	12.67
PF3D7_0801000	Plasmodium exported protein (PHISTc), unknown function	9	12.22	0	0.00	9/0
Signal peptide N=20						
PF3D7_0207600	serine repeat antigen 5 (SERA5)	8	15.15	1	1.81	8.00
PF3D7_0302500	cytoadherence linked asexual protein 3.1 (CLAG3.1)	2	3.25	0	0.00	2/0
PF3D7_0827900	protein disulfide isomerase (PDI8)	5	18.63	1	3.42	5.00
PF3D7_0905400	high molecular weight rhoptry protein 3 (RhopH3)	11	19.84	4	6.24	2.75
PF3D7_0917900	heat shock protein 70 (HSP70-2)	19	36.35	4	7.36	4.75
PF3D7_0929400	high molecular weight rhoptry protein 2 (RhopH2)	25	25.04	6	6.39	4.17
PF3D7_0930300	merozoite surface protein 1 (MSP1)	11	8.37	1	2.85	11.00
PF3D7_1010700	dolichyl-phosphate-mannose protein mannosyltransferase, putative	3	18.39	2	16.55	1.50
PF3D7_1012200	conserved Plasmodium protein, unknown function	5	24.72	0	0.00	5/0
PF3D7_1015200.1/2	cysteine--tRNA ligase, putative (CysRS)	2	3.40	0	0.00	2/0
PF3D7_1105800	conserved Plasmodium protein, unknown function	3	13.53	0	0.00	3/0
PF3D7_1116000	rhoptry neck protein 4 (RON4)	2	1.67	0	0.00	2/0
PF3D7_1116800	heat shock protein 101 (HSP101)	4	6.51	0	0.00	4/0
PF3D7_1129100	parasitophorous vacuolar protein 1 (PV1)	5	14.82	2	5.75	2.50
PF3D7_1222300	endoplasmin, putative (GRP94)	7	12.42	2	3.41	3.50
PF3D7_1232100	60 kDa chaperonin (CPN60)	8	19.36	1	1.67	8.00
PF3D7_1252100	rhoptry neck protein 3 (RON3)	9	5.60	0	0.00	9/0
PF3D7_1454400	aminopeptidase P (APP)	17	29.09	8	13.26	2.13
PF3D7_1471100	exported protein 2 (EXP2)	4	14.98	1	3.83	4.00
TM Domain N=8						
PF3D7_0220000	liver stage antigen 3 (LSA3)	3	2.95	0	0.00	3/0
PF3D7_0801800	mannose-6-phosphate isomerase, putative	2	2.57	1	1.09	2.00

PF3D7_0811200	ER membrane protein complex subunit 1, putative (EMC1)	4	5.21	0	0.00	4/0
PF3D7_0823800	DnaJ protein, putative	3	8.40	0	0.00	3/0
PF3D7_1037300	ADP/ATP transporter on adenylate translocase (ADT)	3	15.62	0	0.00	3/0
PF3D7_1105800	conserved Plasmodium protein, unknown function	3	13.53	0	0.00	3/0
PF3D7_1311800	M1-family alanyl aminopeptidase (M1AAP)	12	17.51	1	2.58	12.00
PF3D7_1459400	conserved Plasmodium protein,	2	7.94	0	0.00	2/0

Table 3.5: Human heats shock 7 identification of co-immunoprecipitation with anti-GFP by LC/MS/MS (Uniprot Human Database)(ratio>2).

Accession Number	Entry name	Protein names	Unique Peptide Number	Peptide Coverage	Unique Peptide Number	Peptide Coverage	Ratio
P34932	HSP74_HUMAN	Heat shock 70 kDa protein 4 (HSP70RY) (Heat shock 70-related protein APG-2)	3	15.238	1	1.667	3
P11021	GRP78_HUMAN	78 kDa glucose-regulated protein (GRP-78) (Endoplasmic reticulum lumenal Ca(2+)-binding protein grp78) (Heat shock 70 kDa protein 5) (Immunoglobulin heavy chain-binding protein) (BiP)	3	21.407	0	8.716	3

3.3.4 Detection of identification proteins in co-immunoprecipitation (co-IP)

In this study, all of the potential interactions between *Pf*Hsp70x, PFE55 were verified by immunoblotting with the available working antibodies including the monoclonal mouse anti-GFP, polyclonal rabbit anti-*Pf*Hsp70x, monoclonal mouse anti-*Pf*Hsp101, polyclonal rabbit anti-*Pf*GBP130, polyclonal rabbit anti-*Pf*PHISTc, monoclonal mouse anti-human Hsp70, polyclonal rabbit anti-*Pf*EXP2 and polyclonal rabbit anti-*Pf*PV1.

So far, four parasite encoded proteins PFE55-GFP, *Pf*HSP70x, *Pf*PHISTc and *Pf*Hsp101 as well as a human heat shock 70 were identified in both co-immunoprecipitation (co-IP) assays with anti-GFP and anti-*Pf*Hsp70x, which were further confirmed by immunoblotting against anti-GFP, anti-*Pf*Hsp70x, anti-*Pf*Hsp101, anti-*Pf*PHISTc and anti-human Hsp70 using co-IP elution, respectively. To rule out non-specific binding during co-IP procedure, a co-IP with anti-GFP was performed on 3D7 wild type parasites; while for the co-IP with anti-*Pf*Hsp70x. the same procedure was applied using non-antibody-conjugated beads as empty control (Figure 3.7 A,B).

*Pf*GBP130 was found to potentially associate with *Pf*Hsp70x in both BN-PAGE and co-IP mass spectrometry data. This interaction was further verified by immunoblot analysis using anti-*Pf*GBP130 (Figure 3.7B). In addition, *Pf*EXP2 and *Pf*PV1 was also verified to be bound with *Pf*Hsp70x but not PFE55 (Figure 3.7A,B)

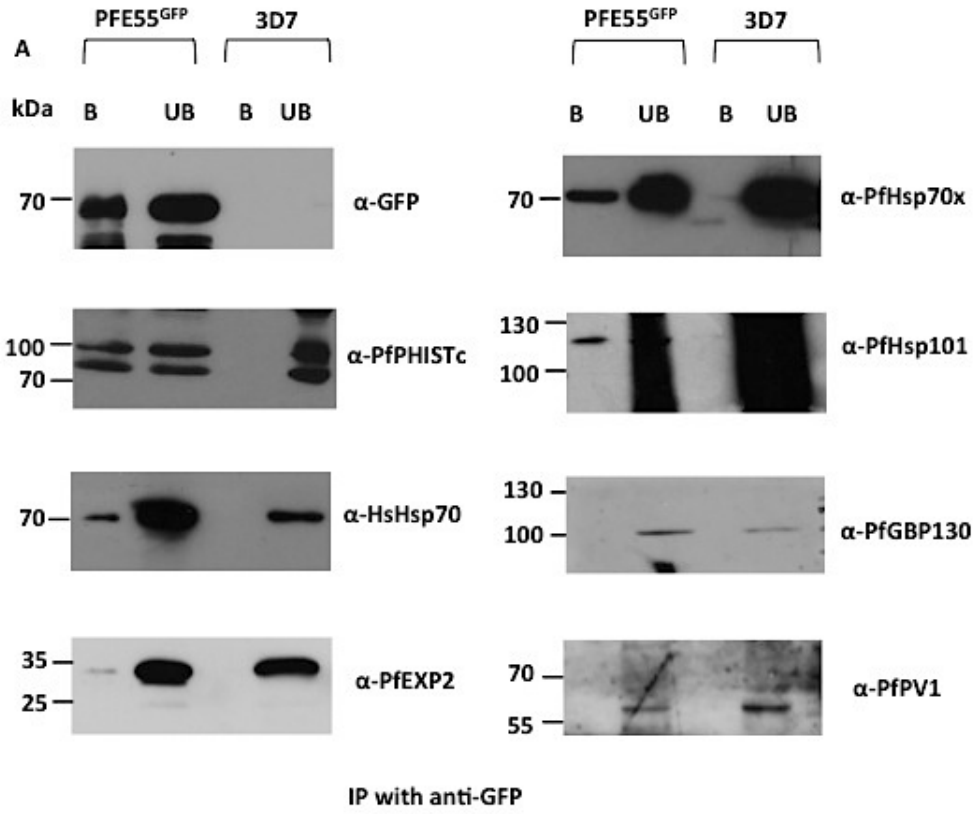

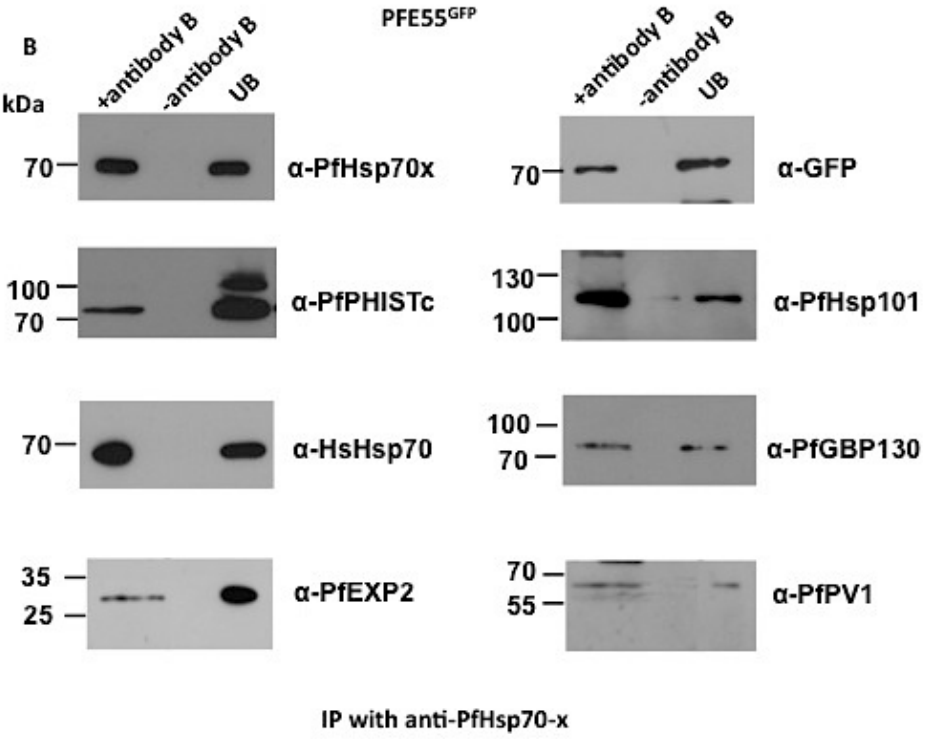

Figure 3.8: Western blot verification of protein-protein interactions.

A. Western blotting analysis of co-Immunoprecipitation using anti-GFP with lysates of PFE55^{GFP} and 3D7 strains (control). B. Western blot analysis of co-Immunoprecipitation with lysates of PFE55^{GFP} strain using *Pf*Hsp70 antibody-conjugated beads or empty bead only (control). UB: lysate. B: binding. The antibodies used including monoclonal mouse anti-GFP, polyclonal rabbit anti-*Pf*Hsp70x, monoclonal mouse anti-*Pf*Hsp101, polyclonal rabbit anti-*Pf*PHISTc monoclonal mouse anti-human Hsp70. polyclonal rabbit anti-*Pf*EXP2, polyclonal rabbit anti-*Pf*GBP130 and polyclonal rabbit anti-*Pf*PV1.

3.4 Protein complex containing *Pf*PHISTc/PFE55/*Pf*Hsp70x

Our mass spectrometry suggests that *Pf*HISTc is incorporated with *Pf*Hsp70x and PFE55, which was further verified by western blotting with anti-*Pf*PHISTc antibody. In order to investigate if the *Pf*PHISTc/PFE55/PfHsp70x containing protein complex contains is a J-dot protein complex and if it localizes to the parasite-infected erythrocyte cytosol; an immunoblot of two- dimensional BN/SDS-PAGE and a co-immunofluorescence were carried out.

3.4.1 Protein complex verification by using western blotting of 2D BN/SDS-PAGE

To further confirm that three exported proteins, PFE55-GFP, *Pf*Hsp70x and *Pf*PHISTc build a protein complex; the immunoblotting of 2D BN/SDS-PAGE was performed on the J-dot fraction of PFE55^{GFP} cell lysate.

The protein sample from 80,000 g (J-dot fraction) was separated on the first dimension on 4-15% gradient BN-PAGE, and then subject to a second dimension of a 10% SDS-PAGE and subsequently detected using specific antibodies including monoclonal mouse anti-GFP, polyclonal rabbit anti-*Pf*Hsp70x, and polyclonal rabbit anti-*Pf*PHSITc; Meanwhile, polyclonal rabbit anti-*Pf*Hsp70-1 was used as negative control. As shown in the figure 3.8, although the signal was not present as a clear spot due to low quality of *Pf*PHISTc antibody; nevertheless, the signal in immunoblotting of the second dimensional gel showed that three of proteins at present at the similar position with high molecular weights around 440kDa. The result suggests *Pf*PHISTc associats with E55-GFP and *Pf*Hsp70x as one of J-dot protein component.

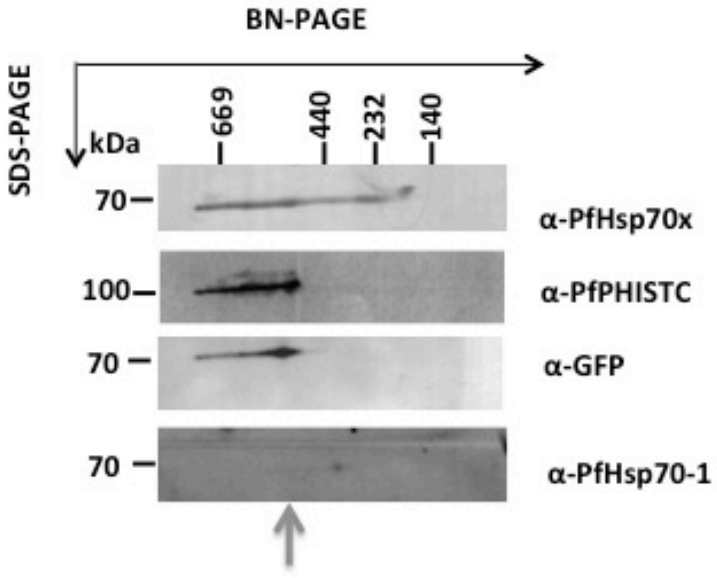

Figure 3.9: Western blotting of 2D BN/SDS-PAGE with J-dots protein complex.

The 80,000 g fraction from PFE55^{GFP} lysate was subjected to 2D BN/SDS-PAGE (4–15% and 10%, respectively), followed by the subsequent immunoblot analysis with monoclonal mouse anti-GFP (1:500 dilution), polyclonal rabbit anti-*Pf*Hsp70x (1:500 dilution), polyclonal rabbit anti-*Pf*PHSITc(1:1000 dilution). Non-specific binding was controlled by immunoblotting with anti-*Pf*Hsp70-1.

3.4.2 *Pf*PHISTc partially localizes to the J-dots

*Pf*PHISTc was likely to be the third component of the J-dots according to the results from co-immunoprecipitation (co-IP) with anti-GFP and anti-*Pf*Hsp70x as well as 2D BN/SDS-PAGE. In pervious a study, it has been shown that *Pf*Hsp70x partially localizes to the J-dots. Here, the immunofluorescence analysis was performed on *Pf*PHISTc^{GFP} transfected parasite line. As shown in the Figure 2.9, *Pf*Hsp70x localizes to the erythrocyte and PV; while *Pf*PHISTc indicated by green fluorescence localizes to erythrocyte. The partial co-localization of *Pf*PHISTc and *Pf*Hsp70x was shown as yellow florescence in the overlay image, which mostly locates in cytosol of the infected red blood cell (Figure 3.9)

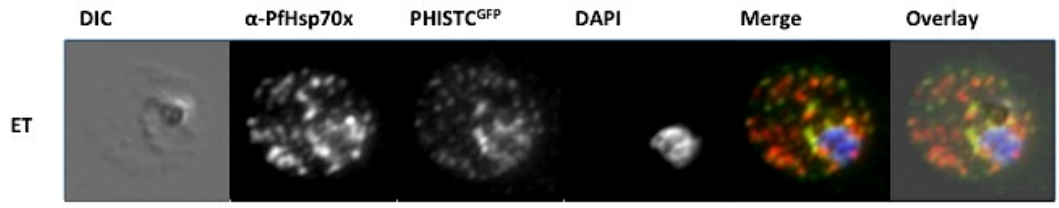

Figure 3.10: *Pf*Hsp70x co-localizes with PfPHISTc.

Fluorescence channels are shown individually in black and white, partial co-localization was observed in merged and overlay images. The polyclonal chicken anti-GFP antibody (green) and polyclonal anti-*P*fHsp70x antibody (red) were used in this analysis.

3.5 *Pf*GEXP18 is another J-dots protein associated with *Pf*Hsp70x

*Pf*GEXP18 is a *Plasmodium* exported protein previously been identified as a gametocyte protein with unknown function, which was identified in both BN-PAGE and pull down assay using anti-*Pf*Hsp70x by LC-MS/MS. Because of the lack of specific antisera against *Pf*GEXP18, GEXP18^{GFP} parasites were generated by Sonja Engels based on 3D7 wild type cell line expression *Pf*GEXP18-GFP fusion protein to further verify the interaction between *Pf*PfHsp70x and *Pf*GEXP18.

A co-immunoprecipitation (co-IP) was carried out on *Pf*GEXP18^{GFP} lysate of *in vivo* cross-linking with monoclonal mouse anti-GFP antibody beads; while 3D7 cell line was

used as control. The binding proteins were eluted and preceded for the immunoblot shown in the Figure 3.10, both of the proteins were observed in the elution.

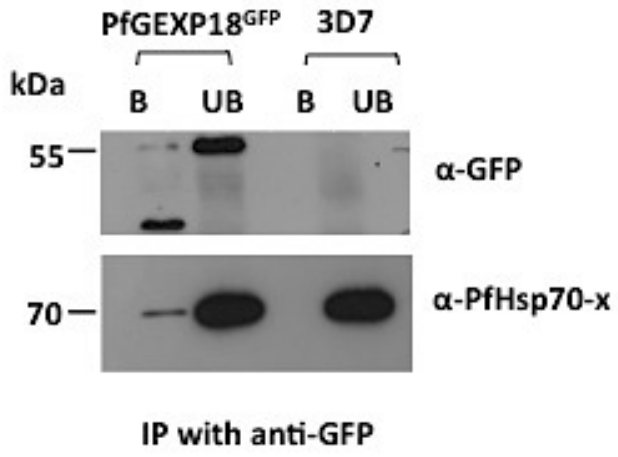

Figure 3.11: Western blot analysis *Pf*GEXP18^{GFP} with *Pf*Hsp70x.

Cell lyate was immunoprecipitated with anti GFP after *in vivo* crosslink cell. B, elution of co-immunoprecipitation, UB, supernatant of lysate, 3D7 wild –type cell line as a negative control. The pulled down complex were analysis by western blotting with antibody anti-GFP and anti-*Pf*Hsp70x.

3.6 *Pf*GBP130 associates with *Pf*Hsp70x and belongs to a new protein complex

*Pf*GBP130 was found to interact with *Pf*Hsp70x according to the result of BN-PAGE as well as co-immunoprecipitation (co-IP). In order to further confirm the specific interaction between them, a co-IP with polyclonal rabbit anti-*Pf*GBP130 was performed on PFE55^{GFP} lysate while the beads without antibody were used as negative control. After elution, both *Pf*GBP130 and *Pf*Hsp70x were detected in the immunoblot analyses using anti-*Pf*GBP130 and anti-*Pf*Hsp70x, respectively, indicating a close contact between each other *in vivo* (Figure 3.11).

In addition, the co-localization analysis of *Pf*GBP130 and *Pf*Hsp70x was performed using monoclonal mouse anti-*Pf*GBP130 and polyclonal rabbit anti-*Pf*Hsp70x. In order

to avoiding the green florescence from GFP, therefore, 3D7 cell line was used in this section. As shown in the figure 3.12, *Pf*GBP130 (labeled in green fluorescence), exhibits more intense signal and appears predominantly in vesicles as well as in the erythrocyte cytoplasm and the PV. It also partially co-localizes with *Pf*Hsp70x as shown by yellow fluorescent in both the PV and erythrocyte.

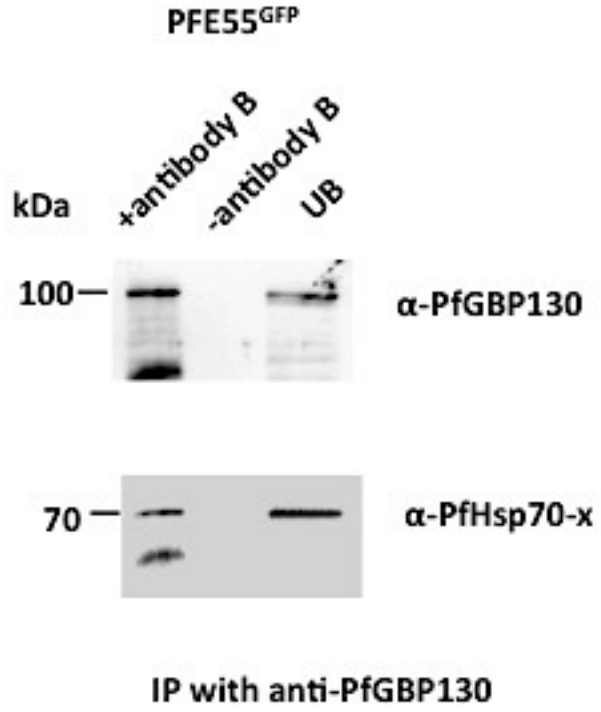

Figure 3.12: Western blot analysis of interaction between *Pf*GBP130 and *Pf*Hsp70x.

Co-Immunoprecipitation with polyclonal rabbit anti-*Pf*GBP130 was performed on PFE55^{GFP} lysate and verified with anti-*Pf*GBP130 and polyclonal rabbit anti-*Pf*Hsp70x. B: elution of co-immunoprecipitation. UB: cell lysate was used as positive control. Co-immunoprecipitation with non-antibody beads were used as negative control.

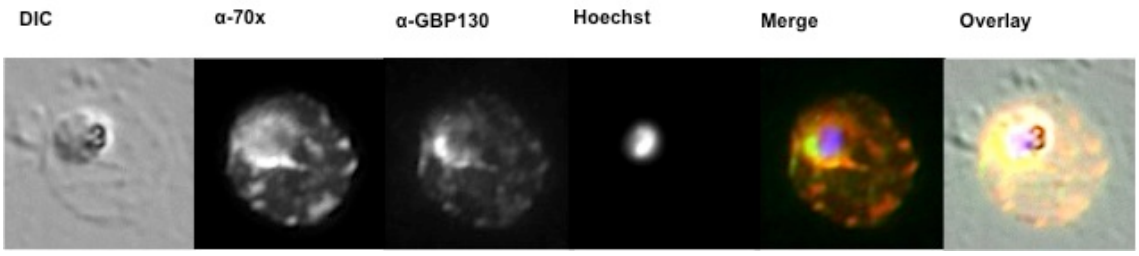

Figure 3.13: *Pf*Hsp70x co-localizes with *Pf*GBP130.

Fluorescence channels are shown individually in black and white, co-localization was observed in merged and overlay images. The monoclonal anti-*Pf*GBP130 antibody (green) and polyclonal anti-*P*fHsp70x (red) were used in the analysis

3.7 The interaction between *Pf*Hsp101 and *Pf*Hsp70x was verified by co-immunoprecipitation with anti-*Pf*Hsp101

*Pf*Hsp101 was found to associate with both *Pf*Hsp40 and *Pf*Hsp70x in co-immunoprecipitation (co-IP) assay. In order to confirm the specific interaction between them, a co-IP assay with monoclonal mouse anti-*Pf*Hsp101 was performed on PFE55^{GFP} lysate and beads without antibody were used as negative control. The binding proteins were eluted and detected by immunoblot analyses using the anti-*Pf*Hsp101, anti-*Pf*Hsp70x and anti-GFP. *Pf*Hsp70x was found in the pull down with *Pf*Hsp101 but not with PFE55-GFP, indicating that *Pf*Hsp70x indeed is in close contact with *Pf*Hsp101 (Figure 3.13).

Besides of co-IP and co-localization analysis of *Pf*Hsp101 and *Pf*Hsp70x was also performed on 3D7 parasite cell line using monoclonal mouse anti-*Pf*Hsp101 and polyclonal rabbit anti-*Pf*Hsp70x antibody. In order to avoiding the green florescence from GFP, 3D7 cell line was used in this analysis instead of PFE55-GFP transgenic cell line. In the previous study, *Pf*Hsp101 has been found as a component of PTEX translocon in the PVM (de Koning-Ward *et al.*, 2009). As shown in the figure 3.4, *Pf*Hsp101 (green fluorescence) surrounded in the membrane; while *Pf*Hsp70x partially co-localized with *Pf*Hsp70x (yellow fluorescence) (Figure 3.14).

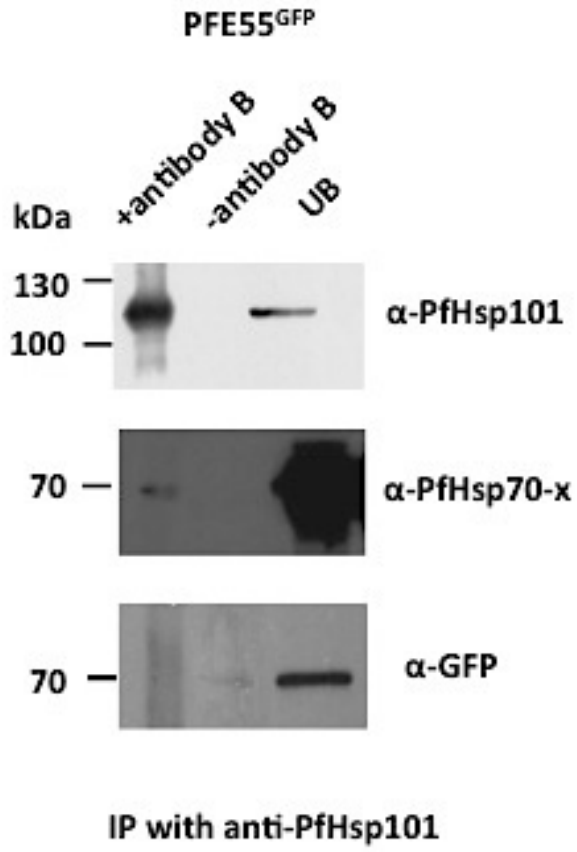

Figure 3.14: Western blotting analysis of interaction between *Pf*Hsp101 and *Pf*Hsp70x.

Co-Immunoprecipitation with monoclonal mouse anti-*Pf*Hsp101 was performed on PFE55^{GFP} lysate and verified with anti-*Pf*Hsp101 and polyclonal rabbit anti-*Pf*Hsp70x. B: elution of co-immunoprecipitation. UB: cell lysate was use as positive control. Co-immunoprecipitation with non-antibody beads was used as negative control.

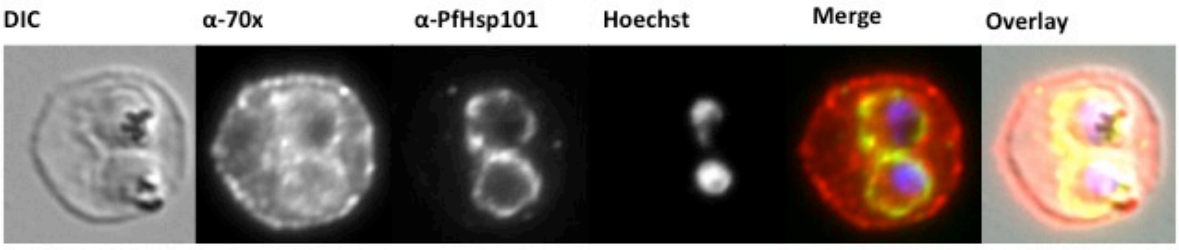

Figure 3.15: *Pf*Hsp70x co-localizes with *Pf*Hsp101.

Fluorescence channels are shown individually in black and white, co-localization was indicated in merge and overlay. The analysis was performed using monoclonal anti-*Pf*Hsp101 (green) and polyclonal anti-*P*fHsp70x (red).

3.8 The interaction between *Pf*Hsp101 and *Pf*Hsp70x is sensitive to proteinase K treatment

3.8.1 LC-MS/MS identification of *Pf*Hsp70x interaction protein from cell lysates after Streptolysin O -Proteinase K protection assay

*Pf*Hsp101 and several more proteins were found in association with *Pf*Hsp70x by co-immunoprecipitation (co-IP) and were further verified with western blotting and co-immunofluorescence assay. To determine subcellular locations of these protein complexes, a streptolysin O with proteinase K protection assay was performed, while saponin lysis was used as the control. After SLO and saponin permeabilization lysis and proteinase K treatment, the pellet fractions were lysed, proceeded by co-IP with anti-*Pf*Hsp70x antibody and identified with following LC-MS/MS and verified with immunoblot (Figure 3.15)

SLO (streptolysine O) is a membrane damage toxin secreted by *Streptococcus pyogenes*. SLO can permeabilize the host red blood cell membrane while leave the PV (parasitophorous vacuole) stays. SLO binds to surface exposed membrane cholesterols and induces a 30nm hole in the membrane (Bhakdi *et al.*, 1985; Jackson *et al.*, 2007). Saponin is a glycoside, which is commonly found in plants and which is known to disintegrate the erythrocyte membrane and the parasitophorous vacuolar membrane of *P. falciparum* and leaves the parasite interacting with cell membrane cholesterol, leading to the permeabilization of the membrane (Beaumelle *et al.*, 1987)

First of all, the *in vivo* cross-linked PFE55^{GFP} cells were permeabilized with streptolysin O. The supernatant fraction contained erythrocyte cytosol; while pellets contained permeablilized red blood cell membrane, PVM, and the intact parasite. After saponin lysis, the supernatant fraction of contained erythrocyte cytosol and PV cytosol, while the pellet contained permeablilized red blood cell membrane, PVM and the intact parasite. The pellet fraction was then treated with proteinase K in order to verify if the protein complexes were located at the parasitophorous vacuole. Proteins whose C terminus exposed to erythrocyte cytosol were degraded.

*Pf*SERP as a soluble PV protein was used as a control to demonstrate that PV was still intact and could be found in the pellet fraction after SLO lysis. In contrast to saponin

lysis, where *Pf*SERP was present in the supernatant at the size of 140kDa, indicating the PVM was lysed successfully lysed. In addition, human Hsp70 was used as a red blood cytosol marker protein that was found in the supernatant fractions in both treatments. *Pf*Aldolase as a parasite cytosol protein was found in the pellet of both SLO and saponin lysate at a size of approximately 45 kDa, which indicates that the parasite remained intact after lysis (Figure 3.16).

The pellet from SLO and saponin lysate was treated with proteinase K followed lysis and co-IP with polyclonal rabbit anti-*Pf*Hsp70x antibody. The identification of binding proteins by mass spectrometry was shown in table 3.6 with two unique peptide matching. Totally, 52 parasite encoded proteins were identified and specific binding protein were selected containing either i) containing a classical N-terminal signal sequence only, ii) having a predicted PEXEL/HT export motif OR an annotation as "exported", or iii) having a hydrophobic domain. Surprisingly, *Pf*Hsp101 was not anymore identified in pulled down with *Pf*Hsp70x after treat with proteinase K, indicating that proteinase K assay break the interaction between *Pf*Hsp101 and *Pf*Hsp70x. Interestingly, PFE55 was found in the pellet fraction associating with *Pf*Hsp70x, in contrast to previous hypothesis that PFE55-*Pf*Hsp70x forms a J-dot protein complex which exclusively localizes to iRBC cytosol (Kulzer *et al.*, 2012). In addition, *Pf*GBP130 was identified to interact with *Pf*Hsp70x in the parasitophorous vacuole, which suggests that the interaction between *Pf*Hsp70x and *Pf*GBP130 was present in both erythrocyte cytosol and parasitophorous vacuole.

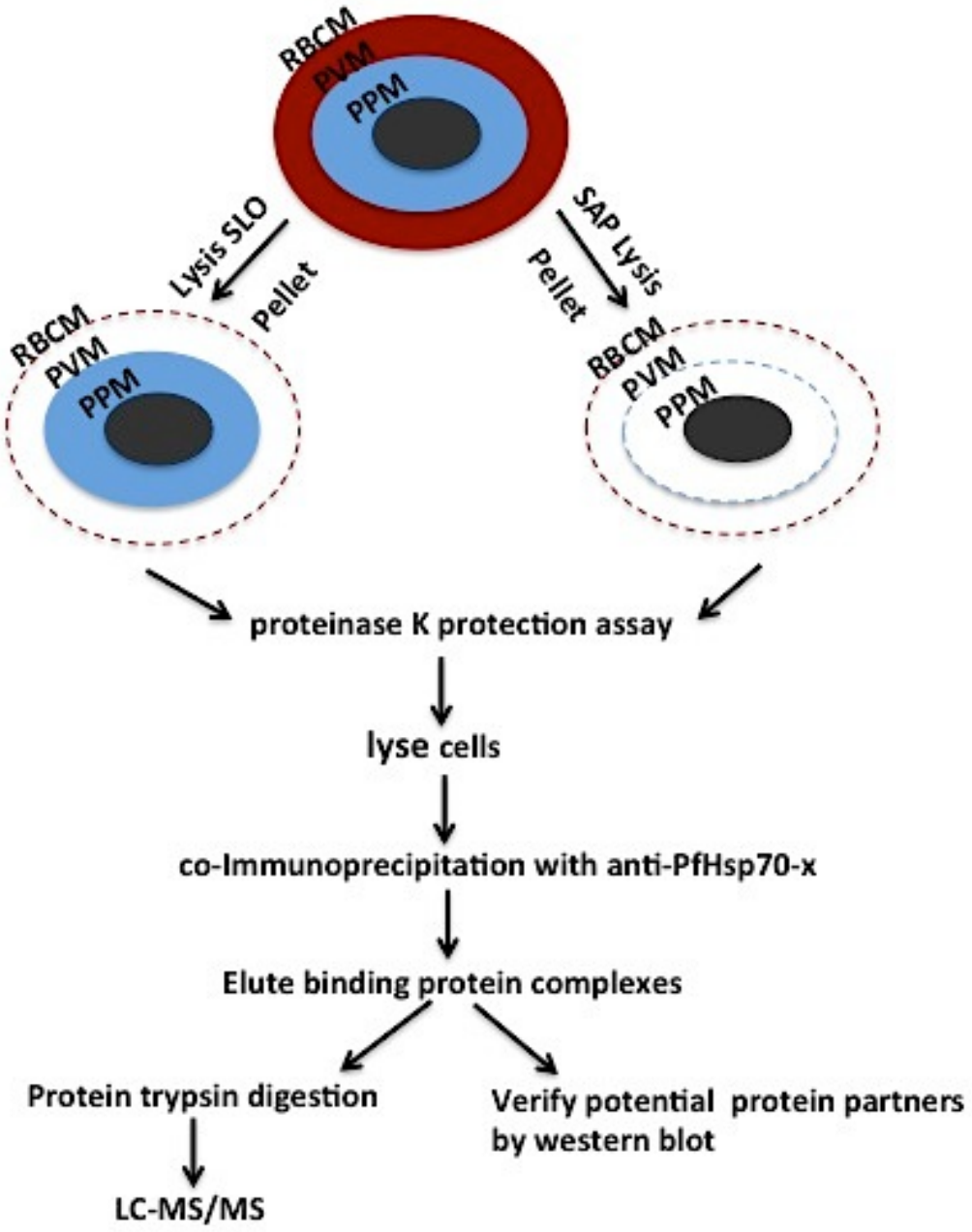

Figure 3.16: A whole work flow of co-IP analysis *Pf*Hsp70x interaction protein after streptolysin O and proteinase K protection assay.

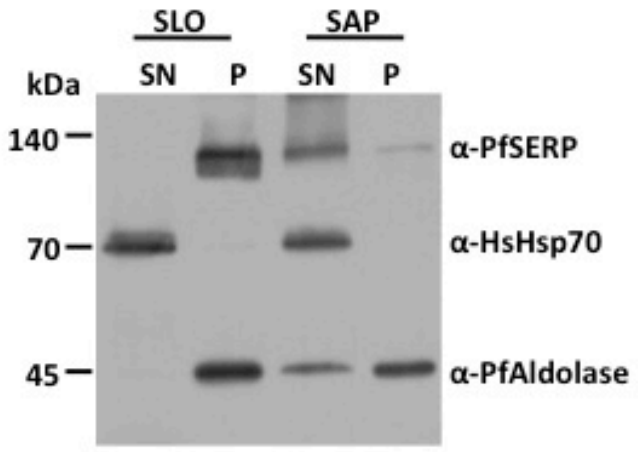

Figure 3.17: Western blotting analyses SLO and saponin lysis.

The PFE55^{GFP} cells were enriched and lysed with SLO and saponin; after centrifugation, the supernatant and pellet were separated and further analyzed by western blotting with polyclonal rabbit anti-*Pf*SERP (parasitophorous vacuole), monoclonal mouse anti-*Pf*Aldolase (parasite cytosol) and monoclonal mouse anti-HsHsp70 (erythrocyte cytosol).

Table 3.6: Co-immunoprecipitation with anti-*Pf*Hsp70x by LC/MS/MS (Plasmodium DB Database)

Exported N=9						
Accession Number	**Protein names**	**Unique Peptide Number**	**Percent Coverage**	**Unique Peptide Number**	**Percent Coverage**	**Ratio**
PF3D7_0501100.1 /2	heat shock protein 40, type II (HSP40)	5	12.935	0	0.00	5/0
PF3D7_1016300	glycophorin binding protein (GBP)	5	42.961	0	0.00	5/0
PF3D7_0831700	heat shock protein 70 (HSP70x)	41	55.523	3	12.08	13.67
Signal peptide N=20						
PF3D7_0827900	protein disulfide isomerase (PDI8)	3	8.075	1	3.42	3.00
PF3D7_0917900	heat shock protein 70 (HSP70-2)	15	26.994	4	7.36	4.75
PF3D7_0929400	high molecular weight rhoptry protein 2 (RhopH2)	3	3.193	6	6.39	4.17
PF3D7_0930300	merozoite surface protein 1 (MSP1)	4	2.384	1	2.85	11.00
PF3D7_1222300	endoplasmin, putative (GRP94)	4	5.725	2	3.41	3.50
PF3D7_1232100	60 kDa chaperonin (CPN60)	3	5.989	1	1.67	3.00

PF3D7_1454400	aminopeptidase P (APP)	15	26.255	8	13.26	2.13
TM Domain N=8						
PF3D7_1311800	M1-family alanyl aminopeptidase (M1AAP)	6	8.111	1	2.58	12.00

3.8.2 Immunoblot analysis of protein interaction with *Pf*Hsp70x after proteinase K assay

The identified proteins were further verified by western blotting against anti-GFP, anti-*Pf*Hsp70x, anti-*Pf*GBP130 and anti-*Pf*Hsp101; while immunoblotting of samples from the saponin-proteinase K assay severed as control.

PFE55-GFP, *Pf*Hsp70x *Pf*Hsp101 and *Pf*GBP130 were detected in the lysate from SLO-proteinase K assay but not in the lysate of the pellet fraction after saponin-proteinase K assay, which indicates that these proteins were present in the PV and PVM. Furthermore, *Pf*Hsp70x, PFE55-GFP, and *Pf*GBP130 were found in the elutes from co-immunoprecipitation (co-IP) verified by immunoblotting, which was consistent with the data from LC-MS/MS (Figure 3.17 B). The result suggests that *Pf*Hsp70x interacts with PFE55-GFP and *Pf*GBP130 in both erythrocyte cytosol and PV.

In section 1.3.3, *Pf*Hsp101 was shown to be interacting with *Pf*Hsp70x identified by LC-MS/MS, and this was further proved by and co-IP with *Pf*Hsp101. However, the interaction between these two proteins was interrupted by proteinase K treatment. Therefore, interaction between *Pf*Hsp70x and *Pf*Hsp101 was most likely mediated by *Pf*EXP2 that is present in the same PTEX translocon complex with *Pf*Hsp101. In addition, *Pf*Hsp70x was binding to this complex cross the PVM and faces the erythrocyte cytosol.

The followed western blotting of SLO lysate verified the *Pf*Hsp101 was not exported into the erythrocyte cytosol (Figure 3.17 A). *Pf*SERP and *Pf*Aldolase, the marker protein for PV and parasite cytosol, respectively, were only detected in the pellet fraction as well as *Pf*Hsp101; while erythrocyte cytosol protein HsHsp70 was found in the supernatant.

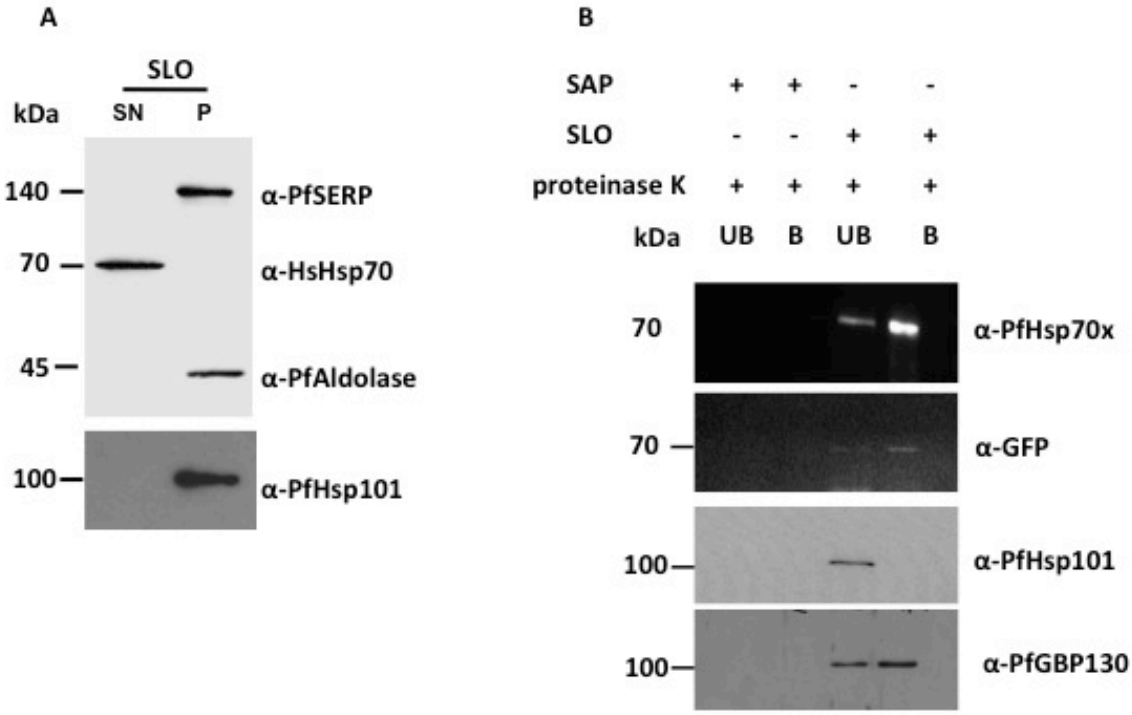

Figure 3.18: Western blotting analysis distribution of different *Pf*Hsp70x complexes in the infect red blood cell.

A: western blotting analysis of lysates from SLO and saponin-Proteinase K protection assays on PFE55^{GFP} cell line; B: Co-immunoprecipitation with anti-*Pf*Hsp70x using the pellet fraction from SLO and saponin-Proteinase K protection assays. B: Elution of co-IP. UB: Lysate.
B: western blotting analysis of *Pf*Hsp101 in different fractions. Antibodies used are listed as following: monoclonal mouse anti-GFP, polyclonal rabbit anti-*Pf*Hsp70x, polyclonal rabbit anti-*Pf*SERP (parasitophorous vacuole), monoclonal mouse anti-*Pf*Aldolase (parasite cytosol) and monoclonal mouse anti-HsHsp70 (erythrocyte cytosol), monoclonal mouse anti-*Pf*Hsp101 and monoclonal mouse anti-*Pf*GBP130.

4 DISCUSSION

Plasmodium falciparum exports more than 400 proteins to the infected red blood cell to modify its host cell in morphology, physiology and function (Hiller *et al.*, 2004; Marti *et al.*, 2004; Sargeant *et al.*, 2006; Maier *et al.*, 2008; Maier *et al.*, 2009). The question of how exported proteins cross the parasitophorous vacuole membrane and how these are further secreted to the red blood cell membrane surface has been raised for long time. Some knowledge was added to this by the identification of highly mobile structures in the iRBC cytosol, referred to as J-dots. J-dots contain two parasite-encoded chaperones Hsp40 (PFE55, PFA660) and *Pf*Hsp70x (Külzer et al. 2010, 2012), in addition, *Pf*Hsp70x was found within parasitophorous vacuole as well. In order to shed some light on the role of the chaperone/co- chaperones complex *Pf*Hsp70x-PFE55 (J-dots) in the infected erythrocyte, in this study, multiple proteomics as well as biochemical methods were used. By those approaches a complete profile of the protein-protein interaction network containing PFE55-*Pf*Hsp70x (J-dots) was obtained. A full overview of the protein-protein interaction network *Pf*Hsp70x/PFE55 is shown in Figure 4.1.

4.1 Investigation of protein complexes localized in J-dots fraction

It is always challenging to purify and identify protein complexes from a large proteome. High abundance proteins such as ribosome proteins, keratin, actin and many others cell compartment proteins always affect especially identification proteins expressed in low quantities. In order to investigate the protein complexes in J-dots, differential centrifugation, BN PAGE, 2D BN/SDS PAGE and LC-MS/MS were used to characterize protein complexes in J-dot.

4.1.1 *Pf*Hsp70x- PFE55 chaperone/co-chaperones are present in a common high molecular weight protein complex

Different centrifugation has been widely used for isolating many organelles such as mitochondria, endosome, Golgi in different species system including *Plasmodium* (Schnaitman and Greenawalt, 1968; Krungkrai *et al.*, 1993; Schroter *et al.*, 1999). It is always used as first purification step combine with the other protein study methods for isolating protein and protein complex. In *Plasmodium* system, it has been successful helping isolate many protein and protein complex, such as Maurer's clefts protein, Rhoptry protein complex (Cao *et al.*, 2009; Pachlatko *et al.*, 2010) Therefore, we also chosen differential centrifugation as the first step to purify the J-dot fraction in our study. In order to get more information of this J-dot protein complex, we separated the J-dot fraction on a BN-PAGE. BN-PAGE is also a mature proteomics technology that has been wildly used for separating both cell lysate protein complex and membrane bound protein complex. The most important issue of BN-PAGE is to choose an appropriate non-ionic detergent for the solubility as well as stability of the protein complex. Külzer and colleagues did not reveal if J-dots are membranous structures (Kulzer *et al.*, 2012). Although, Triton X-100 is suitable for cell lysates of different human cell lines (Camacho-Carvajal *et al.*, 2004), it was not useful for J-dot protein complexes separating in BN-PAGE. In consequence, two other detergents, dodecylmaltoside (DDM) and digitonin, were chosen for dissolution of the J-dot fractions. Upon the addition of DDM, a clear GFP signal was observed at >232KDa. However, by using digitonin, two clear GFP signals were detected, one signal >232KDa, the other one >440 KDa~669KDa. This was further verified by immunoblotting with 2D BN/SDS PAGE, three pairs of GFP and *Pf*Hsp70x signals were observed >223KDa, 440-669KDa and >669KDa. Digitonin is known as a mild detergent that solubilizes and stabilizes supercomplexes while DDM leads to the dissociation of these structures into single protein complexes (Schagger and Pfeiffer, 2000). Therefore, the results indicate that the J-dot protein complex contains *Pf*Hsp70x and PFE55 at least with a molecular weight ~223-440KDa.

4.1.2 LC-MS/MS of BN-PAGE identification of multiple protein complexes containing *Pf*Hsp70x

BN-PAGE has been widely used for studying protein-protein interactions in membranes, total cell and tissue (Schagger *et al.*, 1994; Poetsch *et al.*, 2000; Wittig *et al.*, 2006). In *P. falciparum* studies, it has been successful used for investigation of proteasome complexes and PTEX translocon protein complex (de Koning-Ward *et al.*, 2009; Sessler *et al.*, 2012; Beck *et al.*, 2014). In our study, we try to use BN-PAGE to isolate our protein complex. By coupling LC-MS/MS to BN-PAGE, *Pf*Hsp70x was identified with some exported proteins including PHISTb family protein, *Pf*GEXP18, and *Pf*GBP130, Which gives us a better idea of that *Pf*Hsp70x maybe involved into multiple protein complexes. Unfortunately, we couldn't find PFE55 in BN-PAGE. The possible reason for the lack of PFE55 is due to highly expressed proteins. Most of the proteins that were identified in these two bands belong to several high molecular weight protein complexes including *Plamodium* rhoptry neck (RON) protein complex and low and high rhoptry complexes protein complex (Cowman et al., 2012).

4.2 Protein-protein interaction identification by Co-immunoprecipitation (co-IP) and LC-MS/MS

In order to investigation of components of protein complexes contains PFE55 and *Pf*Hsp70x, co-IP assays with anti-GFP and anti-*Pf*Hsp70x specific antisera were performed on *in vivo* cross-linked PFE55^{GFP} transgenic parasites. The candidate interactions proteins were analysed by LC-MS/MS and immunoblotting, Although, J-dots are found in the iRBC cytosol also many other proteins from different parasite compartments (e.g. parasitophorous vacuole) were found to bind the PFE55/*Pf*Hsp70x co-chaperone-chaperone complex. Therefore, in this study the focus was laid on parasitophorous vacuole and erythrocyte proteins. After selected the candidate proteins according to the subcellular localisation and peptide count ratio. It is not surprise that we found PFE55 identified only interact with six protein including *Pf*Hsp70x, while *Pf*Hsp70x identified interact with much more numbers of proteins. *P. falciparum* genome 43 members of Hsp40 family and only six members of Hsp70 (Botha *et al.*, 2007). Amongst of them, there are 19 members of Hsp40 compare to only one Hsp70 (Hsp70x) predicted exported to the erythrocyte cytosol. Therefore,

PfHsp70x appears to interact with a larger number of substrate proteins than PFE55 (Botha *et al.*, 2007)

4.2.1 *Pf*PHIST_0801 associates with PFE55 and *Pf*Hsp70x at J-dots

There are two proteins *Pf*Hsp101 and PF3D7_0801000, with different localizations, were co-predicated with both anti-GFP and anti-*Pf*Hsp70x. *Pf*PHIST_0801 (PF3D7_0801000) is a member of PHISTc family, which co-immunoprecipitated with both PFE55-GFP and *Pf*Hsp70x, with three- fold and nine- fold unique peptide identification compared to negative control, respectively. This was further verified by immunoblotting of co-IP and co-localization with *Pf*Hsp70x. Moreover, a western blotting of 2D BN/SDS PAGE was employed to confirm that PFE55-GFP, *Pf*Hsp70x and *Pf*PHISTc belong to the same high molecular weight protein complex. Therefore, *Pf*PHIST_0801 was suggested as the third component of the J-dot protein complex by associating with PFE55 and *Pf*Hsp70x in the infected erythrocyte cytosol.

Except *Pf*PHIST_0801, two more PHISTb family proteins PF3D7_1201000 and PF3D7_0401800 were identified by pull downs with *Pf*Hsp70x followed LC-MS/MS. The PHIST (Poly-Helical Interspersed Sub-Telomeric) family is a large protein family with 72 members and is divided into three sub-families including PHISTa, b, c (Sargeant *et al.*, 2006). A recent study found that some of the PHIST family proteins are involved in knobs formation, in contrast to PHISTb (PF3D7_0401800) which is essential for the parasite survival (Maier *et al.*, 2008; Tarr *et al.*, 2014). The latest study showed that PHIST proteins are involved in *Pf*EMP1 trafficking to the cell surface (Oberli *et al.*, 2016). In our previous study, we suggested that J-dots are involved in *Pf*EMP1 trafficking to the host cell based on the fact that *Pf*EMP1 co-localized with Hsp70x during its transport (Kulzer *et al.*, 2012), In this study, this hypothesis was further confirmed by the identification of several PHIST family proteins that interacted with PFE55/*Pf*Hsp70x. Unfortunately, in our study, *Pf*EMP1 was not identified by LC-MS/MS from co-IP neither with anti-GFP nor with anti-*Pf*Hsp70x. It is possible that *Pf*EMP1 was not identified due to the stage dependent interaction of *Pf*Hsp70x and *Pf*EMP1. In our previous study *Pf*Hsp70x and *Pf*EMP1 showed a high co-localization at very early parasite stages (Kulzer *et al.*, 2012). Moreover, *Pf*EMP1 is a high molecular weight protein with low abundance, which makes it difficult to precipitate this protein.

As so many exported proteins were identified to associate with *Pf*Hsp70x it is likely for *Pf*Hsp70x to have a role in the delivery of proteins to their destinations.

4.2.2 *Pf*GEXP18 interacts with Hsp70x at the J-dots

*Pf*GEXP18 is an exported protein with unknown function and found to be expressed in early gametocyte stages and asexual blood stages (Aurrecoechea *et al.*, 2009; Silvestrini *et al.*, 2010). In our study, *Pf*GEXP18 was identified interacted with *Pf*Hsp70x. Because of the lack of a specific antibody of *Pf*GEXP18, a transgenic parasite cell line was generated that expressed a *Pf*GEXP18-GFP fusion protein. During live cell image of the *Pf*GEXP18GFP showed, highly mobile dots that had no fixed direction. Form the morphological point of view *Pf*GEXP18 showed a J-dot like (Kulzer *et al.*, 2012). Moreover, immunofluorescence assay showed that *Pf*GEXP18 co-localized with *Pf*Hsp70x, which indicates that *Pf*GEXP18 is localized at J-dots by incorporation with *Pf*Hsp70x. However, because of lacking the function of *Pf*GEXP18, therefore it is difficult to explain whether *Pf*GEXP18 incorporate with J-dots protein as a partner or be trafficked by J-dots, and this is need to be further investigate in the future.

4.3 *Pf*Hsp70x associate with PTEX translocon

Hsp101/ClpB is belongs to HSP100 protein family, and found in many different species such as bacteria, plants and eukaryotic mitochondria with highly conserved sequences (Lee *et al.*, 1994; Nieto-Sotelo *et al.*, 1999; Doyle and Wickner, 2009). Hsp101/ClpB helps solubilize the aggregate protein formed during the heat stress (Doyle and Wickner, 2009). In addition, many studies found Hsp101/ClpB works incorporation with DnaK/Hsp70 chaperone for aggregate protein degradation (Goloubinoff *et al.*, 1999; Zolkiewski, 1999; Doyle and Wickner, 2009). In our study, parasite-encoded *Pf*Hsp101 was found to specifically interact with both *Pf*Hsp70x as well as PFE55 in co-IP, immunoblotting and co-localization assay. *Pf*Hsp101 is a component of the PTEX translocon which is localized in the parasitophorous vacuole membrane (de Koning-Ward et al., 2009). The role of *Pf*Hsp101 in protein transport was predicated to be in co-operation with some other heat shock proteins to keep exported proteins unfolded, and then transport the protein cross the parasitophorous vacuole membrane by

passing through the pore formed by EXP2 (de Koning-Ward et al., 2009). Others and we have suggested that *Pf*Hsp70x helps in the protein transport by interacting with the PTEX translocon either at the -cis or -trans side of the parasitophorous vacuole membrane (Kulzer *et al.*, 2012; Elsworth *et al.*, 2016). The exported proteins could be chaperoned by *Pf*Hsp70x to keep them unfolded to the PTEX by interaction with *Pf*Hsp101 or help the transport protein refolding after cross the parasitophorous vacuole membrane (de Koning-Ward *et al.*, 2009; Kulzer *et al.*, 2012). Although, some parasite encoded Hsp70s were predicated to interact with *Pf*Hsp101, only *Pf*Hsp70x was found in both parasitophorous vacuole and erythrocyte cytosol. This strongly suggests that *Pf*Hsp70x plays an important role in protein traffic cross parasitophorous vacuole membrane, by interacting with *Pf*Hsp101. In order to elucidate if *Pf*Hsp70x interacts with *Pf*Hsp101 in a *cis*- or *trans*- fashion, a protease K assay was used to digest residual *Pf*Hsp70x of the erythrocyte cytosol. Surprisingly, *Pf*Hsp101 was not identified in a pull down experiment with *Pf*Hsp70x after proteinase K treatment, which suggests that the interaction between *Pf*Hsp101 and *Pf*Hsp70x was broken down by the proteinase K treatment. *Pf*Hsp101 faces towards the parasitophorous vacuole and was thereby protected from protease K treatment which hints towards an indirect interaction of *Pf*Hsp101-*Pf*Hsp70x that is mediated by other parasitophorous vacuole membrane resident factors. Interestingly, another PTEX translocon component, exported protein 2 (EXP2), was identified and verified to interact with *Pf*Hsp70x by LC-MS/MS and western blotting. *Pf*EXP2 is a membrane associate protein forming a channel in the parasitophorous vacuole membrane by which unfolded proteins can pass to reach the erythrocyte cytosol (de Koning-Ward *et al.*, 2009; Molloy, 2014). Therefore, it can be hypothesized that *Pf*EXP2 mediates the binding between *Pf*Hsp70x (erythrocyte cytosol) and *Pf*Hsp101 (parasitophorous vacuole lumen).

A recently study from Elsworth&Sander *et al.*, identified *Pf*PV1 and *Pf*Hsp70x in association with the PTEX translocon core component PTEX150, they suggested that *Pf*Hsp70x associates with PTEX at the erythrocyte side and might there be involved in the refolding of proteins after their path through the PTEX translocon (Elsworth *et al.*, 2016). These observations are consistent with our obtained data which identified an interaction between *Pf*Hsp70x and *Pf*Hsp101, possibly mediated by *Pf*EXP2, at the trans-side of the parasitophorous vacuole membrane. So far, the function of the interaction between *Pf*Hsp70x and PTEX translocon is lacking in our study and we are generating several *Pf*Hsp70x knockdown transgenic parasite lines to reveal the

importance role of *Pf*Hsp70x in protein transport.

4.4 Other protein interactions with *Pf*Hsp70x in the parasitophorous vacuole

In this study, PFE55 and *Pf*GBP130 were both identified as interaction partners of *Pf*Hsp70x in the lumen of parasitophorous vacuole. After proteinase K protection assay, a further verification of the already proven PFE55 interaction with *Pf*Hsp70x in iRBC cytosol was achieved (Kulzer *et al.*, 2010; Kulzer *et al.*, 2012). So far, the function of the PFE55-PfHsp70x complex in the parasitophorous vacuole is unknown. However, some hypothesis suggest that exported proteins could be chaperoned by parasite encoded Hsp70s/40s to keep them in an unfolded state or to unfold proteins before being delivered to *Pf*Hsp101 to pass through the parasitophorous vacuole membrane (Maier *et al.*, 2008; Gehde *et al.*, 2009). Whether the incorporate between the *Pf*Hsp70x and PFE55 support the protein transport through the PTEX translocon or not needs to be further analyzed.

*Pf*GBP130 is known as an exported protein localized in the parasitophorous vacuole and erythrocyte cytosol (Ansorge *et al.*, 1996). *Pf*GBP130 interacts with *Pf*Hsp70x in the parasitophorous vacuole as well as in the erythrocyte cytosol with anti-*Pf*GBP130 of 2D BN/SDS PAGE indicates that the *Pf*GBP130-*Pf*Hsp70x protein complex is potential raised to a supercomplex by binding the J-dot protein complex.

4.5 PFE55 interaction with Human Hsp70

There is the long-standing question of a potential interaction of parasite-encoded type II Hsp40s and human Hsp70 chaperones before exported PfHsp70x found. Since parasite-encoded type II Hsp40s is homologous with the human DnaJB4, cooperation with human Hsp70s might be possible.. In order to address the question of an interaction between human hsp70 and PFE55, all of the raw data was search against human database. There were two HsHsp70 protein identified to interact with PFE55-GFP, HSP74_HUMAN and GRP78_HUMAN, which was highly suggests a chimeric interaction PFE55 and human Hsp70. Also, a recently study of Hsp40 (PFA0660w) shows functionally interacts with *Pf*Hsp70x as a co-chaperone, but not the human Hsp70 (Daniyan *et al.*, 2016) However, the chimeric chaperone-co-chaperone

complexes could assist parasite-exported proteins in refolding after traffic through the PTEX translocon has been described (Charpian and Przyborski, 2008; de Koning-Ward *et al.*, 2009; Gehde *et al.*, 2009). Therefore, in order to better understand the importance interaction between human Hsp70 and PFE55 in protein trafficking, a further study will be continued.

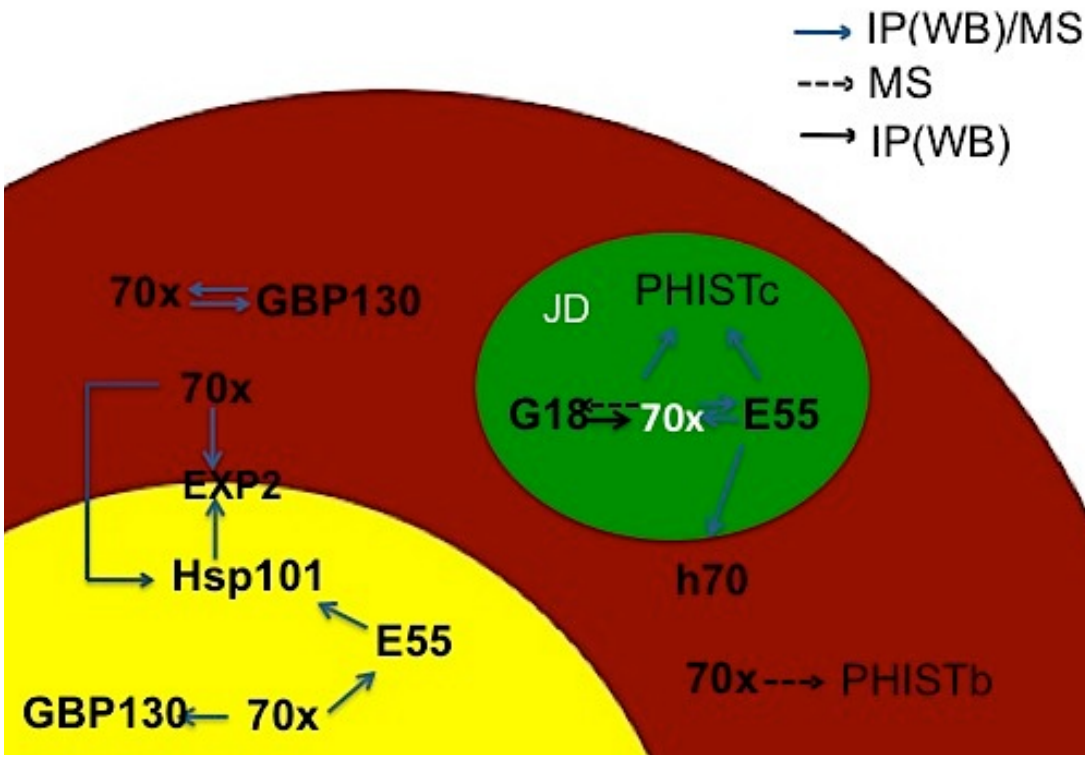

Figure 4.1: Protein-protein interactions network with *Pf*Hsp70x/PFE55 model.

JD: J-dot; red color: erythrocyte cytosol; yellow color: parasitophorous vacuole; IP: immunoprecipitation; WB: western blot; MS: mass spectrometry

4.6 Summary and outlook

As the exported parasite-encoded proteins are responsible for many modifications of host cell, we are always interest in study of protein transporting in the infected iRBC. Our previously study found a parasite-encoded *Pf*Hsp70x was cooperate with parasite-encoded Hsp40s (PFE55/PFA660) in the infected erythrocyte cytosol. Hsp40s (PFE55/PFA660) and *Pf*Hsp70x both are important chaperones and have been implicated involve in several cellular processes in host cell. In order to better understanding the functional of Hsp40 (PFE55) /Hsp70x chaperone/co-chaperones, In this study, we use multiple proteomics analysis method to study the protein-protein interaction and further construct a protein network of Hsp40 (PFE55) /Hsp70x.

It is a challenge to study protein complex in *Plasmodium falciparum* infected red blood cell, a complicated proteome system which originates from two species. Therefore, multiple proteomic methods were carried to purify and characterize protein complexes containing *Pf*Hsp70x, e.g. BN-PAGE, 2D BN/SDS PAGE, co-immunoprecipitation (co-IP). Surprisingly, *Pf*Hsp70x was found to be involved in a multi- protein complex, and Hsp70x protein interactions occurred in both erythrocyte cytosol and parasitophorous vacuole.

In parasite infected erythrocyte cytosol, one protein complex was localized at J-dots including PFE55, *Pf*Hsp70x, *Pf*PHIST_0801 and *Pf*GEXP18. In our previous study, we found that *Pf*EMP1 co-localized with *Pf*Hsp70x at J-dots, which implicated that J-dots play a role for the transport of *Pf*EMP1 to host cell membrane. Unfortunately, so far, we are unable to immunoprecipitate *Pf*EMP1 with *Pf*Hsp70x. Therefore, directly biochemical or genetic evidence to show the function of J-dots is still lacking. However, we cannot exclude the PFE55-*Pf*Hsp70x-PHIST protein complex assists *Pf*EMP1 in transport especially as two further *Pf*PHISTb family proteins were identified as interaction partners of *Pf*Hsp70x. Therefore, the interaction and function between *Pf*Hsp70x and PHIST family protein needs to be further analyzed. So far, the functional of *Pf*GEXP18 is lacking, it is difficult to interpret whether *Pf*GEXP18 is a partners of J-dots or only be trafficked by J-dots. We are trying to generate a *Pf*GEXP18 knockdown parasite to demonstrate of these.

Interestingly, *Pf*Hsp101 and *Pf*EXP2 specifically bind *Pf*Hsp70x. In addition, the interaction between *Pf*Hsp70x and *Pf*Hsp101 spans the parasitophorous vacuole membrane and is mediated by *Pf*EXP2. *Pf*Hsp101 and *Pf*EXP2 are two essential

components of PTEX translocon, which is localized at parasitophorous vacuole membrane and are responsible for the transport of the protein from parasitophorous vacuole to the erythrocyte (de Koning-Ward et al., 2009). A very recent result showed that, another essential component of PTEX complex-PTEX 150 was found to interact with *Pf*Hsp70x (Elsworth *et al.*, 2016). This leads to the hypothesis that *Pf*Hsp70x assists the PTEX translocon in protein transport. It is known that proteins need to be unfolded in order to pass through the translocon and later need to be refolded. This process it is assisted by chaperones/ co-chaperones. *Pf*Hsp70x is the only exported and parasite encoded Hsp70 found involved into multiple protein-protein interaction and further cooperated with PTEX translocon, which make us interpretation of *Pf*Hsp70x has the function of to coordinate protein trafficking. However, direct evidence is lacking. We will further investigate the importance of *Pf*Hsp70x relate to protein traffic by generating multiple *Pf*Hsp70x knockdown transgenic parasite lines.

The discussion of human Hsp70 interaction with parasite encode Hsp40 have been generated for a long time. In our LC-MS/MS data, two human Hsp70 were identified to potentially interact with PFE55, However, due to high homology between human Hsp70 and parasite encoded Hsps, it was difficult to verify with specific. Nevertheless, as Human Hsp70 also interpreted interaction with PTEX translocon, the interaction and function between Human Hsp70-PFE55-*Pf*Hsp70x-PTEX is need to be further analysis.

5 REFERENCE

Aebersold, R. and M. Mann (2003). "Mass spectrometry-based proteomics." Nature **422**(6928): 198-207.

Aikawa, M., Y. Uni, A. T. Andrutis and R. J. Howard (1986). "Membrane-associated electron-dense material of the asexual stages of Plasmodium falciparum: evidence for movement from the intracellular parasite to the erythrocyte membrane." Am J Trop Med Hyg **35**(1): 30-36.

Alano, P. (2007). "Plasmodium falciparum gametocytes: still many secrets of a hidden life." Mol Microbiol **66**(2): 291-302.

Ansorge, I., J. Benting, S. Bhakdi and K. Lingelbach (1996). "Protein sorting in Plasmodium falciparum-infected red blood cells permeabilized with the pore-forming protein streptolysin O." Biochem J **315 (Pt 1)**: 307-314.

Atkinson, C. T. and M. Aikawa (1990). "Ultrastructure of malaria-infected erythrocytes." Blood Cells **16**(2-3): 351-368.

Aurrecoechea, C., J. Brestelli, B. P. Brunk, J. Dommer, S. Fischer, B. Gajria, X. Gao, A. Gingle, G. Grant, O. S. Harb, M. Heiges, F. Innamorato, J. Iodice, J. C. Kissinger, E. Kraemer, W. Li, J. A. Miller, V. Nayak, C. Pennington, D. F. Pinney, D. S. Roos, C. Ross, C. J. Stoeckert, Jr., C. Treatman and H. Wang (2009). "PlasmoDB: a functional genomic database for malaria parasites." Nucleic Acids Res **37**(Database issue): D539-543.

Ay, F., E. M. Bunnik, N. Varoquaux, J. P. Vert, W. S. Noble and K. G. Le Roch (2015). "Multiple dimensions of epigenetic gene regulation in the malaria parasite Plasmodium falciparum: gene regulation via histone modifications, nucleosome positioning and nuclear architecture in P. falciparum." Bioessays **37**(2): 182-194.

Baldi, D. L., K. T. Andrews, R. F. Waller, D. S. Roos, R. F. Howard, B. S. Crabb and A. F. Cowman (2000). "RAP1 controls rhoptry targeting of RAP2 in the malaria parasite Plasmodium falciparum." EMBO J **19**(11): 2435-2443.

Bannister, L. H. and A. R. Dluzewski (1990). "The ultrastructure of red cell invasion in malaria infections: a review." Blood Cells **16**(2-3): 257-292; discussion 293-257.

Baruch, D. I., B. L. Pasloske, H. B. Singh, X. Bi, X. C. Ma, M. Feldman, T. F. Taraschi and R. J. Howard (1995). "Cloning the P. falciparum gene encoding

PfEMP1, a malarial variant antigen and adherence receptor on the surface of parasitized human erythrocytes." Cell **82**(1): 77-87.

Beaumelle, B. D., H. J. Vial and J. R. Philippot (1987). "Reevaluation, using marker enzymes, of the ability of saponin and ammonium chloride to free Plasmodium from infected erythrocytes." J Parasitol **73**(4): 743-748.

Beck, J. R., V. Muralidharan, A. Oksman and D. E. Goldberg (2014). "PTEX component HSP101 mediates export of diverse malaria effectors into host erythrocytes." Nature **511**(7511): 592-595.

Benting, J., D. Mattei and K. Lingelbach (1994). "Brefeldin A inhibits transport of the glycophorin-binding protein from Plasmodium falciparum into the host erythrocyte." Biochem J **300 (Pt 3)**: 821-826.

Berggard, T., S. Linse and P. James (2007). "Methods for the detection and analysis of protein-protein interactions." Proteomics **7**(16): 2833-2842.

Bhakdi, S., J. Tranum-Jensen and A. Sziegoleit (1985). "Mechanism of membrane damage by streptolysin-O." Infect Immun **47**(1): 52-60.

Bhattacharjee, S., C. van Ooij, B. Balu, J. H. Adams and K. Haldar (2008). "Maurer's clefts of Plasmodium falciparum are secretory organelles that concentrate virulence protein reporters for delivery to the host erythrocyte." Blood **111**(4): 2418-2426.

Blisnick, T., M. E. Morales Betoulle, J. C. Barale, P. Uzureau, L. Berry, S. Desroses, H. Fujioka, D. Mattei and C. Braun Breton (2000). "Pfsbp1, a Maurer's cleft Plasmodium falciparum protein, is associated with the erythrocyte skeleton." Mol Biochem Parasitol **111**(1): 107-121.

Blobel, G. and B. Dobberstein (1975). "Transfer of proteins across membranes. I. Presence of proteolytically processed and unprocessed nascent immunoglobulin light chains on membrane-bound ribosomes of murine myeloma." J Cell Biol **67**(3): 835-851.

Blobel, G. and B. Dobberstein (1975). "Transfer of proteins across membranes. II. Reconstitution of functional rough microsomes from heterologous components." J Cell Biol **67**(3): 852-862.

Boddey, J. A., R. L. Moritz, R. J. Simpson and A. F. Cowman (2009). "Role of the Plasmodium export element in trafficking parasite proteins to the infected erythrocyte." Traffic **10**(3): 285-299.

Botha, M., E. R. Pesce and G. L. Blatch (2007). "The Hsp40 proteins of Plasmodium falciparum and other apicomplexa: regulating chaperone power in the parasite and the host." Int J Biochem Cell Biol **39**(10): 1781-1803.

Braun, P. and A. C. Gingras (2012). "History of protein-protein interactions: from egg-white to complex networks." Proteomics **12**(10): 1478-1498.

Bullen, H. E., S. C. Charnaud, M. Kalanon, D. T. Riglar, C. Dekiwadia, N. Kangwanrangsan, M. Torii, T. Tsuboi, J. Baum, S. A. Ralph, A. F. Cowman, T. F. de Koning-Ward, B. S. Crabb and P. R. Gilson (2012). "Biosynthesis, localization, and macromolecular arrangement of the Plasmodium falciparum translocon of exported proteins (PTEX)." J Biol Chem **287**(11): 7871-7884.

Camacho-Carvajal, M. M., B. Wollscheid, R. Aebersold, V. Steimle and W. W. Schamel (2004). "Two-dimensional Blue native/SDS gel electrophoresis of multi-protein complexes from whole cellular lysates: a proteomics approach." Mol Cell Proteomics **3**(2): 176-182.

Cao, J., O. Kaneko, A. Thongkukiatkul, M. Tachibana, H. Otsuki, Q. Gao, T. Tsuboi and M. Torii (2009). "Rhoptry neck protein RON2 forms a complex with microneme protein AMA1 in Plasmodium falciparum merozoites." Parasitol Int **58**(1): 29-35.

Cao, Y., N. Ohwatari, T. Matsumoto, M. Kosaka, A. Ohtsuru and S. Yamashita (1999). "TGF-beta1 mediates 70-kDa heat shock protein induction due to ultraviolet irradiation in human skin fibroblasts." Pflugers Arch **438**(3): 239-244.

Chang, H. H., A. M. Falick, P. M. Carlton, J. W. Sedat, J. L. DeRisi and M. A. Marletta (2008). "N-terminal processing of proteins exported by malaria parasites." Mol Biochem Parasitol **160**(2): 107-115.

Charpian, S. and J. M. Przyborski (2008). "Protein transport across the parasitophorous vacuole of Plasmodium falciparum: into the great wide open." Traffic **9**(2): 157-165.

Cheetham, M. E. and A. J. Caplan (1998). "Structure, function and evolution of DnaJ: conservation and adaptation of chaperone function." Cell Stress Chaperones **3**(1): 28-36.

Chi, A., D. L. Bai, L. Y. Geer, J. Shabanowitz and D. F. Hunt (2007). "Analysis of intact proteins on a chromatographic time scale by electron transfer dissociation tandem mass spectrometry." Int J Mass Spectrom **259**(1-3): 197-203.

Cowman, A. F., D. Berry and J. Baum (2012). "The cellular and molecular basis for malaria parasite invasion of the human red blood cell." J Cell Biol **198**(6): 961-971.

Cowman, A. F. and B. S. Crabb (2006). "Invasion of red blood cells by malaria parasites." Cell **124**(4): 755-766.

Crabb, B. S., B. M. Cooke, J. C. Reeder, R. F. Waller, S. R. Caruana, K. M. Davern, M. E. Wickham, G. V. Brown, R. L. Coppel and A. F. Cowman (1997). "Targeted gene disruption shows that knobs enable malaria-infected red cells to cytoadhere under physiological shear stress." Cell **89**(2): 287-296.

Daniyan, M. O., A. Boshoff, E. Prinsloo, E. R. Pesce and G. L. Blatch (2016). "The Malarial Exported PFA0660w Is an Hsp40 Co-Chaperone of PfHsp70-x." PLoS One **11**(2): e0148517.

de Koning-Ward, T. F., P. R. Gilson, J. A. Boddey, M. Rug, B. J. Smith, A. T. Papenfuss, P. R. Sanders, R. J. Lundie, A. G. Maier, A. F. Cowman and B. S. Crabb (2009). "A newly discovered protein export machine in malaria parasites." Nature **459**(7249): 945-949.

De Maio, A. (1999). "Heat shock proteins: facts, thoughts, and dreams." Shock **11**(1): 1-12.

Dietz, O., S. Rusch, F. Brand, E. Mundwiler-Pachlatko, A. Gaida, T. Voss and H. P. Beck (2014). "Characterization of the small exported Plasmodium falciparum membrane protein SEMP1." PLoS One **9**(7): e103272.

Dobson, S., B. Kar, R. Kumar, B. Adams and S. Barik (2001). "A novel tetratricopeptide repeat (TPR) containing PP5 serine/threonine protein phosphatase in the malaria parasite, Plasmodium falciparum." BMC Microbiol **1**: 31.

Doury, J. C., S. Bonnefoy, N. Roger, J. F. Dubremetz and O. Mercereau-Puijalon (1994). "Analysis of the high molecular weight rhoptry complex of Plasmodium falciparum using monoclonal antibodies." Parasitology **108 (Pt 3)**: 269-280.

Doyle, S. M. and S. Wickner (2009). "Hsp104 and ClpB: protein disaggregating machines." Trends Biochem Sci **34**(1): 40-48.

Elsworth, B., K. Matthews, C. Q. Nie, M. Kalanon, S. C. Charnaud, P. R. Sanders, S. A. Chisholm, N. A. Counihan, P. J. Shaw, P. Pino, J. A. Chan, M. F. Azevedo, S. J. Rogerson, J. G. Beeson, B. S. Crabb, P. R. Gilson and T. F. de Koning-Ward (2014). "PTEX is an essential nexus for protein export in malaria parasites." Nature **511**(7511): 587-591.

Elsworth, B., P. R. Sanders, T. Nebl, S. Batinovic, M. Kalanon, C. Q. Nie, S. C. Charnaud, H. E. Bullen, T. F. de Koning Ward, L. Tilley, B. S. Crabb and P. R. Gilson (2016). "Proteomic analysis reveals novel proteins associated with the Plasmodium

protein exporter PTEX and a loss of complex stability upon truncation of the core PTEX component, PTEX150." Cell Microbiol.

Fenn, J. B., M. Mann, C. K. Meng, S. F. Wong and C. M. Whitehouse (1989). "Electrospray ionization for mass spectrometry of large biomolecules." Science **246**(4926): 64-71.

Fiala, G. J., W. W. Schamel and B. Blumenthal (2011). "Blue native polyacrylamide gel electrophoresis (BN-PAGE) for analysis of multiprotein complexes from cellular lysates." J Vis Exp(48).

Fields, S. and O. Song (1989). "A novel genetic system to detect protein-protein interactions." Nature **340**(6230): 245-246.

Florens, L., M. P. Washburn, J. D. Raine, R. M. Anthony, M. Grainger, J. D. Haynes, J. K. Moch, N. Muster, J. B. Sacci, D. L. Tabb, A. A. Witney, D. Wolters, Y. Wu, M. J. Gardner, A. A. Holder, R. E. Sinden, J. R. Yates and D. J. Carucci (2002). "A proteomic view of the Plasmodium falciparum life cycle." Nature **419**(6906): 520-526.

Fontaine, A., T. Fusai, S. Briolant, S. Buffet, C. Villard, E. Baudelet, M. Pophillat, S. Granjeaud, C. Rogier and L. Almeras (2012). "Anopheles salivary gland proteomes from major malaria vectors." BMC Genomics **13**: 614.

Foth, B. J., N. Zhang, B. K. Chaal, S. K. Sze, P. R. Preiser and Z. Bozdech (2011). "Quantitative time-course profiling of parasite and host cell proteins in the human malaria parasite Plasmodium falciparum." Mol Cell Proteomics **10**(8): M110 006411.

Gardner, M. J., N. Hall, E. Fung, O. White, M. Berriman, R. W. Hyman, J. M. Carlton, A. Pain, K. E. Nelson, S. Bowman, I. T. Paulsen, K. James, J. A. Eisen, K. Rutherford, S. L. Salzberg, A. Craig, S. Kyes, M. S. Chan, V. Nene, S. J. Shallom, B. Suh, J. Peterson, S. Angiuoli, M. Pertea, J. Allen, J. Selengut, D. Haft, M. W. Mather, A. B. Vaidya, D. M. Martin, A. H. Fairlamb, M. J. Fraunholz, D. S. Roos, S. A. Ralph, G. I. McFadden, L. M. Cummings, G. M. Subramanian, C. Mungall, J. C. Venter, D. J. Carucci, S. L. Hoffman, C. Newbold, R. W. Davis, C. M. Fraser and B. Barrell (2002). "Genome sequence of the human malaria parasite Plasmodium falciparum." Nature **419**(6906): 498-511.

Gavazzi, F., B. Lazzari, P. Ciceri, E. Gianazza and A. Viotti (2007). "Wild-type opaque2 and defective opaque2 polypeptides form complexes in maize endosperm cells and bind the opaque2-zein target site." Plant Physiol **145**(3): 933-945.

Gehde, N., C. Hinrichs, I. Montilla, S. Charpian, K. Lingelbach and J. M. Przyborski (2009). "Protein unfolding is an essential requirement for transport across the parasitophorous vacuolar membrane of Plasmodium falciparum." Mol Microbiol **71**(3): 613-628.

Gitau, G. W., P. Mandal, G. L. Blatch, J. Przyborski and A. Shonhai (2012). "Characterisation of the Plasmodium falciparum Hsp70-Hsp90 organising protein (PfHop)." Cell Stress Chaperones **17**(2): 191-202.

Golemis, E. A. and R. Brent (1992). "Fused protein domains inhibit DNA binding by LexA." Mol Cell Biol **12**(7): 3006-3014.

Goloubinoff, P., A. Mogk, A. P. Zvi, T. Tomoyasu and B. Bukau (1999). "Sequential mechanism of solubilization and refolding of stable protein aggregates by a bichaperone network." Proc Natl Acad Sci U S A **96**(24): 13732-13737.

Grau, G. E., G. Bieler, P. Pointaire, S. De Kossodo, F. Tacchini-Cotier, P. Vassalli, P. F. Piguet and P. H. Lambert (1990). "Significance of cytokine production and adhesion molecules in malarial immunopathology." Immunol Lett **25**(1-3): 189-194.

Grover, M., S. Chaubey, S. Ranade and U. Tatu (2013). "Identification of an exported heat shock protein 70 in Plasmodium falciparum." Parasite **20**: 2.

Gruring, C., A. Heiber, F. Kruse, S. Flemming, G. Franci, S. F. Colombo, E. Fasana, H. Schoeler, N. Borgese, H. G. Stunnenberg, J. M. Przyborski, T. W. Gilberger and T. Spielmann (2012). "Uncovering common principles in protein export of malaria parasites." Cell Host Microbe **12**(5): 717-729.

Han, X., A. Aslanian and J. R. Yates, 3rd (2008). "Mass spectrometry for proteomics." Curr Opin Chem Biol **12**(5): 483-490.

Heath, J. R., A. Ribas and P. S. Mischel (2015). "Single-cell analysis tools for drug discovery and development." Nat Rev Drug Discov.

Hiller, N. L., S. Bhattacharjee, C. van Ooij, K. Liolios, T. Harrison, C. Lopez-Estrano and K. Haldar (2004). "A host-targeting signal in virulence proteins reveals a secretome in malarial infection." Science **306**(5703): 1934-1937.

Ho, C. S., C. W. Lam, M. H. Chan, R. C. Cheung, L. K. Law, L. C. Lit, K. F. Ng, M. W. Suen and H. L. Tai (2003). "Electrospray ionisation mass spectrometry: principles and clinical applications." Clin Biochem Rev **24**(1): 3-12.

Hohfeld, J., Y. Minami and F. U. Hartl (1995). "Hip, a novel cochaperone involved in the eukaryotic Hsc70/Hsp40 reaction cycle." Cell **83**(4): 589-598.

Hu, Q., R. J. Noll, H. Li, A. Makarov, M. Hardman and R. Graham Cooks (2005). "The Orbitrap: a new mass spectrometer." J Mass Spectrom **40**(4): 430-443.

Idro, R., K. Marsh, C. C. John and C. R. Newton (2010). "Cerebral malaria: mechanisms of brain injury and strategies for improved neurocognitive outcome." Pediatr Res **68**(4): 267-274.

Jackson, K. E., T. Spielmann, E. Hanssen, A. Adisa, F. Separovic, M. W. Dixon, K. R. Trenholme, P. L. Hawthorne, D. L. Gardiner, T. Gilberger and L. Tilley (2007). "Selective permeabilization of the host cell membrane of Plasmodium falciparum-infected red blood cells with streptolysin O and equinatoxin II." Biochem J **403**(1): 167-175.

Jensen, O. N. (2004). "Modification-specific proteomics: characterization of post-translational modifications by mass spectrometry." Curr Opin Chem Biol **8**(1): 33-41.

Kampinga, H. H. and E. A. Craig (2010). "The HSP70 chaperone machinery: J proteins as drivers of functional specificity." Nat Rev Mol Cell Biol **11**(8): 579-592.

Karas, M. and F. Hillenkamp (1988). "Laser desorption ionization of proteins with molecular masses exceeding 10,000 daltons." Anal Chem **60**(20): 2299-2301.

Kirchhausen, T. (2000). "Three ways to make a vesicle." Nat Rev Mol Cell Biol **1**(3): 187-198.

Knoller, S., S. Shpungin and E. Pick (1991). "The membrane-associated component of the amphiphile-activated, cytosol-dependent superoxide-forming NADPH oxidase of macrophages is identical to cytochrome b559." J Biol Chem **266**(5): 2795-2804.

Krishna, R. G. and F. Wold (1993). "Post-translational modification of proteins." Adv Enzymol Relat Areas Mol Biol **67**: 265-298.

Krungkrai, J., S. R. Krungkrai and A. Bhumiratana (1993). "Plasmodium berghei: partial purification and characterization of the mitochondrial cytochrome c oxidase." Exp Parasitol **77**(2): 136-146.

Kulzer, S., S. Charnaud, T. Dagan, J. Riedel, P. Mandal, E. R. Pesce, G. L. Blatch, B. S. Crabb, P. R. Gilson and J. M. Przyborski (2012). "Plasmodium falciparum-encoded exported hsp70/hsp40 chaperone/co-chaperone complexes within the host erythrocyte." Cell Microbiol **14**(11): 1784-1795.

Kulzer, S., M. Rug, K. Brinkmann, P. Cannon, A. Cowman, K. Lingelbach, G. L. Blatch, A. G. Maier and J. M. Przyborski (2010). "Parasite-encoded Hsp40 proteins define novel mobile structures in the cytosol of the P. falciparum-infected erythrocyte." Cell Microbiol **12**(10): 1398-1420.

Kuss, C., C. S. Gan, K. Gunalan, Z. Bozdech, S. K. Sze and P. R. Preiser (2012). "Quantitative proteomics reveals new insights into erythrocyte invasion by Plasmodium falciparum." Mol Cell Proteomics **11**(2): M111 010645.

LaCount, D. J., M. Vignali, R. Chettier, A. Phansalkar, R. Bell, J. R. Hesselberth, L. W. Schoenfeld, I. Ota, S. Sahasrabudhe, C. Kurschner, S. Fields and R. E. Hughes (2005). "A protein interaction network of the malaria parasite Plasmodium falciparum." Nature **438**(7064): 103-107.

Laemmli, U. K. (1970). "Cleavage of structural proteins during the assembly of the head of bacteriophage T4." Nature **227**(5259): 680-685.

Lambros, C. and J. P. Vanderberg (1979). "Synchronization of Plasmodium falciparum erythrocytic stages in culture." J Parasitol **65**(3): 418-420.

Lanzer, M., H. Wickert, G. Krohne, L. Vincensini and C. Braun Breton (2006). "Maurer's clefts: a novel multi-functional organelle in the cytoplasm of Plasmodium falciparum-infected erythrocytes." Int J Parasitol **36**(1): 23-36.

Lasonder, E., Y. Ishihama, J. S. Andersen, A. M. Vermunt, A. Pain, R. W. Sauerwein, W. M. Eling, N. Hall, A. P. Waters, H. G. Stunnenberg and M. Mann (2002). "Analysis of the Plasmodium falciparum proteome by high-accuracy mass spectrometry." Nature **419**(6906): 537-542.

Lauer, S., J. VanWye, T. Harrison, H. McManus, B. U. Samuel, N. L. Hiller, N. Mohandas and K. Haldar (2000). "Vacuolar uptake of host components, and a role for cholesterol and sphingomyelin in malarial infection." EMBO J **19**(14): 3556-3564.

Lee, C. (2007). "Coimmunoprecipitation assay." Methods Mol Biol **362**: 401-406.

Lee, Y. R., R. T. Nagao and J. L. Key (1994). "A soybean 101-kD heat shock protein complements a yeast HSP104 deletion mutant in acquiring thermotolerance." Plant Cell **6**(12): 1889-1897.

Leech, J. H., J. W. Barnwell, M. Aikawa, L. H. Miller and R. J. Howard (1984). "Plasmodium falciparum malaria: association of knobs on the surface of infected erythrocytes with a histidine-rich protein and the erythrocyte skeleton." J Cell Biol **98**(4): 1256-1264.

Li, D., Y. Fu, R. Sun, C. X. Ling, Y. Wei, H. Zhou, R. Zeng, Q. Yang, S. He and W. Gao (2005). "pFind: a novel database-searching software system for automated peptide and protein identification via tandem mass spectrometry." Bioinformatics **21**(13): 3049-3050.

Li, Z. and P. Srivastava (2004). "Heat-shock proteins." Curr Protoc Immunol **Appendix 1**: Appendix 1T.

Lingelbach, K. and K. A. Joiner (1998). "The parasitophorous vacuole membrane surrounding Plasmodium and Toxoplasma: an unusual compartment in infected cells." J Cell Sci **111 (Pt 11)**: 1467-1475.

Liu, K., L. Qian, J. Wang, W. Li, X. Deng, X. Chen, W. Sun, H. Wei, X. Qian, Y. Jiang and F. He (2009). "Two-dimensional blue native/SDS-PAGE analysis reveals heat shock protein chaperone machinery involved in hepatitis B virus production in HepG2.2.15 cells." Mol Cell Proteomics **8**(3): 495-505.

Loo, R. R., J. D. Cavalcoli, R. A. VanBogelen, C. Mitchell, J. A. Loo, B. Moldover and P. C. Andrews (2001). "Virtual 2-D gel electrophoresis: visualization and analysis of the E. coli proteome by mass spectrometry." Anal Chem **73**(17): 4063-4070.

Macek, B., L. F. Waanders, J. V. Olsen and M. Mann (2006). "Top-down protein sequencing and MS3 on a hybrid linear quadrupole ion trap-orbitrap mass spectrometer." Mol Cell Proteomics **5**(5): 949-958.

Maier, A. G., B. M. Cooke, A. F. Cowman and L. Tilley (2009). "Malaria parasite proteins that remodel the host erythrocyte." Nat Rev Microbiol **7**(5): 341-354.

Maier, A. G., M. Rug, M. T. O'Neill, M. Brown, S. Chakravorty, T. Szestak, J. Chesson, Y. Wu, K. Hughes, R. L. Coppel, C. Newbold, J. G. Beeson, A. Craig, B. S. Crabb and A. F. Cowman (2008). "Exported proteins required for virulence and rigidity of Plasmodium falciparum-infected human erythrocytes." Cell **134**(1): 48-61.

Marti, M., J. Baum, M. Rug, L. Tilley and A. F. Cowman (2005). "Signal-mediated export of proteins from the malaria parasite to the host erythrocyte." J Cell Biol **171**(4): 587-592.

Marti, M., R. T. Good, M. Rug, E. Knuepfer and A. F. Cowman (2004). "Targeting malaria virulence and remodeling proteins to the host erythrocyte." Science **306**(5703): 1930-1933.

Mattson, G., E. Conklin, S. Desai, G. Nielander, M. D. Savage and S. Morgensen (1993). "A practical approach to crosslinking." Mol Biol Rep **17**(3): 167-183.

Matz, J. M., M. J. Blake, H. M. Tatelman, K. P. Lavoi and N. J. Holbrook (1995). "Characterization and regulation of cold-induced heat shock protein expression in mouse brown adipose tissue." Am J Physiol **269**(1 Pt 2): R38-47.

Mayer, M. P., T. Laufen, K. Paal, J. S. McCarty and B. Bukau (1999). "Investigation of the interaction between DnaK and DnaJ by surface plasmon resonance spectroscopy." J Mol Biol **289**(4): 1131-1144.

Meek, J. L. (1980). "Prediction of peptide retention times in high-pressure liquid chromatography on the basis of amino acid composition." Proc Natl Acad Sci U S A **77**(3): 1632-1636.

Miller, L. H., D. I. Baruch, K. Marsh and O. K. Doumbo (2002). "The pathogenic basis of malaria." Nature **415**(6872): 673-679.

Molloy, S. (2014). "Parasite physiology: PTEX in the spotlight." Nat Rev Microbiol **12**(9): 594.

Monti, M., S. Orru, D. Pagnozzi and P. Pucci (2005). "Interaction proteomics." Biosci Rep **25**(1-2): 45-56.

Murphy, S. C., B. U. Samuel, T. Harrison, K. D. Speicher, D. W. Speicher, M. E. Reid, R. Prohaska, P. S. Low, M. J. Tanner, N. Mohandas and K. Haldar (2004). "Erythrocyte detergent-resistant membrane proteins: their characterization and selective uptake during malarial infection." Blood **103**(5): 1920-1928.

Nieto-Sotelo, J., K. B. Kannan, L. M. Martinez and C. Segal (1999). "Characterization of a maize heat-shock protein 101 gene, HSP101, encoding a ClpB/Hsp100 protein homologue." Gene **230**(2): 187-195.

Njunge, J. M., M. H. Ludewig, A. Boshoff, E. R. Pesce and G. L. Blatch (2013). "Hsp70s and J proteins of Plasmodium parasites infecting rodents and primates: structure, function, clinical relevance, and drug targets." Curr Pharm Des **19**(3): 387-403.

Oberli, A., L. Zurbrugg, S. Rusch, F. Brand, M. E. Butler, J. L. Day, E. E. Cutts, T. Lavstsen, I. Vakonakis and H. P. Beck (2016). "Plasmodium falciparum PHIST Proteins Contribute to Cytoadherence and Anchor PfEMP1 to the Host Cell Cytoskeleton." Cell Microbiol.

Operana, T. N. and R. H. Tukey (2007). "Oligomerization of the UDP-glucuronosyltransferase 1A proteins: homo- and heterodimerization analysis by fluorescence resonance energy transfer and co-immunoprecipitation." J Biol Chem **282**(7): 4821-4829.

Pachlatko, E., S. Rusch, A. Muller, A. Hemphill, L. Tilley, E. Hanssen and H. P. Beck (2010). "MAHRP2, an exported protein of Plasmodium falciparum, is an essential component of Maurer's cleft tethers." Mol Microbiol **77**(5): 1136-1152.

Pasloske, B. L., D. I. Baruch, M. R. van Schravendijk, S. M. Handunnetti, M. Aikawa, H. Fujioka, T. F. Taraschi, J. A. Gormley and R. J. Howard (1993). "Cloning and characterization of a Plasmodium falciparum gene encoding a novel high-molecular weight host membrane-associated protein, PfEMP3." Mol Biochem Parasitol **59**(1): 59-72.

Pasvol, G., R. J. Wilson, M. E. Smalley and J. Brown (1978). "Separation of viable schizont-infected red cells of Plasmodium falciparum from human blood." Ann Trop Med Parasitol **72**(1): 87-88.

Pesce, E. R., P. Acharya, U. Tatu, W. S. Nicoll, A. Shonhai, H. C. Hoppe and G. L. Blatch (2008). "The Plasmodium falciparum heat shock protein 40, Pfj4, associates with heat shock protein 70 and shows similar heat induction and localisation patterns." Int J Biochem Cell Biol **40**(12): 2914-2926.

Petta, I., S. Lievens, C. Libert, J. Tavernier and K. De Bosscher (2015). "Modulation of protein-protein interactions for the development of novel therapeutics." Mol Ther.

Pfeiffer, K., V. Gohil, R. A. Stuart, C. Hunte, U. Brandt, M. L. Greenberg and H. Schagger (2003). "Cardiolipin stabilizes respiratory chain supercomplexes." J Biol Chem **278**(52): 52873-52880.

Phizicky, E. M. and S. Fields (1995). "Protein-protein interactions: methods for detection and analysis." Microbiol Rev **59**(1): 94-123.

Poetsch, A., D. Neff, H. Seelert, H. Schagger and N. A. Dencher (2000). "Dye removal, catalytic activity and 2D crystallization of chloroplast H(+)-ATP synthase purified by blue native electrophoresis." Biochim Biophys Acta **1466**(1-2): 339-349.

Pologe, L. G. and J. V. Ravetch (1986). "A chromosomal rearrangement in a P. falciparum histidine-rich protein gene is associated with the knobless phenotype." Nature **322**(6078): 474-477.

Przyborski, J. M., M. Diehl and G. L. Blatch (2015). "Plasmodial HSP70s are functionally adapted to the malaria parasite life cycle." Front Mol Biosci **2**: 34.

Przyborski, J. M., S. K. Miller, J. M. Pfahler, P. P. Henrich, P. Rohrbach, B. S. Crabb and M. Lanzer (2005). "Trafficking of STEVOR to the Maurer's clefts in Plasmodium falciparum-infected erythrocytes." EMBO J **24**(13): 2306-2317.

Qin, K., C. Dong, G. Wu and N. A. Lambert (2011). "Inactive-state preassembly of G(q)-coupled receptors and G(q) heterotrimers." Nat Chem Biol **7**(10): 740-747.

Rigaut, G., A. Shevchenko, B. Rutz, M. Wilm, M. Mann and B. Seraphin (1999). "A generic protein purification method for protein complex characterization and proteome exploration." Nat Biotechnol **17**(10): 1030-1032.

Ritossa, P. (1962). "[Problems of prophylactic vaccinations of infants]." Riv Ist Sieroter Ital **37**: 79-108.

Rosenfeld, J., J. Capdevielle, J. C. Guillemot and P. Ferrara (1992). "In-gel digestion of proteins for internal sequence analysis after one- or two-dimensional gel electrophoresis." Anal Biochem **203**(1): 173-179.

Rug, M. and A. G. Maier (2011). "The heat shock protein 40 family of the malaria parasite Plasmodium falciparum." IUBMB Life **63**(12): 1081-1086.

Salamonsen, R. F., A. M. Tulloh and T. Boyd (1986). "Adaptation of the quadrupole mass spectrometer to multipatient anaesthesia gas monitoring." Anaesth Intensive Care **14**(2): 163-173.

Sali, A., R. Glaeser, T. Earnest and W. Baumeister (2003). "From words to literature in structural proteomics." Nature **422**(6928): 216-225.

Sanders, P. R., G. T. Cantin, D. C. Greenbaum, P. R. Gilson, T. Nebl, R. L. Moritz, J. R. Yates, 3rd, A. N. Hodder and B. S. Crabb (2007). "Identification of protein complexes in detergent-resistant membranes of Plasmodium falciparum schizonts." Mol Biochem Parasitol **154**(2): 148-157.

Sargeant, T. J., M. Marti, E. Caler, J. M. Carlton, K. Simpson, T. P. Speed and A. F. Cowman (2006). "Lineage-specific expansion of proteins exported to erythrocytes in malaria parasites." Genome Biol **7**(2): R12.

Schagger, H. (2001). "Blue-native gels to isolate protein complexes from mitochondria." Methods Cell Biol **65**: 231-244.

Schagger, H., W. A. Cramer and G. von Jagow (1994). "Analysis of molecular masses and oligomeric states of protein complexes by blue native electrophoresis and isolation of membrane protein complexes by two-dimensional native electrophoresis." Anal Biochem **217**(2): 220-230.

Schagger, H. and K. Pfeiffer (2000). "Supercomplexes in the respiratory chains of yeast and mammalian mitochondria." EMBO J **19**(8): 1777-1783.

Schnaitman, C. and J. W. Greenawalt (1968). "Enzymatic properties of the inner and outer membranes of rat liver mitochondria." J Cell Biol **38**(1): 158-175.

Schroter, C. J., M. Braun, J. Englert, H. Beck, H. Schmid and H. Kalbacher (1999). "A rapid method to separate endosomes from lysosomal contents using differential centrifugation and hypotonic lysis of lysosomes." J Immunol Methods **227**(1-2): 161-168.

Schweizer, E., W. Angst and H. U. Lutz (1982). "Glycoprotein topology on intact human red blood cells reevaluated by cross-linking following amino group supplementation." Biochemistry **21**(26): 6807-6818.

Sessler, N., K. Krug, A. Nordheim, B. Mordmuller and B. Macek (2012). "Analysis of the Plasmodium falciparum proteasome using Blue Native PAGE and label-free quantitative mass spectrometry." Amino Acids **43**(3): 1119-1129.

Shonhai, A., A. Boshoff and G. L. Blatch (2007). "The structural and functional diversity of Hsp70 proteins from Plasmodium falciparum." Protein Sci **16**(9): 1803-1818.

Shortt, H. E. (1951). "Life-cycle of the mammalian malaria parasite." Br Med Bull **8**(1): 7-9.

Silvestrini, F., E. Lasonder, A. Olivieri, G. Camarda, B. van Schaijk, M. Sanchez, S. Younis Younis, R. Sauerwein and P. Alano (2010). "Protein export marks the early phase of gametocytogenesis of the human malaria parasite Plasmodium falciparum." Mol Cell Proteomics **9**(7): 1437-1448.

Singh, B., L. Kim Sung, A. Matusop, A. Radhakrishnan, S. S. Shamsul, J. Cox-Singh, A. Thomas and D. J. Conway (2004). "A large focus of naturally acquired Plasmodium knowlesi infections in human beings." Lancet **363**(9414): 1017-1024.

Singh, M., P. Mukherjee, K. Narayanasamy, R. Arora, S. D. Sen, S. Gupta, K. Natarajan and P. Malhotra (2009). "Proteome analysis of Plasmodium falciparum extracellular secretory antigens at asexual blood stages reveals a cohort of proteins with possible roles in immune modulation and signaling." Mol Cell Proteomics **8**(9): 2102-2118.

Smith, D. B. and K. S. Johnson (1988). "Single-step purification of polypeptides expressed in Escherichia coli as fusions with glutathione S-transferase." Gene **67**(1): 31-40.

Smith, G. P. and V. A. Petrenko (1997). "Phage Display." Chem Rev **97**(2): 391-410.

Smith, J. D. (2014). "The role of PfEMP1 adhesion domain classification in Plasmodium falciparum pathogenesis research." Mol Biochem Parasitol **195**(2): 82-87.

Smith, J. D., G. Subramanian, B. Gamain, D. I. Baruch and L. H. Miller (2000). "Classification of adhesive domains in the Plasmodium falciparum erythrocyte membrane protein 1 family." Mol Biochem Parasitol **110**(2): 293-310.

Spielmann, T., P. L. Hawthorne, M. W. Dixon, M. Hannemann, K. Klotz, D. J. Kemp, N. Klonis, L. Tilley, K. R. Trenholme and D. L. Gardiner (2006). "A cluster of ring stage-specific genes linked to a locus implicated in cytoadherence in Plasmodium falciparum codes for PEXEL-negative and PEXEL-positive proteins exported into the host cell." Mol Biol Cell **17**(8): 3613-3624.

Suchanek, M., A. Radzikowska and C. Thiele (2005). "Photo-leucine and photo-methionine allow identification of protein-protein interactions in living cells." Nat Methods **2**(4): 261-267.

Talman, A. M., O. Domarle, F. E. McKenzie, F. Ariey and V. Robert (2004). "Gametocytogenesis: the puberty of Plasmodium falciparum." Malar J **3**: 24.

Tarr, S. J., R. W. Moon, I. Hardege and A. R. Osborne (2014). "A conserved domain targets exported PHISTb family proteins to the periphery of Plasmodium infected erythrocytes." Mol Biochem Parasitol **196**(1): 29-40.

Tobie, J. E. and G. R. Coatney (1961). "Fluorescent antibody staining of human malaria parasites." Exp Parasitol **11**: 128-132.

Towbin, H., T. Staehelin and J. Gordon (1979). "Electrophoretic transfer of proteins from polyacrylamide gels to nitrocellulose sheets: procedure and some applications." Proc Natl Acad Sci U S A **76**(9): 4350-4354.

Tyers, M. and M. Mann (2003). "From genomics to proteomics." Nature **422**(6928): 193-197.

Uckert, W., P. Westermann, I. Hertling and V. Wunderlich (1983). "Chemical crosslinking of major structural proteins within type D retroviruses." Biomed Biochim Acta **42**(2-3): 177-187.

Vahsen, N., C. Cande, J. J. Briere, P. Benit, N. Joza, N. Larochette, P. G. Mastroberardino, M. O. Pequignot, N. Casares, V. Lazar, O. Feraud, N. Debili, S. Wissing, S. Engelhardt, F. Madeo, M. Piacentini, J. M. Penninger, H. Schagger, P. Rustin and G. Kroemer (2004). "AIF deficiency compromises oxidative phosphorylation." EMBO J **23**(23): 4679-4689.

Van Coster, R., J. Smet, E. George, L. De Meirleir, S. Seneca, J. Van Hove, G. Sebire, H. Verhelst, J. De Bleecker, B. Van Vlem, P. Verloo and J. Leroy (2001). "Blue native polyacrylamide gel electrophoresis: a powerful tool in diagnosis of oxidative phosphorylation defects." Pediatr Res **50**(5): 658-665.

van Ooij, C., P. Tamez, S. Bhattacharjee, N. L. Hiller, T. Harrison, K. Liolios, T. Kooij, J. Ramesar, B. Balu, J. Adams, A. P. Waters, C. J. Janse and K. Haldar (2008). "The malaria secretome: from algorithms to essential function in blood stage infection." PLoS Pathog **4**(6): e1000084.

Vincensini, L., S. Richert, T. Blisnick, A. Van Dorsselaer, E. Leize-Wagner, T. Rabilloud and C. Braun Breton (2005). "Proteomic analysis identifies novel proteins of the Maurer's clefts, a secretory compartment delivering Plasmodium falciparum proteins to the surface of its host cell." Mol Cell Proteomics **4**(4): 582-593.

von Bohl, A., A. Kuehn, N. Simon, V. N. Ngongang, M. Spehr, S. Baumeister, J. M. Przyborski, R. Fischer and G. Pradel (2015). "A WD40-repeat protein unique to malaria parasites associates with adhesion protein complexes and is crucial for blood stage progeny." Malar J **14**(1): 435.

Waller, K. L., B. M. Cooke, W. Nunomura, N. Mohandas and R. L. Coppel (1999). "Mapping the binding domains involved in the interaction between the Plasmodium falciparum knob-associated histidine-rich protein (KAHRP) and the cytoadherence ligand P. falciparum erythrocyte membrane protein 1 (PfEMP1)." J Biol Chem **274**(34): 23808-23813.

Walter, S. and J. Buchner (2002). "Molecular chaperones--cellular machines for protein folding." Angew Chem Int Ed Engl **41**(7): 1098-1113.

Waterkeyn, J. G., M. E. Wickham, K. M. Davern, B. M. Cooke, R. L. Coppel, J. C. Reeder, J. G. Culvenor, R. F. Waller and A. F. Cowman (2000). "Targeted mutagenesis of Plasmodium falciparum erythrocyte membrane protein 3 (PfEMP3) disrupts cytoadherence of malaria-infected red blood cells." EMBO J **19**(12): 2813-2823.

Wilkins, M. (2009). "Proteomics data mining." Expert Rev Proteomics **6**(6): 599-603.

Wittig, I., H. P. Braun and H. Schagger (2006). "Blue native PAGE." Nat Protoc **1**(1): 418-428.

Yamada, T. and P. Bork (2009). "Evolution of biomolecular networks: lessons from metabolic and protein interactions." Nat Rev Mol Cell Biol **10**(11): 791-803.

Yang, B., Y. J. Wu, M. Zhu, S. B. Fan, J. Lin, K. Zhang, S. Li, H. Chi, Y. X. Li, H. F. Chen, S. K. Luo, Y. H. Ding, L. H. Wang, Z. Hao, L. Y. Xiu, S. Chen, K. Ye, S. M. He and M. Q. Dong (2012). "Identification of cross-linked peptides from complex samples." Nat Methods **9**(9): 904-906.

Young, J. C., V. R. Agashe, K. Siegers and F. U. Hartl (2004). "Pathways of chaperone-mediated protein folding in the cytosol." Nat Rev Mol Cell Biol **5**(10): 781-791.

Zabrouskov, V. and J. P. Whitelegge (2007). "Increased coverage in the transmembrane domain with activated-ion electron capture dissociation for top-down Fourier-transform mass spectrometry of integral membrane proteins." J Proteome Res **6**(6): 2205-2210.

Zhang, H., X. Tang, G. R. Munske, N. Tolic, G. A. Anderson and J. E. Bruce (2009). "Identification of protein-protein interactions and topologies in living cells with chemical cross-linking and mass spectrometry." Mol Cell Proteomics **8**(3): 409-420.

Zolkiewski, M. (1999). "ClpB cooperates with DnaK, DnaJ, and GrpE in suppressing protein aggregation. A novel multi-chaperone system from Escherichia coli." J Biol Chem **274**(40): 28083-28086.

6 SUPPLEMENT

Table S1: Full list of proteome identification of co-immunoprecipitation against with anti-GFP by LC/MS/MS (Plasmodium DB database).

Exported N=5						
Accession Number	**Protein names**	**Unique Peptide Number**	**Peptide Coverage**	**Unique Peptide Number**	**Peptide Coverage**	**Ratio**
PF3D7_0501100.1/2	heat shock protein 40, type II (HSP40)	6	15.42	0	0.00	6/0
PF3D7_0801000	Plasmodium exported protein (PHISTc), unknown function	3	4.10	0	0.00	3/0
PF3D7_1401100	DnaJ protein, putative	8	22.56	1	1.83	8.00
PF3D7_1407800	plasmepsin IV (PM4)	3	12.70	1	4.68	3.00
PF3D7_0831700	heat shock protein 70 (HSP70-x)	17	34.87	6	15.46	2.83
Signal peptide N=3						
PF3D7_1116800	heat shock protein 101 (HSP101)	5	9.27	0	0.00	5/0
PF3D7_0929400	high molecular weight rhoptry protein 2 (RhopH2)	7	7.33	4	5.01	1.75
PF3D7_1471100	exported protein 2 (EXP2)	3	9.76	2	8.36	1.50
TM Domain N=2						
PF3D7_1408100	plasmepsin III (HAP)	2	5.97	0	0.00	2/0
PF3D7_1311800	M1-family alanyl aminopeptidase (M1AAP)	7	11.43	6	9.68	1.17
No signal N=31						
PF3D7_1361800	conserved Plasmodium protein, unknown function	8	4.65	0	0.00	8/0
PF3D7_1308200	carbamoyl phosphate synthetase (cpsSII)	6	3.92	0	0.00	6/0
PF3D7_1441400	FACT complex subunit SSRP1, putative (FACT-S)	6	14.63	0	0.00	6/0
PF3D7_0307100	40S ribosomal protein S12, putative	4	36.88	0	0.00	4/0
PF3D7_0517000	60S ribosomal protein L12, putative	4	34.55	0	0.00	4/0
PF3D7_1410600	eukaryotic translation initiation factor 2 gamma subunit, putative	4	15.48	0	0.00	4/0
PF3D7_1225800	ubiquitin-activating enzyme E1 (UBA1)	3	3.42	0	0.00	3/0
PF3D7_1338100	26S proteasome regulatory subunit RPN3, putative (RPN3)	3	8.95	0	0.00	3/0
PF3D7_1027800	60S ribosomal protein L3 (RPL3)	2	7.77	0	0.00	2/0
PF3D7_1103100	60S acidic ribosomal protein P1, putative (RPP1)	2	22.03	0	0.00	2/0
PF3D7_1136400	signal recognition particle subunit SRP72, putative (SRP72)	3	5.08	0	0.00	2/0
PF3D7_1238800	acyl-CoA synthetase (ACS11)	2	3.79	0	0.00	2/0

PF3D7_1367000	suppressor of kinetochore protein 1, putative (SKP1)	2	14.82	0	0.00	2/0
PF3D7_1369700	U2 small nuclear ribonucleoprotein A', putative	2	12.57	0	0.00	2/0
PF3D7_1203700	nucleosome assembly protein (NAPL)	6	14.70	1	2.59	6.00
PF3D7_1451100	elongation factor 2 (eEF2)	5	8.29	1	1.08	5.00
PF3D7_1416500	NADP-specific glutamate dehydrogenase (GDH1)	4	14.68	1	4.04	4.00
PF3D7_0708800	heat shock protein 110 (HSP110c)	7	12.37	2	3.44	3.50
PF3D7_0322000	peptidyl-prolyl cis-trans isomerase (CYP19A)	3	18.13	1	7.02	3.00
PF3D7_0708400	heat shock protein 90 (HSP90)	11	20.27	4	7.38	2.75
PF3D7_1441200	60S ribosomal protein L1, putative	2	13.36	1	5.53	2.00
PF3D7_0802000	glutamate dehydrogenase, putative (GDH3)	5	3.94	3	2.51	1.67
PF3D7_1436000	glucose-6-phosphate isomerase (GPI)	5	11.92	3	6.39	1.67
PF3D7_1011800	PRE-binding protein (PREBP)	3	2.81	2	1.93	1.50
PF3D7_1034900	methionine--tRNA ligase (MRScyt)	3	4.50	2	3.15	1.50
PF3D7_1341200	60S ribosomal protein L18, putative	3	14.67	2	7.61	1.50
PF3D7_1460700	60S ribosomal protein L27 (RPL27)	3	20.55	2	15.07	1.50
PF3D7_0818900	heat shock protein 70 (HSP70)	12	16.54	9	17.43	1.33
PF3D7_1357800	T-complex protein 1 subunit delta (CCT4)	4	11.34	3	13.04	1.33
PF3D7_1444800	fructose-bisphosphate aldolase (FBPA)	9	24.39	7	26.83	1.29
PF3D7_0621200	pyridoxine biosynthesis protein PDX1 (PDX1)	6	28.24	5	28.24	1.20

Table S2: Full list of proteome identification of co-immunoprecipitation against with anti-*Pf*Hsp70x by LC/MS/MS (Plasmodium DB database).

Exported N=9						
Accession Number	**Protein names**	**Unique Peptide Number**	**Peptide Coverage**	**Unique Peptide Number**	**Peptide Coverage**	**Ratio**
PF3D7_0831700	heat shock protein 70 (HSP70-x)	38	57.44	3	12.08	12.67
PF3D7_0402400	Plasmodium exported protein, unknown function (GEXP18)	6	36.61	0	0.00	6/0
PF3D7_1016300	glycophorin binding protein (GBP)	6	46.48	0	0.00	6/0
PF3D7_0501100.1/2	heat shock protein 40, type II (HSP40)	4	15.92	0	0.00	4/0
PF3D7_1201000	Plasmodium exported protein (PHISTb), unknown function	4	6.28	0	0.00	4/0
PF3D7_0401800	Plasmodium exported protein (PHISTb), unknown function	2	4.46	0	0.00	2/0

	(PfD80)					
PF3D7_0721100	conserved Plasmodium protein, unknown function	2	9.84	0	0.00	2/0
PF3D7_1001400	alpha/beta hydrolase, putative	2	3.47	0	0.00	2/0
PF3D7_0801000	Plasmodium exported protein (PHISTc), unknown function	9	12.22	0	0.00	9/0
Signal peptide N=3						
PF3D7_1252100	rhoptry neck protein 3 (RON3)	9	5.60	0	0.00	9/0
PF3D7_1012200	conserved Plasmodium protein, unknown function	5	24.72	0	0.00	5/0
PF3D7_1116800	heat shock protein 101 (HSP101)	4	6.51	0	0.00	4/0
PF3D7_1105800	conserved Plasmodium protein, unknown function	3	13.53	0	0.00	3/0
PF3D7_0302500	cytoadherence linked asexual protein 3.1 (CLAG3.1)	2	3.25	0	0.00	2/0
PF3D7_1015200.1/2	cysteine--tRNA ligase, putative (CysRS)	2	3.40	0	0.00	2/0
PF3D7_1116000	rhoptry neck protein 4 (RON4)	2	1.67	0	0.00	2/0
PF3D7_0930300	merozoite surface protein 1 (MSP1)	11	8.37	1	2.85	11.00
PF3D7_0207600	serine repeat antigen 5 (SERA5)	8	15.15	1	1.81	8.00
PF3D7_1232100	60 kDa chaperonin (CPN60)	8	19.36	1	1.67	8.00
PF3D7_0827900	protein disulfide isomerase (PDI8)	5	18.63	1	3.42	5.00
PF3D7_0917900	heat shock protein 70 (HSP70-2)	19	36.35	4	7.36	4.75
PF3D7_0929400	high molecular weight rhoptry protein 2 (RhopH2)	25	25.04	6	6.39	4.17
PF3D7_1471100	exported protein 2 (EXP2)	4	14.98	1	3.83	4.00
PF3D7_1222300	endoplasmin, putative (GRP94)	7	12.42	2	3.41	3.50
PF3D7_0905400	high molecular weight rhoptry protein 3 (RhopH3)	11	19.84	4	6.24	2.75
PF3D7_1129100	parasitophorous vacuolar protein 1 (PV1)	5	14.82	2	5.75	2.50
PF3D7_1454400	aminopeptidase P (APP)	17	29.09	8	13.26	2.13
PF3D7_1010700	dolichyl-phosphate-mannose protein mannosyltransferase, putative	3	18.39	2	16.55	1.50
PF3D7_1324900	L-lactate dehydrogenase (LDH)	13	51.58	9	56.96	1.44
TM Domain N=8						
PF3D7_0811200	ER membrane protein complex subunit 1, putative (EMC1)	4	5.21	0	0.00	4/0
PF3D7_0220000	liver stage antigen 3 (LSA3)	3	2.95	0	0.00	3/0
PF3D7_0823800	DnaJ protein, putative	3	8.40	0	0.00	3/0
PF3D7_1037300	ADP/ATP transporter on adenylate translocase (ADT)	3	15.62	0	0.00	3/0
PF3D7_1105800	conserved Plasmodium protein, unknown function	3	13.53	0	0.00	3/0
PF3D7_1459400	conserved Plasmodium protein, unknown function	2	7.94	0	0.00	2/0
PF3D7_1311800	M1-family alanyl aminopeptidase (M1AAP)	12	17.51	1	2.58	12.00

PF3D7_0801800	mannose-6-phosphate isomerase, putative	2	2.57	1	1.09	2.00
No signal N=31						
PF3D7_1034900	methionine--tRNA ligase (MRScyt)	11	15.97	0	0.00	11/0
PF3D7_1410200	cytidine triphosphate synthetase	11	17.13	0	0.00	11/0
PF3D7_0205900	26S proteasome regulatory subunit RPN1, putative (RPN1)	8	13.35	0	0.00	8/0
PF3D7_1104000	phenylalanine--tRNA ligase beta subunit	8	22.31	0	0.00	8/0
PF3D7_1145400	dynamin-like protein (DYN1)	8	10.63	0	0.00	8/0
PF3D7_1453800	glucose-6-phosphate dehydrogenase-6-phosphogluconolactonase (GluPho)	8	10.99	0	0.00	8/0
PF3D7_0525100	acyl-CoA synthetase (ACS10)	7	14.41	0	0.00	7/0
PF3D7_1355100	DNA replication licensing factor MCM6 (MCM6)	7	9.58	0	0.00	7/0
PF3D7_1012600	GMP synthetase (GMPS)	6	14.78	0	0.00	6/0
PF3D7_1417800	DNA replication licensing factor MCM2 (MCM2)	6	12.46	0	0.00	6/0
PF3D7_0305500	conserved Plasmodium protein, unknown function	5	1.65	0	0.00	5/0
PF3D7_0822600	protein transport protein SEC23 (SEC23)	5	12.52	0	0.00	5/0
PF3D7_1117700	GTP-binding nuclear protein RAN/TC4 (RAN)	5	33.18	0	0.00	5/0
PF3D7_1134000	heat shock protein 70 (HSP70-3)	5	16.14	0	0.00	5/0
PF3D7_1224300	polyadenylate-binding protein, putative (PABP)	5	8.57	0	0.00	5/0
PF3D7_1317100	DNA replication licensing factor MCM4 (MCM4)	5	9.85	0	0.00	5/0
PF3D7_0803800	proteasome subunit beta type-4	4	20.00	0	0.00	4/0
PF3D7_0808400	coatomer subunit epsilon, putative (SEC28)	4	17.27	0	0.00	4/0
PF3D7_1136300	tudor staphylococcal nuclease (TSN)	4	4.10	0	0.00	4/0
PF3D7_1353900	proteasome subunit alpha type-7, putative	4	24.07	0	0.00	4/0
PF3D7_1437900	HSP40, subfamily A, putative (ERdj3)	4	16.75	0	0.00	4/0
PF3D7_1464900	ATP-dependent zinc metalloprotease FTSH, putative	4	8.78	0	0.00	4/0
PF3D7_1474800	proteasome subunit alpha type-1, putative	4	27.17	0	0.00	4/0
PF3D7_0527000	DNA replication licensing factor MCM3, putative (MCM3)	3	4.16	0	0.00	3/0
PF3D7_0903400	DEAD/DEAH box helicase, putative	3	1.62	0	0.00	3/0
PF3D7_1008400	26S protease regulatory subunit 4, putative (RPT2)	3	6.03	0	0.00	3/0
PF3D7_1008700	tubulin beta chain	3	8.76	0	0.00	3/0

PF3D7_1008900	adenylate kinase (AK1)	3	18.60	0	0.00	3/0
PF3D7_1127100	deoxyuridine 5'-triphosphate nucleotidohydrolase (dUTPase)	3	22.54	0	0.00	3/0
PF3D7_1130400	26S protease regulatory subunit 6A, putative (RPT5)	3	7.75	0	0.00	3/0
PF3D7_1208900	protein phosphatase, putative	3	3.33	0	0.00	3/0
PF3D7_1213800	proline--tRNA ligase (PRS)	3	5.63	0	0.00	3/0
PF3D7_1235700	ATP synthase subunit beta, mitochondrial	3	9.28	0	0.00	3/0
PF3D7_1239000	HD superfamily phosphohydrolase protein	3	8.04	0	0.00	3/0
PF3D7_1250700	conserved Plasmodium protein, unknown function	3	24.86	0	0.00	3/0
PF3D7_1402300	26S proteasome regulatory subunit RPN6 (RPN6)	3	6.31	0	0.00	3/0
PF3D7_1451100	elongation factor 2 (eEF2)	3	4.69	0	0.00	3/0
PF3D7_0109200	mRNA cleavage factor-like protein, putative	2	15.09	0	0.00	2/0
PF3D7_0109500	N-acetyltransferase, putative	2	16.77	0	0.00	2/0
PF3D7_0211800	asparagine--tRNA ligase (AsnRS)	2	3.28	0	0.00	2/0
PF3D7_0315100	eukaryotic translation initiation factor 4E (eIF4E)	2	7.05	0	0.00	2/0
PF3D7_0319600	elongation factor 1 (EF-1), putative	2	20.51	0	0.00	2/0
PF3D7_0416800	small GTP-binding protein sar1 (SAR1)	2	15.63	0	0.00	2/0
PF3D7_0529500	cell cycle regulator protein, putative	2	15.08	0	0.00	2/0
PF3D7_0619500	acyl-CoA synthetase (ACS12)	2	2.30	0	0.00	2/0
PF3D7_0807500	proteasome subunit alpha type-6, putative	2	8.85	0	0.00	2/0
PF3D7_0826700	receptor for activated c kinase (RACK)	2	6.50	0	0.00	2/0
PF3D7_0933600	mitochondrial-processing peptidase subunit beta, putative (MAS1)	2	5.79	0	0.00	2/0
PF3D7_1012700	NLI interacting factor-like phosphatase, putative (NIF4)	2	1.53	0	0.00	2/0
PF3D7_1015200.3	cysteine--tRNA ligase, putative	2	3.40	0	0.00	2/0
PF3D7_1034400	flavoprotein subunit of succinate dehydrogenase (SDHA)	2	4.12	0	0.00	2/0
PF3D7_1106000	RuvB-like helicase 2 (RUVB2)	2	4.00	0	0.00	2/0
PF3D7_1126200	40S ribosomal protein S18, putative	2	23.72	0	0.00	2/0
PF3D7_1206700	eukaryotic translation initiation factor 5, putative	2	4.60	0	0.00	2/0
PF3D7_1211700	DNA replication licensing factor MCM5, putative (MCM5)	2	3.96	0	0.00	2/0
PF3D7_1231100	ras-related protein Rab-2 (RAB2)	2	11.74	0	0.00	2/0
PF3D7_1239600	hydroxyethylthiazole kinase (ThzK)	2	3.16	0	0.00	2/0
PF3D7_1247400	FK506-binding protein (FKBP)-	2	9.54	0	0.00	2/0

	type peptidyl-prolyl isomerase (FKBP35)					
PF3D7_1251300	thymidylate kinase (TMK)	2	9.05	0	0.00	2/0
PF3D7_1323100	60S ribosomal protein L6, putative	2	18.42	0	0.00	2/0
PF3D7_1338100	26S proteasome regulatory subunit RPN3, putative (RPN3)	2	11.53	0	0.00	2/0
PF3D7_1341900	V-type proton ATPase subunit D, putative	2	7.29	0	0.00	2/0
PF3D7_1342800	phosphoenolpyruvate carboxykinase (PEPCK)	2	4.12	0	0.00	2/0
PF3D7_1346300	DNA/RNA-binding protein Alba 2 (ALBA2)	2	11.37	0	0.00	2/0
PF3D7_1346400	conserved Plasmodium protein, unknown function	2	0.38	0	0.00	2/0
PF3D7_1353800	proteasome subunit alpha type-4, putative	2	19.51	0	0.00	2/0
PF3D7_1361100	protein transport protein Sec24A (SEC24A)	2	3.40	0	0.00	2/0
PF3D7_1419300	glutathione S-transferase (Schweizer *et al.*)	2	11.37	0	0.00	2/0
PF3D7_1420600	pantothenate kinase, putative (PANK)	2	4.62	0	0.00	2/0
PF3D7_1426700	phosphoenolpyruvate carboxylase (PEPC)	2	2.53	0	0.00	2/0
PF3D7_1445100	histidine--tRNA ligase, putative	2	2.12	0	0.00	2/0
PF3D7_0802000	glutamate dehydrogenase, putative (GDH3)	15	16.75	0	0.00	15
PF3D7_0708800	heat shock protein 110 (HSP110c)	13	23.60	0	0.00	13/0
PF3D7_1219100	clathrin heavy chain, putative	11	7.26	1	0.60	11.00
PF3D7_1357800	T-complex protein 1 subunit delta (CCT4)	11	29.68	1	28.92	11.00
PF3D7_0922600	glutamine synthetase, putative	9	23.76	1	2.03	9.00
PF3D7_1011800	PRE-binding protein (PREBP)	9	8.17	1	1.05	9.00
PF3D7_1235600	serine hydroxymethyltransferase (SHMT)	8	19.36	1	1.67	8.00
PF3D7_0524000	karyopherin beta (KASbeta)	7	9.17	1	1.16	7.00
PF3D7_0818200	14-3-3 protein (14-3-3I)	7	38.93	1	6.87	7.00
PF3D7_0708400	heat shock protein 90 (HSP90)	12	24.16	2	5.64	6.00
PF3D7_0932300	M18 aspartyl aminopeptidase (M18AAP)	6	15.79	1	2.46	6.00
PF3D7_0627800	acetyl-CoA synthetase, putative (ACS)	5	6.62	1	1.00	5.00
PF3D7_1403900	serine/threonine protein phosphatase CPPED1, putative (CPPED1)	5	17.11	1	4.03	5.00
PF3D7_1350100	lysine--tRNA ligase (KRS1)	9	17.84	2	4.29	4.50
PF3D7_1325100	phosphoribosylpyrophosphate synthetase	4	13.27	1	4.12	4.00
PF3D7_1349200	glutamate--tRNA ligase, putative	4	5.68	1	1.39	4.00
PF3D7_1362200	RuvB-like helicase 3 (RUVB3)	4	14.49	1	3.31	4.00
PF3D7_1436000	glucose-6-phosphate isomerase (GPI)	8	18.48	2	3.80	4.00

PF3D7_1026800	40S ribosomal protein S2 (RPS2)	7	38.78	2	11.41	3.50
PF3D7_1015600	heat shock protein 60 (HSP60)	10	26.72	3	6.55	3.33
PF3D7_0214000	T-complex protein 1 subunit theta (CCT8)	3	5.35	1	2.77	3.00
PF3D7_0517000	60S ribosomal protein L12, putative	3	28.49	1	15.15	3.00
PF3D7_0934500	V-type proton ATPase subunit E, putative	3	11.49	1	5.53	3.00
PF3D7_1438900	thioredoxin peroxidase 1 (Trx-Px1)	3	27.18	1	21.03	3.00
PF3D7_1470900	proteasome subunit beta type-2, putative	3	23.59	1	11.68	3.00
PF3D7_0915400	6-phosphofructokinase (PFK9)	42	40.41	15	12.41	2.80
PF3D7_0619400	cell division cycle protein 48 homologue, putative	5	8.82	2	3.62	2.50
PF3D7_1229500	T-complex protein 1 subunit gamma (CCT3)	10	23.06	4	7.57	2.50
PF3D7_1311900	V-type proton ATPase catalytic subunit A (vapA)	5	14.08	2	7.04	2.50
PF3D7_1338200	60S ribosomal protein L6-2, putative	5	31.22	2	13.12	2.50
PF3D7_1447000	40S ribosomal protein S5	5	20.96	2	8.09	2.50
PF3D7_1120100	phosphoglycerate mutase, putative (PGM1)	7	45.20	3	12.00	2.33
PF3D7_1343000	phosphoethanolamine N-methyltransferase (PMT)	14	70.68	6	29.70	2.33
PF3D7_1012400	hypoxanthine-guanine phosphoribosyltransferase (HGPRT)	11	56.28	5	41.99	2.20
PF3D7_0322900	40S ribosomal protein S3A, putative	2	11.45	1	9.16	2.00
PF3D7_0516200	40S ribosomal protein S11	2	18.54	1	18.54	2.00
PF3D7_0727400	proteasome subunit alpha type-5, putative	2	13.67	1	4.69	2.00
PF3D7_0813900	40S ribosomal protein S16, putative	4	32.64	2	15.97	2.00
PF3D7_0907700	subunit of proteaseome activator complex, putative	4	16.85	2	10.04	2.00
PF3D7_0920800	inosine-5'-monophosphate dehydrogenase (IMPDH)	2	7.06	1	2.35	2.00
PF3D7_1357900	pyrroline-5-carboxylate reductase	2	12.98	1	12.21	2.00
PF3D7_1439900	triosephosphate isomerase (TIM)	6	33.47	3	21.37	2.00
PF3D7_1441200	60S ribosomal protein L1, putative	2	11.06	1	5.53	2.00
PF3D7_1460700	60S ribosomal protein L27 (RPL27)	2	15.07	1	13.70	2.00
PF3D7_0818900	heat shock protein 70 (HSP70)	9	16.25	5	16.25	1.80
PF3D7_0621800	nascent polypeptide associated complex alpha chain, putative	5	42.39	3	23.91	1.67
PF3D7_1446200	M17 leucyl aminopeptidase (LAP)	8	17.03	5	15.87	1.60
PF3D7_1410600	eukaryotic translation initiation factor 2 gamma subunit,	3	9.68	2	9.46	1.50

	putative					
PF3D7_0621200	pyridoxine biosynthesis protein PDX1 (PDX1)	4	13.29	3	22.26	1.33
PF3D7_0608800	ornithine aminotransferase (Tobie and Coatney)	5	12.56	4	13.53	1.25
PF3D7_1357000	elongation factor 1-alpha	10	23.25	8	24.15	1.25
PF3D7_1462800	glyceraldehyde-3-phosphate dehydrogenase (GAPDH)	16	59.05	13	62.32	1.23
PF3D7_1444800	fructose-bisphosphate aldolase (FBPA)	6	20.87	5	25.75	1.20
PF3D7_1015900	enolase (Waterkeyn *et al.*)	15	42.60	13	62.78	1.15
PF3D7_1105400	40S ribosomal protein S4, putative	2	13.79	6	27.59	0.33

7 ACKNOWLEDGMENTS

During these three years time, I got lots of help from many people from different countries, without their contribution and support I would never finish my thesis.

First of all, let me first express my gratitude to my supervisor Prof. Dr. Jude M. Przyborski for his support and guidance to complete this work. The entire project is preceded with his great ideas and helpful advices. I would like to thank my thesis committee members Prof. Dr. Jude M. Przyborski, Prof. Dr. Uwe G. Maier, Prof. Dr. Alfred Batschauer and Prof. Dr. Ralf Jacob. Thank you for all the advices and suggestions, and kindly spend time on reading and reviewing my thesis.

I would like also to thank the DFG 1580 for granting me a PhD fellowship.

It is a great pleasure to spend these three years in my working group. My colleagues support me not only for my work but also during my daily life in Marburg. Many thanks to Sonja and Mathias giving help during my thesis preparation. I also want to give my gratitude to all of my lovely colleagues, Dr. Baumeister, Dr. Kollisch, Mrs Bonarius-Meidt, Mareike, Dr. Sabrine, Dr. Thuva, Dr.Jyotsna, Dr. Preetish, Volker and all students.

I am really thankful and grateful to my family for their supporting and understanding. I also want to thank for my lovely friend Binbin and Lilin to company me in the Marburg.